AD-A130 495 INTERNATIONAL CONFERENCE ON SOLID FILMS AND SURFACES (2ND) (ICSFS-2) PROG. (U) MARYLAND UNIV COLLEGE PARK JUN 81 N00014-81-C-0039 1/2

UNCLASSIFIED F/G 7/4 NL

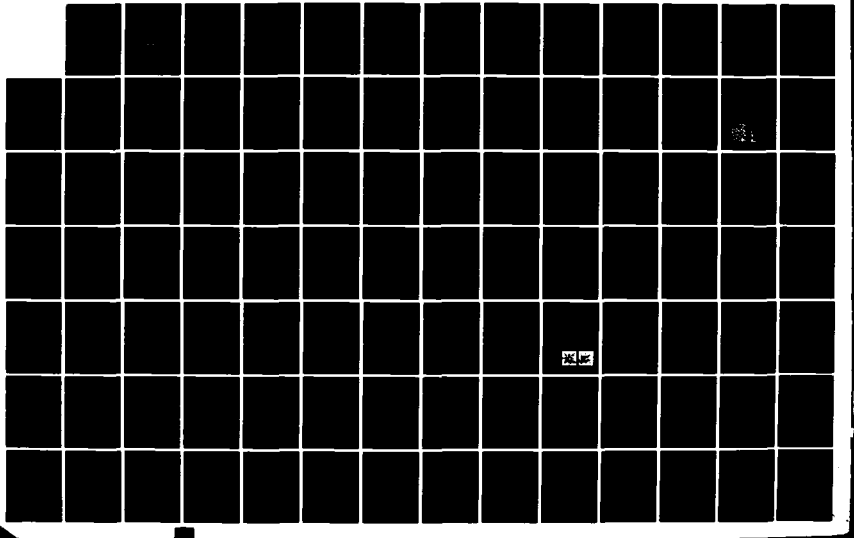

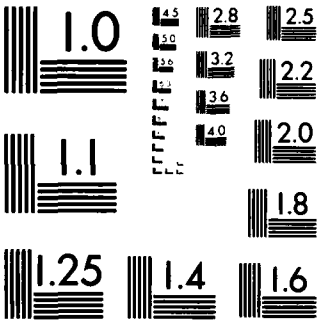

MICROCOPY RESOLUTION TEST CHART
NATIONAL BUREAU OF STANDARDS-1963-A

PROGRAM AND ABSTRACTS

ICSFS-2

INTERNATIONAL CONFERENCE ON SOLID FILMS AND SURFACES

8th–11th June, 1981

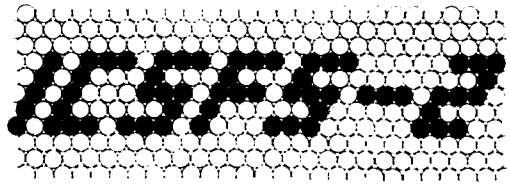

Sponsored by:
Department of Energy,
Office of Naval Research, and
University of Maryland

University of Maryland
College Park, U.S.A.

DEPARTMENT OF THE NAVY
OFFICE OF NAVAL RESEARCH
RESIDENT REPRESENTATIVE
2110 G STREET, NW
WASHINGTON, DC 20037

IN REPLY REFER TO

3510-10-2

TO 6124
4-26-83

From: ONR Resident Representative, ~~George Washington University~~ National Academy of Sciences
To: Code 427
Attn: Larry Cooper
Subj: Contract N00014-81-6-0039 with U MD of Maryland
acceptance of final technical report

1. It is requested that the certificate below be executed, and a signed copy thereof be returned to this office as soon as practicable in order that further closeout actions under the subject contract will not be unduly delayed.

FIRST ENDORSEMENT on ONRRR/GWU ltr, dtd , Ser

From:

To: John Christensen, Code 612A

1. The undersigned hereby certifies that the Contractor has completed the technical performance required under

SIGNATURE

DATE

UNIVERSITY OF MARYLAND

COLLEGE PARK, MARYLAND 20742

DEPARTMENT OF PHYSICS AND ASTRONOMY
301-454-3401

Division of Mathematical and Physical
Sciences and Engineering

April 8, 1983

Mr. John Christianson
Office of Naval Research
Department of Navy
800 N. Quincy Street
Arlington, VA 22217

Dear Mr. Christianson:

I understand from our Office of Sponsored Programs that you need a final technical report on Contract N00014-81-G-0039, A00001. This contract was in partial sponsorship of the Third International Conference on Solid Films and Surfaces, which was held at the University of Maryland 8 - 11 June, 1981. I have pleasure in enclosing a Program and Abstract Book, which gives a detailed outline of all the papers presented at the Conference and I hope you will find that this will therefore serve as the technical report.

I am returning to our Office of Sponsored Programs, as requested, DD form 882, duly signed and completed as a negative report.

If you have any further questions, I will be happy to try to answer them.

Sincerely,

Robert L. Park

Robert L. Park
Professor of Physics

RLP:ps

Enc.

Code 427
322-102
Larry Cooper
19th Floor

2ND INTERNATIONAL CONFERENCE ON SOLID FILMS AND SURFACES

University of Maryland

8 - 11 June, 1981

INTERNATIONAL ADVISORY COMMITTEE

R. L. Park, Co-Chairman
J. E. Rowe, Co-Chairman
R. Ueda, Co-Chairman
M. Balkanski
R. A. Baragiola
E. Bauer
B. K. Chakraverty
A. A. Chernov
R. Dobrozemsky
R. Harman
M. Henzler
Z. Y. Hua
J. D. Joannopoulos
B. A Joyce
J. W. Mayer
W. Mönch
S. Nakamura
J. Pendry
V. Ponec
M. W. Roberts
J. L. Robins
G. Shimaoka
B. J. Slagsvold
W. E. Spicer
V. S. Sundaram
E. J. Suoninen
J. H. van der Merwe

LOCAL COMMITTEE

Robert L. Park, Chairman
Theodore L. Einstein
J. William Gadzuk
Rolfe E. Glover, III
Ray Kaplan
Ron N. Lee
E. Lander McConkey
Pamela Solomos
Vicki J. Zell

2ND INTERNATIONAL CONFERENCE ON SOLID FILMS AND SURFACES

College Park, Maryland

8 - 11 June, 1981

hosted by

UNIVERSITY OF MARYLAND, COLLEGE PARK

PROGRAM

Sunday, June 7

4:00 - 10:00 p.m.	Registration (Main Concourse)
7:00 - 10:00 p.m.	Wine and cheese reception (Volunteer Firefighters Room)

Monday, June 8

8:00 a.m.	Registration booth opens
8:45 a.m.	Welcome by Robert L. Gluckstern, Chancellor
9:00 a.m.	Plenary Session (Main Auditorium) Chairman: J. W. Gadzuk
1:40 p.m.	Session M-A: Thickness and Morphology of Films (Room 0123) Chairman: R. Ueda
1:40 p.m.	Session M-B: Chemisorption (Room 1105) Chairman: T. L. Einstein
1:40 p.m.	Session M-C: Ion Beams and Sputtering (Room 1123) Chairman: W. N. Unertl

Tuesday, June 9

9:00 a.m.	Plenary Session (Main Auditorium) Chairman: R. Kaplan
1:40 p.m.	Session Tu-A: Deposition and Properties of Thin Films (Room 0123) Chairman: J. E. Rowe
1:40 p.m.	Session Tu-B: Semiconductor Surfaces and Heterostructures (Room 1105) Chairman: F. Koch
1:40 p.m.	Session Tu-C: Core Level Spectroscopy (Room 1123) Chairman: R. N. Lee
8:15 p.m.	Pennsylvania Ballet (Tawes Theater, Campus) (Tickets free to first 30 purchasers of $2.00 Activities Card)*

Wednesday, June 10

9:00 a.m.	Plenary Session (Main Auditorium) Chairman: R. E. Glover, III
1:40 p.m.	Session W-A: Semiconductor Films (Room 0123) Chairman: L. J. Brillson

*A Summer Activities Card entitles the holder not only to attend the Ballet at no extra charge but also to use the sports facilities at the University.

1:40 p.m.	Session W-B: Surface Phases (Room 1105) Chairman: M. Henzler
1:40 p.m.	Session W-C: Metal Surfaces (Room 1123) Chairman: G. G. Kleiman
7:00 p.m.	Banquet (Chesapeake/Ft. McHenry Room)

Thursday, June 11

9:00 a.m.	Plenary Session (Main Auditorium) Chairman: C. R. Anderson
1:40 p.m.	Session Th-A: Epitaxy and Segregation (Room 0123) Chairman: E. Bauer
1:40 p.m.	Session Th-B: Electron Energy Loss Spectroscopy and Optical Methods (Room 1105) Chairman: A. Bradshaw
1:40 p.m.	Session Th-C: Adsorption (Room 1123) Chairman: L. D. Roelofs

Monday, June 8, 1981

Plenary Session

Main Auditorium

8:45 Welcome: Robert L. Gluckstern, Chancellor, University of Maryland

9:00 Keynote Lecture: Determination and Application of the Atomic Geometries of Solid Surfaces. C. B. DUKE

9:45 Low Energy Electron Diffraction Analysis of Surface Structures. J. B. PENDRY

10:30 Extended Absorption Fine Structure Analysis of Surface Structure. T. L. EINSTEIN

11:15 Ion Backscattering Analysis of Surface Structures. W. N. UNERTL

Session M-A: Thickness and Morphology of Films (Room 0123)

1:40 Determination of Anodic Oxide Film Thickness by a Luminescence Method. L. D. ZEKOVIĆ, V. V. UROŠEVIĆ and B. JOVANIĆ

2:00 The Estimation of the Thickness of Material Examined by the X-Ray Continuum Isochromat Method. J. AULEYTNER, K. ŁAWNICZAK-JABŁONSKA and K. GLEGOŁA

2:20 Application of an Electron-Matter Interaction Theory for the Solid Film Thickness Measurement. C. LANDRON

2:40 Determination of Surface Roughness from X-Ray Diffraction Measurements on Thin Films. W. FISCHER and P. WISSMANN

3:00 New Application of ESCA (XPS). O. K. T. WU, G. G. PETERSON, W. J. LaROCCA and E. M. BUTLER

3:20 Characterization of [001] Tilt Boundaries in Bicrystalline Thin Films of Gold by High-Resolution Transmission Electron Microscopy. F. COSANDEY and C. L. BAUER

3:40 Low Loss Surface Imaging Studies of Thin Film Growth. D. A. SMITH and M. M. J. TREACY

4:00 Investigation of Morphology of Surfaces Using the Method of Defocused Electron Microscopy Images. S. K. MAKSIMOV, V. D. VERNER, G. N. GAIDUKOV, V. L. YEGOROV, N. I. MAISURADZE and A. P. FILIPPOV

4:20 The Use of Defocused Electron Images in Search for Atomic Surface Relief. S. K. MAKSIMOV, S. N. BEZRYADIN, V. D. VERNER, V. L. YEGOROV and N. I. MAISURADZE

4:40 Studies of the Thin Films of Li-B Alloys. H. KEZUKA and K. IWAMURA

5:00 Investigation of Growth Surface and Fine Structure of C.V.D. W-Re-Films. G. M. DEMYASHEV, Y. V. LAKHOTKIN, A. I. KRASOVSKY and R. K. CHUZHKO

5:20 Structure and Shape of Epitaxial Metal Clusters., M. J. YACAMÁN, P. SCHABES and T. OCAÑA

Session M-B: Chemisorption (Room 1105)

1:40 Direct Calculation of Experimentally Measurable Chemisorptive Parameters from Theoretical Quantum Chemical Cluster Models. M. E. SCHWARTZ

2:00 Copper Atoms and Cluster Isolated in Oxygen Matrices. D. SCHMEISSER, K. JACOBI and D. M. KOLB

2:20 Physisorption and Chemisorption of Oxygen on Tin at Low Temperature. G. S. CHOTTINER, R. E. GLOVER, III and R. L. PARK

2:40 A Study of Oxygen Adsorption on Ti(001) Using Photon Stimulated Desorption. D. M. HANSON, R. STOCKBAUER and T. E. MADEY

3:00 Oxygen Chemisorbed on Ti(0001). B. T. JONKER, J. F. MORAR and R. L. PARK

3:20 Comparison of the Interaction of CO with Mo(001) and Ni(001). R. V. KASOWSKI

3:40 The Structure of CO on Ni(111). F. P. NETZER and T. E. MADEY

4:00 Thermal Desorption of CO, O_2 and CH_4 Molecules from Ni(111) Single Crystals. G. A. SARGENT, J. CHAO and G. B. FREEMAN

4:20 A Study of Nitric Oxide Adsorption on Copper (100) and (110). J. F. WENDELKEN

4:40 High-Resolution Angle-Resolved Photoemission Studies of the Interaction between Atomic Chlorine and Cu(001) and Cu(111) Surfaces. A. GOLDMANN and D. WESTPHAL

5:00 Ammonia on Iridium (111): Adsorption Kinetics and Band Structure. R. J. PURTELL, R. P. MERRILL, T. HUGHBANKS, R. HOFFMANN, S. B. CHRISTMAN and T. N. RHODIN

5:20 Pulsed Laser Atom-Probe Study of Clean and Oxygen Covered Silicon. G. L. KELLOGG

Session M-C: Ion Beams and Sputtering (Room 1123)

1:40 The Sputtering of Molecular Ions from Surfaces in Secondary Ion Mass Spectrometry. M. L. YU

2:00 Resonant Ionization of Short-Lived Neutral Molecules as a Mechanism for Sputtered Molecular Ion Creation. K. J. SNOWDON, W. HEILAND and E. TAGLAUER

2:20 Mechanism of Ejection of F^+ from LiF Surfaces by Ion Neutralization. J. A. SCHULTZ, P. T. MURRAY, R. KUMAR and J. W. RABALAIS

2:40 Transmission Electron Microscope Study of Ion Beam Induced Interfacial Reactions in Molybdenum Thin Films on Silicon. L. J. CHEN, L. S. HUNG and J. W. MAYER

3:00 Anodization and Rutherford Backscattering Measurements of Superimposed Metal Film - GaAs Structures. J. D. CANADAY and C. W. FISCHER

3:20 Surface Pre-Treatment Dependent Formation of Molybdenum Nitride by Low Energy N_2^+ Bombardment. N. SHAMIR, D. A. BALDWIN and J. W. RABALAIS

3:40 Molybdenum Nitride Film Growth under N_2^+ and N^+ Impact on a Molybdenum Surface: Energy and Dose Dependence. D. A. BALDWIN, N. SHAMIR and J. W. RABALAIS

4:00 Formation of N-Layers in Silicon Bombarded by Low-Energy Oxygen Ions. V. A. LABUNOV and V. E. BORISENKO

4:20 Dynamic Simulation of Changes in Near Surface Composition during Ion Bombardment. M. L. ROUSH, T. D. ANDREADIS, F. DAVARYA and O. F. GOKTEPE

4:40 Stainless-Steel Oxidation Investigation, Using Nuclear Techniques for Surface Studies, with an Automated Scanning Proton Microbeam: Experimental System and Results. J. M. CALVERT and L. F. REQUICHA FERREIRA

5:00 Sputtering Yield Calculations for Light Ions Incident on Wall In Tokamak. T.-W. XU, Z.-T. FAN and Q.-C. HE

Tuesday, June 9, 1981

Plenary Session

Main Auditorium

9:00 Interaction of Metals with Semiconductor Surfaces. L. J. BRILLSON

9:45 Subband Physics: Energy Bands and Transport Properties of an Interfacial Charge Layer. F. KOCH

10:30 Electronic Surface States of II-VI Compound Semiconductors. T. TAKAHASHI and A. EBINA

11:15 Atomistic or Molecular Processes on Clean Surfaces: Recent Advances. R. UEDA

Session Tu-A: Deposition and Properties of Thin Films (Room 0123)

1:40 Film and Surface Studies by MEED. G. SHIMAOKA

2:00 Electrical Properties of Sputtered RuO_2 Films. M. TAKEUCHI, K. MIWADA and H. NAGASAKA

2:20 Preparation and Characterization of Thin Dielectric Films. V. S. DHARMADHAKARI

2:40 Substrate Biased R.F. Sputtering of Zinc Oxide Films. D. K. MURTI

3:00 Production and Properties of Sputtered Thin Films for Solar Selective Absorbing Surfaces. G. L. HARDING and S. CRAIG

3:20 Carbon Thin Films Obtained by Means of R.F. Plasma-Decomposition of Hydrocarbon. Y. ONUMA, Y. KATO and K. HORI

3:40 Characterization of Plasma Nitride. H. KOYAMA

4:00 The Surface Temperature of a Substrate during the Vacuum Evaporation. Y. H. SHEN

4:20 Polarization in Dielectric Films due to Uncompensated Mobile Charge. V. P. ROMANOV

4:40 Structure of Thin Film Ag-O-Cs Photocathode and its Dark Current. Q.-D. WU

Session Tu-B: Semiconductor Surfaces and Heterostructures (Room 1105)

1:40 On the Electronic Properties of Ge:GaAs (110) Heterostructures. H. GANT, R. MURSHALL and W. MÖNCH

2:00 Intermixing and the Mechanism for Schottky Barrier Formation. W. E. SPICER, P. SKEATH, C. Y. SU and I. LINDAU

2:20 Field Effect Spectroscopy of Fast Surface States at Oxidized GaAs Surfaces. E. W. KREUTZ and P. SCHROLL

2:40 Surface Studies of InP by Electron Energy Loss Spectroscopy and Auger Electron Spectroscopy. C. W. TU and A. R. SCHLIER

3:00 Unified Theory of Intrinsic States, Core Excitons, and Defect-Induced States at Semiconductor Surfaces. R. E. ALLEN and J. D. DOW

3:20 Angular Resolved Photoemission Measurements on Clean and Hydrogen Covered Ge(111) Surfaces. R. D. BRINGANS and H. HÖCHST

3:40 Interface State and Oxide Charge Generation in the Si-SiO_2 System by Photoinjection of Carriers. E. W. KREUTZ

4:00 Charge Transport and Storage in Ion Implanted Metal-Oxide-Semiconductor Structures. L. AUGULIS and L. PRANEVIČIUS

4:20 On the Acceptor Nature, Formed in the Surface Layer at Silicon Thermal Evaporation. L. N. ALEKSANDROV, R. N. LOVYAGIN and L. N. SAFRONOV

4:40 Relationship between the Polar Surfaces of CdS Crystals and some Properties of CdS-Cu_2S and CdS-CdTe Heterojunctions. A. KOBAYASHI

5:00 Development and Characterization of a Monochristalline Silicon Solar Cell. N. KESRI

Session Tu-C: Core Level Spectroscopy (Room 1123)

1:40 A Quantum Effect in Surface Plasmon Excitation. P. LONGE and S. M. BOSE

2:00 Incident-Energy Dependence of the 3p Electron Energy-Loss Spectra of Nickel. T. JACH and C. J. POWELL

2:20 Absolute Core Level Binding Energies for 4d Transition Elements. Y. S. CHEE, B. SLAGSVOLD, J. F. MORAR, R. L. PARK and R. N. LEE

2:40 The Appearance Potential Spectroscopies of Evaporated Thin Lanthanum Films. J. ZHUGE, X. L. PAN and Z. Y. HUA

3:00 Soft X-Ray Appearance-Potential Spectra of Rare Earth Ho and Ho-Ni Alloy. D. CHOPRA and H. K. CHUNG

3:20 Resonant Photoelectron Appearance Potential Spectroscopy. Z. Y. HUA, J. ZHUGE and X. L. PAN

3:40 Appearance Potential Spectra of Semiconductors. J. F. MORAR and R. L. PARK

4:00 Evidence for Screening Effects in the Carbon KVV Auger Lineshape of Intercalated Graphite. B. I. DUNLAP, D. E. RAMAKER and J. S. MURDAY

4:20 Auger Line Shape Analyses for Epitaxial Growth in the Cu/Cu, Ag/Ag, and Ag/Cu Systems. R. W. VOOK and Y. NAMBA

4:40 Surface Chemical Characterization by Auger Signal Decomposition: Silicon Nitride H. H. MADDEN and G. C. NELSON

5:00 XPS Studies of the Photodecomposition of AgCl. J. SHARMA, P. DiBONA and D. A. WIEGAND

5:20 Electron Spectroscopic Study of Phase Transition $V_2O_5 \rightarrow V_6O_{13}$. I. CURELARU, E. SUONINEN and E. MINNI

Wednesday, June 10, 1981

Plenary Session

Main Auditorium

9:00 Order in Two Dimensions. L. D. ROELOFS

9:45 LEED Studies of Surface Imperfections. M. HENZLER

10:30 Clean Surface Reconstruction of BCC{001} Metals. A. J. MELMED and W. R. GRAHAM

11:15 Epitaxy of Metal Films. E. BAUER

12:00 Misfit Accommodation at Interface by Dislocations. J. WOLTERSDORF

Session W-A: Semiconductor Films (Room 0123)

2:00 Dopant Incorporation Studies in Silicon Molecular Beam Epitaxy (Si MBE). F. G. ALLEN, S. S. IYER and R. A. METZGER

2:20 On the Nature of Electron Irradiation Damage in Hydrogenated Amorphous Silicon. H. SCHADE

2:40 Optical and Electrical Properties of Hydrogenated Amorphous Silicon Films Deposited by Tetrode RF Sputtering. Y. GEKKA, Y. KIMURA and T. MATSUMORI

3:00 Coupled Electron-LO Phonon Modes of GaAs-$A\ell_xGa_{1-x}As$ Multilayer Systems. S. DAS SARMA

3:20 The Substrate Heating Effects on Ion-Beam Sputter-Deposited $CuInS_2$ and GaP Thin Films. J.-R. CHEN, C.-C. NEE, H.-L. HWANG, L. LU and Y.-C. LIU

3:40 Recent Studies of ZnS Films: Evaporation, Growth and Laser Irradiation Effects. T. N. CHIN, O. W. O'NEILL and P. E. HOUSER

4:00 Multi-Layer Film Structure for Light Sources. L. N. ALEKSANDROV and A. S. IVANZEV

4:20 Field Effect Studies on MIS Structures of PbTe Films. A. L. DAWAR, O. P. TANEJA, P. KUMAR, S. K. PARADKAR and P. C. MATHUR

4:40 Electrical Effect of Na, Ag, and Tl Impurities on Lead Telluride Thin Films. A. L. DAWAR, O. P. TANEJA, S. K. PARADKAR, P. KUMAR and P. C. MATHUR

5:00 Electrical Effect of Hydrogen on SnTe Thin Films. A. L. DAWAR, O. P. TANEJA, B. K. SACHAR, A. O. MOHAMMED, P. KUMAR, S. K. PARADKAR and P. C. MATHUR

Session W-B: Surface Phases (Room 1105)

2:00 Direct Measurement of Pair Energies in Adatom-Adatom Interactions on a Metal Surface. R. CASANOVA and T. T. TSONG

2:20 Correlation between Adatom-Adatom Pair Interactions and Adlayer Superstructure Formation: Si on W{110}. T. T. TSONG and R. CASANOVA

2:40 The Role of Three-Adatom Interactions in Two-Dimensional Phase Diagrams. N. C. BARTELT, T. L. EINSTEIN and P. E. HUNTER

3:00 Exact Solutions for Ising Model Multisite Correlations on the Honeycomb and Triangular Lattices. C. H. MÚNERA, J. H. BARRY and T. TANAKA

3:20 Theory of dc Conductivity for a Two-Dimensional Superionic Conductor on the Honeycomb Lattice. T. TANAKA, N. L. SHARMA, C. H. MUNERA and J. H. BARRY

3:40 Observation of the Structural Transition Pt(100) 1×1→hex by LEED Intensities. K. HEINZ, E. LANG, K. STRAUSS and K. MULLER

4:00 Structures of Cs-Adlayers on Reconstructed Ir, Pt and Au Surfaces. K. MÜLLER, E. LANG, H. ENDRISS and K. HEINZ

4:20 Direct Determination of the Size Distribution of Adsorbed-Layer Islands from LEED Beam Intensity-vs-Angle Profiles. L. H. ZHAO, T. M. LU, P. K. WU and M. G. LAGALLY

4:40 LEED, AES, ELS, Surface Conductivity and Work Function Measurements Study of Reconstruction Modes of (110)SnO_2. E. DE FRÉSART, J. DARVILLE and J. M. GILLES

5:00 Phase Diagram of Oxygen on Nickel (100). D. E. TAYLOR and R. L. PARK

5:20 Hydrogen Atom Diffraction from Ordered Xenon Overlayers Adsorbed on the (0001) face of Graphite. T. H. ELLIS, S. IANNOTTA, G. SCOLES and U. VALBUSA

Session W-C: Metal Surfaces (Room 1123)

2:00 Temperature Dependence in UV Photoemission from Cu(111). H. MÅRTENSSON, P.-O. NILSSON and J. KANSKI

2:20 Reflection High Energy Diffraction by the Ag(001), Ag(111) and Ag(110) Surfaces. P. A. MAKSYM and J. L. BEEBY

2:40 Non-Adiabatic Scattering from Metal Surfaces. J. W. GADZUK

3:00 Ab-initio Atom Cluster Models of Carbon Surfaces. W. H. FINK

3:20 Magnetic Moments at the Surface of 3d Transition Metals. J. DORANTES-DÁVILA and J. L. MORÁN-LÓPEZ

3:40 A New Polarization Model of Changes in the Work Function for Bare and Covered Transition Metal Surfaces. E. SHUSTOROVICH and E. C. BAETZOLD

4:00 Interionic Interactions at Metallic Surfaces. R. N. BARNETT, C. L. CLEVELAND and U. LANDMAN

4:20 Method of Determination of the Electron Structure of Films. S. N. BEZRYADIN, Y. K. VEKILOV and V. D. VERNER

Thursday, June 11, 1981

Plenary Session

Main Auditorium

9:00 Vibrational Spectra of Adsorbed Atoms and Molecules. A. M. BRADSHAW

9:45 Inelastic Tunneling. J. KLEIN

10:30 Angular-Resolved Photoemission. F. R. McFEELY

11:15 X-Ray Excited Auger Studies of Metals and Alloys. G. G. KLEIMAN

Session Th-A: Epitaxy and Segregation (Room 0123)

1:40 Investigation of Order-Disorder and Segregation Behavior on $Cu_3Au(100)$ and (110) Surfaces by LEIS(TOF). T. M. BUCK, G. H. WHEATLEY and L. MARCHUT

2:00 First Stage of Au/Ag(111) Epitaxy using Ion Scattering, LEED and Auger Analyses. R. J. CULBERTSON, L. C. FELDMAN and P. J. SILVERMAN

2:20 Iron-Cobalt Alloys: The Importance of Iron Surface Segregation for the Order-Disorder Theory and for Catalysis Reactions. G. ALLIE, C. LAUROZ, P. VILLEMAIN, M. COULON and C. VANVOREN

2:40 Thin Silver Films on Al(100). W. F. EGELHOFF, JR.

3:00 Au, Ag and Cu-films on Si(111) Surfaces Studied by Auger Electron Spectroscopy. R. WEISSMANN, G. FISCHER and K. MÜLLER

3:20 Measurement of the Intrinsic Stress as a Method for the In Situ Investigation of the Structure and Growth of Thin Films. R. KOCH, H. P. MARTINZ and R. ABERMANN

3:40 A New Method for Metal Electroreflectance Measurements Using Metal-Insulator-Metal Structures. J. P. GOUDONNET, G. CHABRIER, G. NIQUET and P. VERNIER

4:00 Autonodulation of Composition of Complex Semiconductor Epitaxial Films. S. K. MAKSIMOV, E. N. NAGDAYEV and L. A. BONDARENKO

4:20 Diataxial Growth of Semiconductors. E. I. GIVARGIZOV, N. N. SHEFTAL and V. I. KLYKOV

4:40 Defect States in a WO_3 Film Grown on a W(111) Surface. H. HÖCHST and R. D. BRINGANS

Session Th-B: Electron Energy Loss Spectroscopy and Optical Methods (Room 1105)

1:40 EELS Study of Formic Acid on Pt(111)-O. N. R. AVERY

2:00 The Role of Electrodynamic Interactions on Energy Loss Intensities and Vibrational Frequencies of Adsorbed Molecules. B. I. DUNLAP and P. R. ANTONIEWICZ

2:20 Some Aspects and Results of Quantitative Electron-Loss Spectroscopy. Y. MARGONINSKI

2:40 Transmission of Monochromatic 0-15 eV Electrons Through Thin Films Organic Solids. L. SANCHE

3:00 Electron-Energy-Loss Electronic and Vibronic Spectroscopy of Matrix-Isolated-Benzene and Multilayer-Benzene Films. L. SANCHE and M. MICHAUD

3:20 Electron-Spectroscopic Studies of $LiNbO_3$ and $LiTaO_3$ Surfaces. V. H. RITZ and V. M. BERMUDEZ

3:40 Surface-enhanced Raman Scattering from Chemisorbed Pyridine on Ag(111): Dependence on Bonding Orientation: P. N. SANDA, J. E. DEMUTH, J. C. TSANG, L. M. WARLAUMONT and K. CHRISTMANN

Session Th-C: Adsorption (Room 1123)

1:40 Kinetic Equations for Physisorption. H. J. KREUZER

2:00 Surface Potentials of Benzene Derivative Monolayers and Submonolayers at the Mercury/Nitrogen Interface. R. J. KINZIG

2:20 Alkoxy Complexes on Lithium–Identification and Geometry. S. GATES, J. A. SCHULTZ, L. G. PEDERSEN and R. C. JARNAGIN

2:40 Interactions of Lithium with Dry Air. C. R. ANDERSON and R. N. LEE

3:00 Evaluation of Surface Cleaning Procedures. R. G. MUSKET, C. A. COLMENARES, D. M. MAKOWIECKI, W. McLEAN, R. G. MEISENHEIMER and W. J. SIEKHAUS

3:20 H_2O Interaction with Ni(110): Auto-catalytic Decomposition in the Temperature Range from 400–550 K C. BENNDORF, C. NOBL, M. RUSENBERG and F. THIEME

3:40 Hartree–Fock Theory of Multilayer Physisorption. H. J. KREUZER, P. SUMMERSIDE and R. TESHIMA

4:00 Ion Formation from Solid Surfaces due to very rapid Energy Transfer. F. R. KRUEGER

4:20 A Study of Gas Conduction in Evacuated Solar Energy Thermal Collectors. B. WINDOW and G. HARDING.

MONDAY MORNING, JUNE 8, 1981

Plenary Session

Main Auditorium

Chairman: J. W. GADZUK

8:45 Welcome by Robert L. Gluckstern, Chancellor

9:00 Keynote Lecture: Determination and Application of the Atomic Geometries of Solid Surfaces.
C. B. DUKE

9:45 Low Energy Electron Diffraction Analysis of Surface Structures
J. B. PENDRY

10:30 Extended Absorption Fine Structure Analysis of Surface Structure
T. L. EINSTEIN

11:15 Ion Backscattering Analysis of Surface Structures.
W. N. UNERTL

DETERMINATION AND APPLICATION OF THE ATOMIC GEOMETRIES OF SOLID SURFACES

C.B. Duke
Xerox Webster Research Center
Xerox Square-114, Rochester, NY, 14644

In order to calculate the electronic charge density and excitation spectra associated with a surface the positions of the atomic constituents in the vicinity of the surface must be known. These positions, in turn, may be evaluated either by minimizing the total energy of the surface using a model to calculate this energy or by analyzing experimental spectra using a model embodying both these positions and a description of the physical phenomena giving rise to the observed spectra. This paper is devoted to an assessment of the accuracy with which these positions can be determined by state-of-the-art analyses of experimental measurements, specifically elastic low-energy electron diffraction (ELEED), ion scattering spectroscopy (at both medium and high energies), photoemission spectroscopy (PES), and surface sensitive variants of extended X-ray fine structure (EXAFS) intensities. The methodology is that of comparing the results of various techniques as applied to specific systems. We consider three clean metal surfaces [Al(111), Pt(111), and Ni(110)], one clean semiconductor surface [GaAs(110)], and two metal-overlayer systems [O and CO adsorbed on Ni(100)]. Our major finding is that when carefully and accurately applied, the various methods provide structural results which are consistent to within about 0.1A. Perusal of the literature reveals larger discrepancies which, however, have exhibited a tendency to disappear as a function of increasing time once conflicting results become sufficiently precisely specified that the origin of the discrepancies can be identified and resolved. The examples of Pt(111), GaAs(110) and CO on Ni(100) provide explicit examples of the convergence of the various spectroscopies to common results with the passage of time.

LOW ENERGY ELECTRON DIFFRACTION ANALYSIS OF SURFACE STRUCTURES

J.B. Pendry

SRC Daresbury Laboratory, Warrington, WA4 4AD

LEED as a technique for surface structure determination has come of age in the past five years. Improved methods of analysis, especially the use of reliability factors and fast data-collection procedures, have led to a large number of solved structures and advances of the technique to more complex surface systems of more than academic interest. Perhaps most significant in this respect is the ability to look at molecules on surfaces with the accompanying shift of emphasis from the surfaces reaction to the adsorption, to questions of molecular conformation to the surface. Subsidiary techniques such as EELS and photoemission will be important in arriving at "first guesses" for such systems. A comparison will be made between the effectiveness of LEED as a surface technique and of its major competitors such as surface EXAFS. Some speculations will be made about possible future developments.

EXTENDED ABSORPTION FINE STRUCTURE ANALYSIS OF SURFACE STRUCTURE

T. L. Einstein
Department of Physics and Astronomy, University of Maryland
College Park, Maryland 20742

With extended absorption fine structure techniques one can determine directly, by a weighted Fourier transform, the distance between atoms in a material. Typical accuracies are ±0.05 Å or better. The essence of these techniques is simple. An incident beam of X-rays or electrons excites a core electron into an outgoing spherical state. Backscattering from nearby atoms increases or decreases the amplitude of this final state at the central atom, depending on the ratio of the interatomic spacing to the electron wave length. This interference leads to a weak sinusoidal modulation (fine structure) of the absorption probability as the energy of the electron is ramped. "Extended" refers to final-state electrons well above threshold (by at least 50-100 eV), where the mean free path is short. Only atoms near the absorbing atom are seen. Thus, long-range order is irrelevant, in contrast to LEED or ion backscattering. Another reason for considering just the extended fine structure is that multiple scattering effects that plague LEED are minimal: the atomic scattering function is peaked in the forward direction and 180° backscattered electrons produce most of the fine structure.

In order for the Fourier transform procedure to work simply, it is important that the final-state electron be an angular momentum eigenstate. For an incident X-ray beam (EXAFS), the dipole selection rule readily provides this feature. Similarly, a high-energy (~100 keV) electron beam can be used and small-angle scattering measured (EXELFS). In both methods the excitation cross-section is small, forcing one to use films of order 500 Å thickness. In the X-ray case surface sensitivity has been achieved (SEXAFS) by collecting electrons emitted during deexcitation of the core hole (rather than measuring the absorption coefficient). To achieve adequate signal, SEXAFS requires a powerful X-ray source, typically a storage ring. Extended fine structure can also be measured with equipment found in most surface science laboratories by using appearance potential spectroscopy (EAPFS). Here a lower energy electron beam (~1 keV) impinges on the sample. The derivative of the excitation probability with respect to incident energy is measured; either X-rays or electrons emitted in the core deexcitation are collected. For a K-edge, calculation shows that the second electron is predominantly s-wave rather than p-wave.

After amplifying these ideas, the talk will consider applications to oxides of Al, Ni, and Si to demonstrate the capabilities of SEXAFS and EAPFS. Critical comparisons of the two methods will be stressed. Advantages of SEXAFS include less beam damage and availability of beam polarization. Advantages of EAPFS include superior data range and use of a beam source that is stable, modulable, convenient, and readily available. Both methods compete well with plane-wave diffraction techniques as a probe of local structure for ordered structures, and make it possible to measure structure directly in systems with little or no order.

ION BACKSCATTERING ANALYSIS OF SURFACE STRUCTURES*

W. N. Unertl[+]

Laboratory for Surface Science and Technology and
Department of Physics
University of Maine
Orono, Maine 04469

Backscattering of 0.1 to 2 MeV ions from single crystal surfaces is a powerful new tool for studying surface crystallography. It's surface sensitivity arises from a combination of Rutherford scattering, ion channeling and the electronic stopping power. The scattering process can be analysed using simple classical models and Monte Carlo simulations. Absolute measurements are facilitated by the availability of Bi implanted silicon standards. Ion backscattering provides information which complements that obtained by other surface sensitive techniques. The method has been used to study small relaxations, adsorbed atom locations, reconstruction of clean and adsorbate covered surfaces, and displacive phase transitions. It also shows promise as a method for studying surface lattice dynamics including correlated vibrations and as a method for studying epitaxial growth and interfacial structure.

*Supported in part by the National Science Foundation under grant DMR8020840.

[+]Member of Attached Staff, Chalk River Nuclear Laboratory, AECL, Chalk River, Ontario, Canada

Monday afternoon, June 8, 1981

Session M-A: Thickness and Morphology of Films

(Room 0123)

Chairman: R. UEDA

1:40 Determination of Anodic Oxide Film Thickness by a Luminescence Method. L. D. ZEKOVIĆ, V. V. UROŠEVIĆ and B. JOVANIĆ

2:00 The Estimation of the Thickness of Material Examined by the X-Ray Continuum Isochromat Method. J. AULEYTNER, K. ŁAWNICZAK-JABŁONSKA and K. GŁEGOŁA

2:20 Application of an Electron-Matter Interaction Theory for the Solid Film Thickness Measurement. C. LANDRON

2:40 Determination of Surface Roughness from X-Ray Diffraction Measurements on Thin Films. W. FISCHER and P. WISSMANN

3:00 New Application of ESCA (XPS). O. K. T. WU, G. G. PETERSON, W. J. LaROCCA and E. M. BUTLER

3:20 Characterization of [001] Tilt Boundaries in Bicrystalline Thin Films of Gold by High-Resolution Transmission Electron Microscopy. F. COSANDEY and C. L. BAUER

3:40 Low Loss Surface Imaging Studies of Thin Film Growth. D. A. SMITH and M. M. J. TREACY

4:00 Investigation of Morphology of Surfaces Using the Method of Defocused Electron Microscopy Images. S. K. MAKSIMOV, V. D. VERNER, G. N. GAIDUKOV, V. L. YEGOROV, N. I. MAISURADZE and A. P. FILIPPOV

4:20 The Use of Defocused Electron Images in Search for Atomic Surface Relief. S. K. MAKSIMOV, S. N. BEZRYADIN, V. D. VERNER, V. L. YEGOROV and N. I. MAISURADZE

4:40 Studies of the Thin Films of Li-B Alloys. H. KEZUKA and K. IWAMURA

5:00 Investigation of Growth Surface and Fine Structure of C.V.D. W-Re-Films. G. M. DEMYASHEV, Y. V. LAKHOTKIN, A. I. KRASOVSKY and R. K. CHUZHKO

5:20 Structure and Shape of Epitaxial Metal Clusters. M. J. YACAMÁN, P. SCHABES and T. OCAÑA

Determination of anodic oxide film thickness by a luminescence method

Lj.D.Zeković*, V.V.Urošević and B.Jovanić

Institute of Physiscs, 11001 Beograd, P.O.Pox 57 and
*Department of Physics, Faculty of Science, 11001 Beograd,
P.O.Box 550, Yugoslavia.

In this work we use interference effect[1] wich takes place in electroluminescence of thin anodic films in order to determine film thickness and/or some other film characteristics. The experiment has been performed with constant DC current (5 mA/cm^2), Pt cathode and very pure electropolished Al anodes in an organic electrolyte (ammonium tartarate), the axis of the optical and detection system (condensor, optical monochromator and photon counter) being parallel to the film surface. The acceptance angle of the optical system was rather low (~5°). In this case multiple reflections take place wich lead to the interference of Lummer-Gehrke type, as shown on the figure. It is experimentaly proved that odd maxima correspond to normal components of the electric vector and even maxima to parallel components. It is shown that this phenomenon can be used for determination of film thickness and anodizing rate if refraction index of Al_2O_3 is known, or vice versa to check optical constants of Al and Al_2O_3 if anodizing rate is known. Using for n_0 a value 1,57 , we obtained for anodizing rate 1,4 nm/V, wich is in excellent aggreement with other measurements.

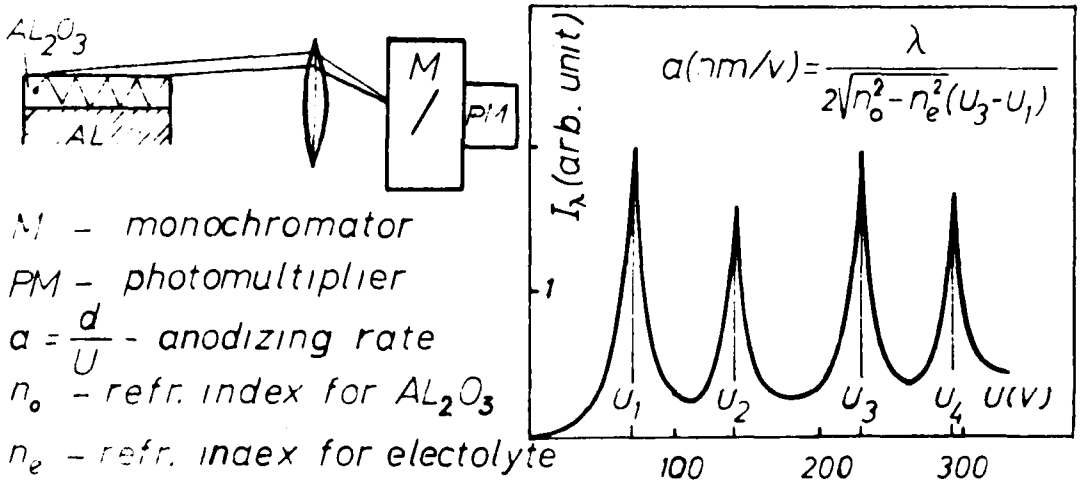

1. Lj.D.Zeković and V.V.Urošević, Thin Solid Films, Vol.78, No3, (1981), pp.279-286

The estimation of the thickness of material examined by the X-ray continuum isochromat method.

J. Auleytner, K. Ławniczak-Jabłonska, K.Glegoła
Institute of Physics, Polish Academy of Sciences,
Warszawa, Poland

The method of the X-ray continuum isochromat is one of the X-ray emission methods which can be in studies of the empty electron valence states in solids [1,2]. The sampling depth of the emission spectroscopies is equal to micrometers and these methods are not considered to be surface sensitive. This problem is different in the case of the isochromat method. The isochromat is excited by the electron beam with energy E_o which is close to the measured energy of the X-ray continuns radiation. The primary structure of the isochromat is created by such electrons which do not lose energy in inelastic collisions. Thus, the material thickness examined by the isochromat method is determined by the inelastic mean free path of electrons in solid. In the present work the inelastic mean free paths were calculated for electron energy E_o equal to 2400, 5400, 8000 and 19600 eV in aluminium, nickel, tungsten, molibdenium and gold. Only few experimental data fore these energies can be found in the literature. The mean free paths were also estimated experimentally by the isochromat method. The energy of the primary electron beam in experiment was E_o = 5420 eV. Several layers of gold were evaporated on electropolished surfaces of tungsten and molibdenium. The thickness of these layers were equal to 40, 90, 240 and 380 Å. The isochromats of these layers were measured and compared with isochromat for pure gold. The contribution of the substrate and the overlayer to the recorded isochromat was estimated from the isochromat taken for pure metals. The nonhomogeneity of the overlayer was accounted for in estimation of the sampled thickness. The agreement between theoretically calculated and experimentaly determined mean free paths were rather good.

References:

1. K.Ulmer, Phys.Rev.Lett., 3 (1959) 519
2. R.P.Tartie and R.J.Liefeld, Phys.Rev., 1?, 7 (1975) 3411.

APPLICATION OF AN ELECTRON-MATTER INTERACTION THEORY FOR THE SOLID FILM THICKNESS MEASUREMENT

Claude LANDRON
Département de Physique
Faculté des Sciences et Techniques
Sfax -TUNISIE-

Abstract

Electron Probe Microanalyser are available with many different geometries of electron beam incidence angle and X-ray take off angle. Change in electron beam incidence angle affects the production of X rays as a function of electron backscattering and of distance from the target surface. Change in take off angle affects the X rays absorption into the specimen.

The intensity of characteristic X rays excited by electron bombardment into solid film depends upon the distribution with depth of primary electron beam. The behavior of the electron distribution function is governed by the Boltzmann transport equation.

It is shown that the X ray intensity emitted is proportional to the mean depth of electron penetration which depends upon :

a) the electron beam incidence angle ;

b) the film thickness ;

c) the degree to which electrons are scattered along their trajectories. The form for the dependance of X ray intensity on mean depth is derived by considering the electron diffusion process.

The agreement with a Monte Carlo simulation method is good and an advantage of these technique over Monte Carlo calculation is the reduced computer time, and a betterment of accuray, and it is possible to calculate other quantities of interest.

Determination of Surface Roughness from X-Ray Diffraction Measurements on Thin Films

W. Fischer and P. Wissmann
Institut für Physikalische und Theoretische Chemie der Universität,
Egerlandstraße 3, 8520 Erlangen, FRG

In certain cases the x-ray diffraction spectrum of thin films shows characteristic secondary maxima which lie symmetrically about the primary maximum. Important informations regarding the roughness of the films can be deduced from a quantitative analysis of the intensity profile of these secondary maxima.

The method is explained for the example of gold films epitaxially grown on silicon (111) single-crystals. These films (thickness range 20 - 200 Å) show a typical (111) single-crystal structure without grain boundaries or lattice faults. High sensitivity of the x-ray diffraction analyzer has been achieved by means of a doubly focussing crystal monochromator, step scanning unit and impulse height discriminator. The resolving power is, then, sufficient to detect the 4^{th} and 5^{th} secondary maximum of a 77 Å thick film without problems, although the secondary maxima exhibit intensities of the order of only 3 % of the primary peak intensity.

The quantitative evaluation is performed on the basis of a meander model of surface roughness. By comparing theoretical and experimental reflex intensity data the step height of the grooves in the surface is found to be about one interlattice plane distance, indicating that the gold films under investigation possess a very high degree of plane parallelism. The results are in excellent agreement with literature data on LEED pattern and electrical conductivity of the films. The limits of the proposed method are reached, however, when step height is more than threefold interlattice distance, because at such step heights interference phenomena force the secondary maxima to disappear.

NEW APPLICATION OF ESCA (XPS)

by

C. K. T. Wu, G. G. Peterson, W. J. LaRocca and E. M. Butler

Gould Inc., Gould Laboratories
40 Gould Center
Rolling Meadows, Illinois 60008

The effects of surface roughness on Auger Electron Spectroscopy (AES) and Electron Spectroscopy for Chemical Analysis (ESCA or XPS) have been a problem in surface analysis. In the present paper, the quantitative relationship between surface area and ESCA signal intensity was studied using a variety of electrodeposited foils. The foil surfaces studied here can be classified into two categories: Type A is cone-shaped (diameter: ~ 5μ, height: ~ 5μ) and Type B is cone-shaped with small nodules (diameter: ~1μ) on the surface. The morphology of the foils was studied by Scanning Electron Microscopy. The surface area was measured by the Brunauer, Emett and Teller (BET) gas adsorption technique and light scattering experiments. The ESCA signal intensities of the foils were studied before and after gold deposition. The results indicate that there is a strong correlation between surface area data and ESCA signal intensities, for both Type A and Type B foils. Thus, it is concluded that ESCA can be used to obtain not only surface chemical information but also physical information such as relative surface area.

TYPE A x1000

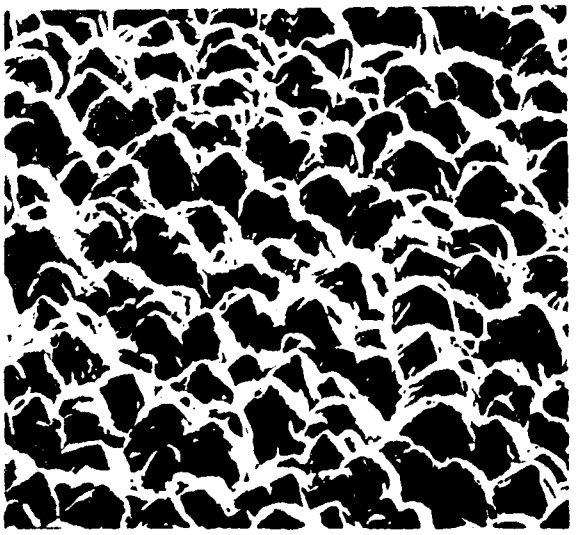

TYPE B x1000

Characterization of [001] Tilt Boundaries in Bicrystalline Thin Films of Gold by High-Resolution Transmittion Electron Microscopy

F. Cosandey and C. L. Bauer

Department of Metallurgy & Materials Science
Carnegie-Mellon University
Pittsburgh, PA 15213 USA

Selected [001] tilt boundaries in bicrystalline thin films of gold, corresponding to angles of misorientation ranging from 5 to 39°, have been examined by high-resolution transmission electron microscopy in order to characterize concomitant structure of low-angle, high-angle, and coincidence grain boundaries. These films are produced by vapor deposition and subsequent epitaxial growth on bicrystalline substrates of NaCl so that exact misorientation of the grains and essential characteristics of the grain boundary, such as preferred inclination and dislocation misfit structure, are transmitted from the underlying substrate to the bicrystalline film. The high degree of perfection of the resultant boundaries, uniform and controlled thickness of the films, and optimum inclination of the boundary plane for lattice-fringe imaging make these films ideally suited for systematic investigation of grain-boundary structure by high-resolution transmission electron microscopy.

Both bright-field and lattice-fringe images reveal that [001] tilt boundaries in gold are characterized by a regular array of primary relaxations and a more widely spaced array of secondary relaxations. Excellent agreement between experimental results and the O-lattice theory indicates that primary relaxations in the boundary occur between points of the O lattice in a periodic manner, whereas satisfactory agreement between results and the DSC-lattice theory indicates that secondary relaxations in the boundary are associated with secondary dislocations, which accommodate small deviations from exact coincidence orientations. These results represent the first time that both primary and secondary relaxations have been observed concurrently near coincidence orientations and, therefore, help to further elucidate the atomic (dislocation) structure of special grain boundaries.

Low Loss Surface Imaging Studies of Thin Film Growth

D.A. Smith and M.M.J. Treacy
IBM T.J. Watson Research Center
Yorktown Heights, N.Y. 10598

Conventional transmission electron microscopy (CTEM) has provided extensive data concerning the nucleation and growth of thin films. However, it is usually difficult to deduce much information about surface topography of thin films from electron micrographs. Such knowledge is relevant to a full understanding of island growth, island coalescence and the origin of defects in thin films. The scanning transmission electron microscope (STEM) has the advantage over the CTEM in that it may be operated either in its usual mode, to provide transmission images from thin films, or from tilted samples to provide "low-loss" surface images. By employing a modified specimen support in conjunction with a high tilt cartridge, this versatility can be exploited to allow comparison of transmission and surface images from the same region in thin films.[1] Here we report on the use of this surface sensitive low loss technique, as well as conventional scanning electron microscopy, to study the topography of thin films, mainly of copper, silver and gold, at successive stages of growth and after heat treatment.

(1) M.M.J. Treacy, W. Krakow, D.A. Smith and G. Trafas, to be published in Appl. Phys. Letts.

INVESTIGATION OF MORPHOLOGY OF SURFACES USING THE METHOD OF DEFOCUSED ELECTRON MICROSCOPY IMAGES

by S.K.Maksimov, V.D.Verner, G.N.Gaidukov,
V.L.Yegorov, N.I.Maisuradze, A.P.Filippov
Institute of Electronic Technology, Moscow, USSR

The ultimate possibilities of electron microscopy in detecting small surface relief defects via the method defocused micrographs has been studied experimentally and by means of a computer modelling of micrographs. Calculation were carried out in the framework of the column approximation, for the two-beam case, using the Howie-Whelan equation for the model of elastically conjugated defects.

The phase variations are due to the different length of scattering column and the displacements because of the misfit in the defect-substrate system. Displacement components were found to be equal to:

$$4\pi G U_1 = -M_0\left\{-\frac{x_1}{R^3} + (1-2\nu)\left[\frac{2x_1}{(R+x_3)^3} - \frac{2x_1+x_3}{R(R+x_3)^2}\right]\right\}$$

$$4\pi G U_2 = -M_0\left\{-\frac{x_2}{R^3} + (1-2\nu)\left[\frac{2x_2}{(R+x_3)^3} - \frac{2x_2+x_3}{R(R+x_3)^2}\right]\right\}$$

$$4\pi G U_3 = -M_0\left\{-\frac{x_3}{R^3} + (1-2\nu)\,\frac{x_3}{R(R+x_3)^2}\right\}, \quad R^2 = x_1^2 + x_2^2 + x_3^2$$

where G - is the elasticity of shear; ν , the Poisson coefficient; M_0, a coefficient which depends on: a) the misfit of parameters, b) the defect height, c) the defect area; x_1, x_2, x_3 are coordinates. The model in question corresponds to the type of conjuation with the matrix has been revealed. Irrespective of the model the defocused contrast method enables one to discover surface defects with heights of 10 A. For irregularities with heights of a few dozens of A the method enables an estimation of their height. The actual approach to height estimations depends on the character of the defect-matrix conjugation.

Calculated defocused images for different models and experimental defocused images of defects such as islets and steps are presented.

R e f e r e n c e s

1. Ya.B.Hehoozin, A.S.Dzuba, B.L.Indenbom, N.I.Ovcharenko, Kristallografiya (in Russian), 18, 3, 800, 1973.
2. V.Novitskii, Teoriya Uprugosti (in Russian), Moscow, Mir Publishers, 1975, p. 241.

THE USE OF DEFOCUSED ELECTRON IMAGES IN SEARCH FOR ATOMIC SURFACE RELIEF

By S.K.Maksimov, S.N.Bezryadin, V.D.Verner, V.L.Yegorov, N.I.Maisuradze
Institute of Electronic Technology, Moscow, USSR.

Method of defocused images results in the development of the phase contrast in the electron micrographs which enables one to visualize the surface relief irregularities with heights of the order of a few angströms. In this paper we report on the investigations of the formation regularities of the defocused electron microscopy images with the purpose of optimisation of surface relief investigation methods. The following results were obtained.

1) The rectangular step. The contrast in the image of the rectangular step depends on a) the aperture size of objective lens, b) the amounts of defocusing Δz, c) the on-step phase shift $\Delta\varphi$. The optimal conditions for the maximum contrast in the defocused image are:

$$\Delta z_o \approx d^2/\lambda,\ D_o \approx \lambda f/d,\ K_o \approx \sin(\Delta\varphi) \qquad \ldots (1)$$

where Δz_o is the optimal defocusing; d, the micrograph resolution on points; λ^o, the electron wavelength; D_o, the optimal diaphragm size for the objective lens; f, the focal length of the objective lens.

2) Smooth step. The phase shift approximated as follows:

$(\Delta\varphi_o/\pi)\arctan(x/\Delta x_o)$, where x is the coordinate of the illuminated region along the axis perpendicular to the step front; Δx_o, the effective width of the step. The condition (1) for the objective lens aperture remains the same, whereas the condition for the optimal defocusing is varied:

$$\Delta z_o \approx (12\,\Delta x_o d)/\lambda \qquad \ldots (2)$$

3)Rectangular band. For the band widths exceeding the doubled resolution of micrographs are produced under the optimal observation conditions of the rectangular step (1). For the smaller widths the optimal defocusing is:

$$\Delta z_o \approx (\Delta x_o)^2/1.2\lambda \qquad \ldots (3)$$

In this case the maximum contrast is equal to $K_o \approx 1.5 \sin(\Delta\varphi)$.

4) Periodic system of equal height rectangular bands. At interband spacings exceeding d separate bands are resolved. The optimal conditions for the maximum contrast in the image correspond to those for a single rectangular band (3). For the interband spacings of the order of the resolution Δx_o there develops a periodic system of interference bands with the amount of contrast $K_o \approx 1.5 \sin(\Delta\varphi)$. The magnitude of the period equals the periodicity of bands in the sample. In this case the optimal defocusing is given by (3).

5) Periodic system of equal height steps. At interstep spacings exceeding the microscope resolution 2d the optimal observation conditions are given by (1). In the other cases the optimal conditions are the same as (2) for the smooth step. In this case for Δx_o one should take the total length of the irregularity.

6) Pyramid shaped system of equal height steps. In this case the intensity in the defocused image is identical to that for the case 5 of the periodic system of equal height steps reflected symmetrically in the plane passing through the middle of the top band.

Irrespective of the model the defocused contrast enables a detection of the surface defects with 3 ÷ 5 angströms heights. The maximum sensitivity of the defocused images is realized when the foil thickness is equal to $\xi_g(n + 1/2)$ for the transmitted wave and $n\xi_g$ for the diffracted waves (ξ_g is the extinction distance).

STUDIES OF THE THIN FILMS OF Li-B ALLOYS

Hiroshi KEZUKA and Kokuyo IWAIURA

College of Engineering, Hosei University,
Kajino, Koganei, Tokyo (Japan)

Alloys of lithium-boron are of great interest as anode materials for Li-S batteries. Main purpose is to obtain the compound films of Li-B with stoichiometry near 1:1 and to examine the structure of these films by electron diffraction method. The thin films of Li-B alloys have been prepared on glass substrates in a vacuum of 10^{-6} Torr making use of the reaction of lithium and boron by Sandwich-Type-Evaporation-Method[1]. In this method Li-B films are deposited using $LiBH_4$ and lithium-metal in the order of Li-B from Ta-boat first, Li-B and Li from another Ta-boat second and Li-B last continuously to make a sandwich structure. As the result, it is found from electron diffraction patterns analysis that the Li-B films 1 μm thick deposited at 450°C have interplanar spacings (d=3.37, 2.09 A) which correspond to those of Li_3B_{14} compound[2]. On the other hand, $LiAl_xB_{1-x}$ films have been prepared evaporating Al and (Li-B + Li) at the substrate temperature of 350°C by the Sandwich-Type-Evaporation-Method. In the case of $LiAl_xB_{1-x}$ ($x \geq 0.5$) films, the electron diffraction patterns are in agreement with A(h) sets of NaCl-type LiAl compound; (111), (200), (220), (311) and (400) planes are appeared.

1) H. Kezuka and K. Iwaiura, Thin Solid Films 29 (1975) No1, 11
2) Dalle[illegible] et al., J. Electrochem. Soc.: SOLID-STATE SCIENCE AND TECHNOLOGY, [illegible] (1[illegible])

INVESTIGATION OF GROWTH SURFACE AND FINE STRUCTURE OF C.V.D. W-Re-FILMS

G.M.Demyashev, Yu.V.Lakhotkin, A.I.Krasovsky, R.K.Chuzhko
Institute of Physical Chemistry Academy of Sciences of the USSR,
II7071, Moscow, USSR

In our work electron microscopy [1] investigations of the morphology of the growth surface and dislocation structure of films W-Re alloy, obtained by reducing unter vacuum from mixture of hexafluorides with hydrogen [2] : $(WF_6+ReF_6)+H_2 \rightarrow (W\text{-}Re)+HF$ are carrud ont. The deposition of the films is under about ~2kPa total pressure of the reactants initial molar ratio is $H_2/(WF_6 + ReF_6) = 14$ and temperature is about ~700°C.

The W-Re alloy is a α-solid solution Re (up to 9%) in W with an intrinsic growth texture [001], the degree of grain orientation of which is about 80%. Typical forms produced on the film surface are tetrahedral growth pyramids.

There are also such morphological peculiarities of the growth surface which can be explained by elementary processes of crystallization. Grains of [001], [011], [111] orientation are studied in the textured W-Re films. On the basis of the results obtained the grains [001] can be classified into three types. Type I - grains having dislocation density (ρ) of about $10^9 cm^{-2}$ in which mixed dislocations with Burgers vectors $\bar{b}=a/2\langle 111\rangle$ and $\bar{b}=a\langle 100\rangle$ are uniformly distributed. Type II - grains with ρ of about $10^8 cm^{-2}$ in which edge and mixed dislocations are present with $\bar{b}_2 = a/2\langle 111\rangle$. Type III - grains with of about $10^7 cm^{-2}$ in which mixed (occasionally screw) dislocations with $\bar{b} = a\langle 100\rangle$ are mainly distributed. This regularity is probably associated with the non-uniform distribution of he in grains. For ρ of some grains [001] in the centre is I to I,5 order of magnitude as low as that at the boundary, which is also associated with the non-uniform distribution of Re [3] . Grains [111] comprise mainly screw and edge dislocations with $\bar{b} = a/2\langle 111\rangle$ which form low-angle boundaries. Grains [011] comprise mainly edge and mixed dislocations with $\bar{b} = a/2\langle 111\rangle$. In grains [011] and [111] ρ is on average I,5 order of magnitude as high as that in [001] [4], which is due to the growth conditions and crystallization mechanism [5]. The dislocation density of the W-Re alloy is on the average I to I,5 order of magnitude as high as that in W prepared under the same conditions using a similar technique.

Based on the investigation results obtained, the regularities of formation of the growth surface morphology and the fine structure of the C.V.D. W-Re-films, ase discussed in the report.

REFERENCES:

[I] Edington J.W. Practical Electron Microscopy in Materials Science. Vol.I-5. Eindhoven.Macmillan Philips Tech. I974-I977.
[2] Holman W.R. and Huegel F.J. - J.Vac.Sci.Technol., II, (I974)70I.
[3] Holman W.R. and Huegel F.J. - Proceedings of the Conference on Chemical Vapor Deposition of Refr.Metals, Allous and Comp. Ed.by Schaffhauser Gatlinburg,Tennessee,Sep.I2-I4,I967,p.I27.
[4] Demyashev G.M., Chuzhko R.K., Tshalych A.E., Evko E.I. - 6th International Conference on Crystal Growth,Moscau,I0-I6 Sep I980, p.360-363.
[5] Chuzhko R.K., Andreyev Yu.V., Kleyner L.M., Khaldeyev G.V. - Fizika Metallov i Metallovedenie (Russ.), 49, No.3, (I980)579.

STRUCTURE AND SHAPE OF EPITAXIAL METAL CLUSTERS

by

M. José Yacamán, P. Schabes and T. Ocaña
Instituto de Física, U.N.A.M.
Apartado Postal 20-364
México 20, D. F.

The structure of small gold particles produced by evaporation on alkali halide surfaces is studied using ultra-high resolution electron microscopy. During the growth two main types of particles are observed; five-fold (icosahedral and decahedral) and regular fcc structures. Ultra-high resolution projected potential images of icosahedral particles are obtained. The images show that the interatomic distance along a radial direction do not change substantially. Particle distorsions predicted by energy calculations based on a pair wise Lennard-Jones potential are not observed. The different shapes of the fcc particles are studied. The shapes found are octahedral, rombic, pyramidal, cubo-octahedral and irregular ones.

The influence of substrate steps on the degree of epitaxy is also studied by the weak beam dark field method. It is found that for KCl substrates the particles nucleated along the steps are in average of the same type that those in the terraces. However in the stage in which coalescence starts the nuclei produced on the steps tend to be icosahedral, while those in the terraces are mainly regular fcc. That effect seems to be related to changes on the diffusivity along the steps.

Monday afternoon, June 8, 1981

Session M-B: Chemisorption

(Room 1105)

Chairman: T. L. EINSTEIN

1:40 Direct Calculation of Experimentally Measurable Chemisorptive Parameters from Theoretical Quantum Chemical Cluster Models. M. E. SCHWARTZ

2:00 Copper Atoms and Cluster Isolated in Oxygen Matrices. D. SCHMEISSER, K. JACOBI and D. M. KOLB

2:20 Physisorption and Chemisorption of Oxygen on Tin at Low Temperature. G. S. CHOTTINER, R. E. GLOVER, III and R. L. PARK

2:40 A Study of Oxygen Adsorption on Ti(001) Using Photon Stimulated Desorption. D. M. HANSON, R. STOCKBAUER and T. E. MADEY

3:00 Oxygen Chemisorbed on Ti(0001). B. T. JONKER, J. F. MORAR and R. L. PARK

3:20 Comparison of the Interaction of CO with Mo(001) and Ni(001). R. V. KASOWSKI

3:40 The Structure of CO on Ni(111). F. P. NETZER and T. E. MADEY

4:00 Thermal Desorption of CO, O_2 and CH_4 Molecules from Ni(111) Single Crystals. G. A. SARGENT, J. CHAO and G. B. FREEMAN

4:20 A Study of Nitric Oxide Adsorption on Copper (100) and (110). J. F. WENDELKEN

4:40 High-Resolution Angle-Resolved Photoemission Studies of the Interaction between Atomic Chlorine and Cu(001) and Cu(111) Surfaces. A. GOLDMANN and D. WESTPHAL

5:00 Ammonia on Iridium (111): Adsorption Kinetics and Band Structure. R. J. PURTELL, R. P. MERRILL, T. HUGHBANKS, R. HOFFMANN, S. B. CHRISTMAN and T. N. RHODIN

5:20 Pulsed Laser Atom-Probe Study of Clean and Oxygen Covered Silicon. G. K. KELLOGG

Direct Calculation of Experimentally Measurable Chemisorptive Parameters from Theoretical Quantum Chemical Cluster Models

Maurice E. Schwartz
Department of Chemistry
St. Patrick's College,
National University of Ireland
Maynooth Co. Kildare
Ireland

and

Department of Chemistry* and
Radiation Laboratory
University of Notre Dame
Notre Dame, Indiana 46556
USA

Experimental techniques can now provide direct information about interatomic distances (from extended x-ray absorption fine structure measurements), vibrational frequencies (from electron energy loss spectroscopy), and core-electron binding energies (from x-ray photoelectron spectroscopy) for atoms and molecules chemisorbed on surfaces. This means that direct, explicit predictions from cluster calculations can now be reliably tested. We have been developing and applying a valence-only electronic structure theory, based on model-potential representations of the core electrons, which allow for accurate molecular orbital calculation of energy vs geometry, and therefore for both bond-length and vibrational frequency calculations. By putting in a real, all-electron atom for any particular atom whose core electrons are of interest, we can also calculate directly and accurately core electron binding energies. This overall approach is to be contrasted, for example, to the scattered-wave X_α molecular orbital scheme which has often been applied in cluster problems, but whose inability to calculate reliable total energy/geometry data means that its utility rests on rather indirect comparison with experiment, e.g., in density of state inferences. As one example of our work, the chemisorbed O atom on the (111) face of Aℓ has been modeled by small clusters, of which the minimal model is $OAℓ_3$. We predict an O-Aℓ distance of 1.81A° (experiment: 1.79 ± 0.05A°), an O 1s binding energy of 531.7 eV (experiment 531.3 ± 0.2 eV), and an O-Aℓ surface vibrational frequency of about 394 cm^{-1} (≡49 meV, experiment not known). Other studies of NO and $Aℓ_n$, and of O on Zn_n will be discussed in connection with experimental data and other theoretical considerations.

*Permanent address.

COPPER ATOMS AND CLUSTER ISOLATED IN OXYGEN MATRICES

D. SCHMEISSER, K. JACOBI and D. M. KOLB
Fritz-Haber Institut der Max-Planck Gesellschaft,
Faradayweg 4-6, D-1000 BERLIN 33, Germany

UV photoemission studies have been performed on Cu atoms and Cu clusters isolated in oxygen matrices. The experiments were performed in an UHV system equipped with a He resonance lamp and a double pass cylindrical mirror analyzer. The matrices were prepared by cocondensing Cu and oxygen onto a gallium film as substrate. Ga films have been prepared by evaporation on a metal rod, which could be cooled down to 7K by liquid helium.

Photoelectron spectroscopy of metal particles isolated in reactive matrices offers a new possibility to study chemisorption systems. By controlled warming up the matrices the physisorbed matrix gas desorbs leaving the clusters within chemisorbed molecules. Due to the higher number of chemisorption sites of such clusters compared to surfaces large signals have been found for the chemisorbed molecules.

Here we show that there is no observable chemical interaction between copper atoms and the oxygen matrix at 7K. An additional shift in the ionization potentials due to different relaxation mechanismns in the final state is obtained by comparing to recent data of condensed oxygen as well as to data of copper atoms and clusters isolated in rare gas matrices. By warming to room temperature two different chemisorption states of oxygen can be destinquished. Between 40K and 100K molecular chemisorbed oxygen is observed in accordance with the data found on polycristalline Cu and Ga surfaces. Above 200K molecular and dissoziated oxygen coexist, while at room temperature only atomic oxygen remains. The size of the Cu clusters causes only small differences in the emission patterns of oxygen in its different chemisorption states.

PHYSISORPTION AND CHEMISORPTION OF OXYGEN ON TIN AT LOW TEMPERATURE*

G. S. Chottiner,+ R. E. Glover, III, and Robert L. Park
University of Maryland, College Park, Md. 20740 U.S.A.

Controlled amounts of oxygen gas from a source whose temperature can be varied between 100 K and 500 K are condensed on clean, annealed tin films being held at 5 K. Changes caused by the presence of oxygen are followed by means of measurements of the electrical resistance of the films, which are on the order of 200 Å thick.[1] Initial condensation causes a very small increase in resistance after which the resistance remains constant as long as the low temperature is maintained. The small size of this effect rules out the possibility that appreciable numbers of conduction electrons are localized in chemical bonds and, together with other evidence, suggests that oxygen is adsorbed in a molecular form. When the oxygen coated tin films are heated an irreversible increase in resistance is observed starting at about 13 K. This is believed to be associated with the transition from the physisorbed to the chemisorbed state of oxygen. At a given stage in the reaction the rate is found to increase rapidly with the temperature while at a fixed temperature the rate decreases as the reaction progresses and molecular oxygen is consumed. Measurements of the rate as a function of temperature lead to activation energies on the order of 40 meV for submonolayer coverages of oxygen during the initial stage of the reaction. The activation energy increases if the initial coverage of molecular oxygen is increased and also increases as the reaction of the molecular oxygen progresses. The latter effect has been observed with silver, lead, and nickel in addition to tin films. These results can be interpreted in terms of interaction between the adsorbed oxygen molecules. The conduction decrease caused by chemisorption of a single oxygen molecule has been estimated from the resistance increase caused by complete reaction of a known initial coverage of O_2. The result is used to find the absolute number of molecules reacting per time. The "attempt frequency" determined in this way is on the order of 10^7 sec^{-1} for the initial stage of the reaction. This is much smaller than typical phonon frequencies and suggests that special conditions, perhaps a particular orientation or location, have to be met before the transition from physisorbed to chemisorbed oxygen can take place.

*Supported in part by the Department of Energy.

+Present address: Case Western Reserve University, Cleveland, Ohio, 44106, U.S.A.

[1]Experiments of this type were pioneered by W. Ruhl, Z. Physik 176, 409 (1963). See also G. Chottiner and R. E. Glover, III, J. Vac. Sci. & Tech. 15, 429 (1978).

A Study of Oxygen Adsorption on Ti(001) Using Photon Stimulated Desorption

David M. Hanson*, Roger Stockbauer
and
Theodore E. Madey
Surface Science Division
National Bureau of Standards
Washington, D.C. 20234

Synchrotron radiation at the NBS SURF II facility (25 eV<hν<75eV) has been employed to study the adsorption of oxygen and coadsorption of hydrogen plus oxygen on a Ti(001) surface, using photon stimulated desorption (PSD), electron stimulated desorption (ESD), and ultraviolet photoemission spectroscopy (UPS). A cylindrical mirror analyzer was used for both ion and electron energy analysis. The ESD and PSD products observed for oxygen exposures > 1 Langmuir are O^+ ions having a most probable kinetic energy of ∿ 3 eV. The photon energy dependence of the PSD ion yield is in good agreement with the major features of the constant-final-state secondary electron yield although there are some differences in detail. This demonstrates that the O^+ desorption is associated with the production of a Ti 3p core hole, consistent with the Knotek-Feibelman Auger decay mechanism. The dependence of O^+ ion yield on oxygen coverage and surface temperature is compared with UPS and work function measurements. These data indicate that surface oxidation occurs at temperatures as low as 100 K, and that at least a fraction of the surface oxide is electronically similar to the maximal valence compound TiO_2.

The PSD ion yield observed following coadsorption of hydrogen and oxygen on Ti(001) is found to be sensitive to surface impurities.

*Institute of Physical Science and Technology, University of Maryland. NBS SURF Fellow 1980-1981. Permanent address: Department of Chemistry, State University of New York, Stony Brook, New York 11790

OXYGEN CHEMISORBED ON Ti(0001)*

B. T. Jonker, J. F. Morar and Robert L. Park
Department of Physics and Astronomy
University of Maryland
College Park, Maryland 20742

The system O_2 on Ti(0001) has been investigated using appearance potential spectroscopy (APS), Auger electron spectroscopy (AES), low energy electron diffraction (LEED), and work function measurements obtained by the field emission retarding potential (FERP) technique. As a probe of the unfilled density of states, APS was used to investigate the behavior of the unfilled portion of a band of surface states previously observed on polycrystalline samples[1] and more recently predicted for the (0001) surface to occur at the Fermi level and to extend a few tenths of an eV on either side of it.[2] These states were suppressed upon exposure to oxygen and either broadened or shifted below the Fermi level with increasing temperature. The work function steadily increased with oxygen exposure from a clean surface value of 4.58 ± 0.05 eV, leveling off at approximately 5.3 eV as the surface became saturated with oxygen. The initially diffuse low coverage p(2x2) LEED superstructure formed upon exposure at room temperature was significantly improved upon flashing the sample to 250° C. This was accompanied by an abrupt decrease of 0.15 eV in the work function, though AES revealed no decrease in the amount of oxygen on the surface. The LEED observations and measurements of the oxyge AES signal vs exposure enabled a rough estimate of absolute coverage to be obtained.

[1] Y. Fukuda, W. T. Elam, and Robert L. Park, Surface Sci. 1, 278 (1978).

[2] P. J. Feibelman, J. A. Appelbaum and D. R. Hamann, Phys. Rev. B20, 1433 (1979).

*This work was supported by the National Science Foundation under Grant DMR-79-00323.

Comparison of the Interaction of CO With Mo(001) and Ni(001). R. V. KASOWSKI, Central Research and Development Department*, E. I. du Pont de Nemours and Co., Experimental Station, Wilmington, Delaware 19898--The extended muffin tin orbital (EMTO) energy band method has been used to perform the first ab initio self-consistent calculation of the electronic structure of a) CO on Mo(001) in a c(1x1) array and b) CO on Ni(001) in a c(2x2) array. A local density potential with alpha equal to 0.7 is used. For both calculations, the CO 4σ state gives rise to one peak in the density of states (DOS), while the CO 5σ and 1π states overlap to yield a second peak. The peak in the DOS due to overlapping 1π and 5σ is at -7.6 ev (relative to E_F) for Ni and -7.3 ev for Mo. The 4σ peak occurs at -10.4 ev for Mo and -12.1 ev for Ni. Ionization potential (IP) measurements have reported peaks at -7.8 ev and -10.8 ev for Ni and -7.6 and a broad tail for Mo. Our Ni DOS agrees with experiment provided that the very localized CO 4σ electrons undergo a final state relaxation of approximately 1.5 ev. The 1π and 5σ electrons interact strongly with the Ni electrons and need not undergo such a strong final state relaxation. Similar arguments have previously been proposed by Shirley, et. al.[1].

Finally, we will show that the CO molecular levels mix strongly with the Mo levels resulting in strong back-bonding. Approximately 0.5 electrons are tied up in back bonds. For CO on Ni, the back-bonding is very weak in comparison. Thus, arguments will be presented as to how the strong back-bonding leads to association of CO on Mo but not on Ni.

1) D. A. Shirley, J. Vacuum Sci. Technol. 12 (1979) 280.

*Contribution No. 4060

THE STRUCTURE OF CO ON Ni(111)

Falko P. Netzer* and Theodore E. Madey
Surface Science Division
National Bureau of Standards
Washington, DC 20234

We have used electron stimulated desorption ion angular distributions (ESDIAD), low energy electron diffraction (LEED), and temperature programmed desorption (TPD) to study the adsorption of CO on Ni(111), at temperatures as low as 80 K. The LEED data are consistent with published work.[1] For low coverages, the CO layer is disordered; a c(4x2) pattern appears at coverages $\theta \sim 0.5$ (the maximum coverage at 300 K). At lower temperatures, the CO coverage increases to a saturation value of $\theta \simeq 0.57$, and a well-defined ($\sqrt{7}$ x $\sqrt{7}$)R19° LEED pattern forms. From TPD, only one binding state is seen (peak temperature of 450 K) for $\theta \lesssim 0.45$; species having lower desorption temperatures populate at higher coverages. Upon adsorption at 300 K, the only ESD ion observed is O^+, with desorption centered about the direction perpendicular to the surface. At high coverages at 80 K, CO^+ is also observed. The ESDIAD patterns for saturation coverage in the range 80-260 K indicate off-normal ion emission in addition to the normal component.

These ESD/ESDIAD data suggest that for $\theta \lesssim 0.5$, CO is adsorbed in bridging sites with the molecular axis perpendicular to the surface. At the higher coverages achievable below $\sim$ 300 K, CO can adsorb in non-bridging sites as well, and a fraction of the adsorbed CO molecules have their molecular axes randomly tilted with respect to the surface normal. Upon heating the CO layer formed at 80 K ($\theta \simeq 0.57$), the CO^+ ion yield maximizes at $\sim$ 240 K when the ($\sqrt{7}$ x $\sqrt{7}$)R19° LEED pattern is well-defined. The CO^+ yield therefore reflects the ordering behavior in the adsorbate layer at temperatures below the onset of desorption and indicates a shift of a fraction of CO molecules from bridging to non-bridging sites, in agreement with electron energy loss spectroscopy (EELS) data.[1]

(1) W. Erley, H. Wagner and H. Ibach, Surface Science 80, 612 (1979).

* Guest Worker, NBS and Visiting Associate Professor of Physics, University of Maryland. Permanent address: University of Innsbruck, Austria

THERMAL DESORPTION OF CO, O_2 and CH_4 MOLECULES FROM Ni(111) SINGLE CRYSTALS

by

Gordon A. Sargent, J. Chao and G. B. Freeman, Department of Metallurgical Engineering and Materials Science and the Institute for Mining and Minerals Research, University of Kentucky, Lexington, KY 40506

Abstract

The thermal desorption of CO, O_2 and CH_4 molecules from a Ni(111) single crystal surface has been studied using the techniques of Low Energy Electron Diffraction (LEED), Auger Electron Spectroscopy (AES) and Mass Spectroscopy. The surface of the nickel crystal was exposed to the above gases at pressures from 10^{-9} to 10^{-5} torr. at room temperature and at 100°C. Surface structures and bonding were studied by the above techniques. The absolute coverage of the molecules on the surface was measured for the above experimental conditions and activation energies for thermal desorption were measured for each molecule.

A STUDY OF NITRIC OXIDE ADSORPTION ON COPPER (100) AND (110)*

J. F. Wendelken
Solid State Division, Oak Ridge National Laboratory
Oak Ridge, Tennessee 37830

ABSTRACT

The adsorption of nitric oxide on single crystal copper (100) and (110) surfaces has been studied with the techniques of electron energy loss vibrational spectroscopy, low energy electron diffraction and thermal desorption spectroscopy. In the case of Cu(110), molecular adsorption of NO is confirmed by vibrational spectroscopy to occur with a crystal temperature of 80 K for very low exposures. For exposures exceeding 1.2 Langmuirs, dissociation occurs with the vibrational spectra indicating atomic oxygen retained on the surface and located at the long bridge site. Comparison of low energy electron diffraction patterns with those obtained by exposure to oxygen alone indicates that atomic nitrogen also remains on the surface following dissociation. Vibrational frequencies obtained using two isotopic forms of NO, ^{14}NO and ^{15}NO, are assigned to the stretching and bending modes of NO and indicate a molecule strongly tilted relative to the surface normal in a predissociation state. Dissociation occurs at temperatures above 113 K with the atomic species again retained on the surface. Adsorption of nitric oxide on Cu(100) was found to be more complicated. A published XPS study reports the observation of a disproportionation reaction in which $2(NO) \rightarrow N_2O + O$ at 85 K with the N_2O desorbing at a temperature of 110 K.[1] In the present study, vibrational spectra indicate a change in molecular species between low exposure ($\sim$ 1 Langmuir) and high exposure ($\sim$ 10 Langmuir) cases for T < 100 K. Depending on exposure and temperature, evidence is found for the presence of NO, N_2O, N_2 and O. In contrast to adsorption of NO on Cu(110), a large fraction of the NO dissociates upon initial exposure with Cu(100). All species containing nitrogen are found to desorb below room temperature with desorption of N_2 and N_2O occurring below 150 K. The presence of N_2O is thus confirmed but is shown not to be the only molecular species present.

1) D. W. Johnson, M. H. Matloob, and M. W. Roberts, J. C. S. Chem. Comm., 40 (1978).

*Research sponsored by the Division of Materials Sciences, U. S. Department of Energy, under Contract W-7405-eng-26 with Union Carbide Corporation.

High-resolution angle-resolved photoemission studies of the interaction between atomic Chlorine and Cu(001) and Cu(111) surfaces

A. Goldmann and D. Westphal

Laboratorium für Festkörperphysik, Universität - GH - Duisburg

D-4100 Duisburg, Germany

We have studied photoemission from an ordered c(2x2) Cl-overlayer on Cu(001) at good angular ($\Delta\theta < 1^{o}$) and energy (ΔE =100 meV)resolution. Normal emission spectra taken at photon energies $\hbar\omega$ = 17, 21, 27 and 41 eV exhibit the angular momentum character of adsorption-induced structures at 1.95 eV (FWHM = 100 meV), 3.45 eV and 5.4 eV. Using linearly polarized light we deduced their spatial orientation. Their energy dispersion is mapped out along $\bar{\Gamma}\bar{X}$ and $\bar{\Gamma}\bar{M}$ of the surface Brillonin Zone. From the change in work function upon adsorption and assuming fourfold hollow positions, we derive a charge transfer to chlorine of about 0.1 e_{o}. Our model thus requires empty Cl-states, some of which we observed in the angular resolved secondary electron spectra. The results are discussed in the context of recent theoretical work.

Significant modification of Cu d-band emission is observed upon Cl adsorption, which makes the concept of "difference spectra" very questionable. We have studied in some detail the coverage dependence of changes in d-band features at normal emission from Cu(001) and Cu(111). Both adsorbate and substrate states are strongly dependent on Cl coverage. These results will be discussed, in connection with off-normal emission data, using a model of Cl-Cl interaction through the subtrate.

Spectra taken from chlorine-covered surfaces show features originating from Cu bulk transitions, which are not observed on clean Cu due to symmetry constraints. This observation may be important when using polarization selection rules and will be discussed.

Ammonia on Iridium (111): Adsorption Kinetics and Band Structure

Robert J. Purtell*
Department of Chemical Engineering
University of California, Berkeley, Ca. 94720

Robert P. Merrill
School of Chemical Engineering
Cornell University, Ithaca, N. Y. 14850

Tim Hughbanks and Roald Hoffmann
Department of Chemistry
Cornell University, Ithaca, N.Y. 14850

Stan B. Christman
Bell Labs, Murray Hill, N.J. 07974

Thor N. Rhodin
Dept. of Eng. and Appl. Phys.
Cornell University, Ithaca, N. Y., 14850

The adsorption kinetics and coverage for ammonia on iridium (111) have been measured as a function of sample temperature. The sticking coefficient vs. coverage was obtained by monitoring the reflectivity of a calibrated ammonia beam from an iridium surface as a function of dose time. Ammonia is seen to adsorb via a Langmuir adsorption isotherm with a precursor state.

LEED measurements with nanoamp beam currents show second-order spots due to an ammonia overlayer which could be due to a (2x2) sturcture or three domains of a (2x1) overlayer. Evidence is seen for an order-disorder transition at lower coverages. Angle resolved photoemission measurements on a (2x1) domain are analysed in terms of pi and sigma overlap between neighboring molecules.

Angle resolved photoemission work was done at the Tantalus 1 storage ring at the Univ. of Wisc. Synchrotron Radiation Center. LEED work was done at Bell Labs, Murray Hill, N.J.. Band structure calculations were done at Cornell University.

*. Present address: IBM Thomas Watson Research Center, Yorktown Hts., N. Y. 10598

Pulsed Laser Atom-Probe Study of Clean and Oxygen Covered Silicon*

G. L. Kellogg
Sandia National Laboratories†
Albuquerque, New Mexico 87185

The chemisorption of oxygen on clean silicon surfaces has been investigated using the recently developed Pulsed Laser-Atom-Probe[1] (PLAP). In this technique, surface atoms are removed as positive ions by applying a short duration laser pulse to a field emitter sample subjected to a high electric field. The chemical identities of the desorbed ions are determined by time of flight mass spectroscopy. This method of ion production eliminates the high voltage electrical pulses used in conventional time of flight-atom-probes and thus permits surface analysis of high resistivity materials previously unaccessable to these techniques. In the present study the PLAP technique was used to analyze surfaces of silicon, both clean and exposed to oxygen. The primary objective was to identify the adsorption state (i.e., molecular or atomic) of the oxygen. Mass spectra of clean silicon surfaces contained various Si species which changed with changing desorption conditions. At relatively high fields (approaching the dc evaporation field) and low laser power Si^{2+} and Si^{+} were the predominant species. As the field was lowered and the laser power increased, silicon clusters (Si_x^+ with $x = 2,3$, and 4 were also detected. After oxygen exposure (low temperature dosing followed by heating to room temperature), mass 32 was detected, but not mass 16. This indicates that the oxygen adsorbed in molecular form. Analysis of samples exposed under varying degrees of temperature and dosage level are currently in progress and should provide useful information for the development of realistic models of silicon oxidation.

*This work was supported by the U. S. Department of Energy under contract DE-AC04-76-DP00789.

†A U. S. Department of Energy facility.

[1]G. L. Kellogg and T. T. Tsong, J. Appl. Phys. 51, 1184 (1981).

Monday afternoon, June 8, 1981

Session M-C: Ion Beams and Sputtering

(Room 1123)

Chairman: W. N. UNERTL

1:40 The Sputtering of Molecular Ions from Surfaces in Secondary Ion Mass Spectrometry. M. L. YU

2:00 Resonant Ionization of Short-Lived Neutral Molecules as a Mechanism for Sputtered Molecular Ion Creation. K. J. SNOWDON, W. HEILAND and E. TAGLAUER

2:20 Mechanism of Ejection of F^+ from LiF Surfaces by Ion Neutralization. J. A. SCHULTZ, P. T. MURRAY, R. KUMAR and J. W. RABALAIS

2:40 Transmission Electron Microscope Study of Ion Beam Induced Interfacial Reactions in Molybdenum Thin Films on Silicon. L. J. CHEN, L. S. HUNG and J. W. MAYER

3:00 Anodization and Rutherford Backscattering Measurements of Superimposed Metal Film - GaAs Structures. J. D. CANADAY and C. W. FISCHER

3:20 Surface Pre-Treatment Dependent Formation of Molybdenum Nitride by Low Energy N_2^+ Bombardment. N. SHAMIR, D. A. BALDWIN and J. W. RABALAIS

3:40 Molybdenum Nitride Film Growth under N_2^+ and N^+ Impact on a Molybdenum Surface: Energy and Dose Dependence. D. A. BALDWIN, N. SHAMIR and J. W. RABALAIS

4:00 Formation of N-Layers in Silicon Bombarded by Low-Energy Oxygen Ions. V. A. LABUNOV and V. E. BORISENKO

4:20 Dynamic Simulation of Changes in Near Surface Composition during Ion Bombardment. M. L. ROUSH, T. D. ANDREADIS, F. DAVARYA and O. F. GOKTEPE

4:40 Stainless-Steel Oxidation Investigation, Using Nuclear Techniques for Surface Studies, with an Automated Scanning Proton Microbeam: Experimental System and Results. J. M. CALVERT and L. F. REQUICHA FERREIRA

5:00 Sputtering Yield Calculations for Light Ions Incident on Wall in Tokamak. T.-W. XU, Z.-T. FAN and Q.-C. HE

The Sputtering of Molecular Ions from Surfaces in Secondary Ion Mass Spectrometry

Ming L. Yu
IBM T. J. Watson Research Center
Yorktown Heights, NY 10598

It is well known that secondary ion mass spectrometry offers the opportunity for direct identification of molecular species on surfaces[1]. However, the formation mechanisms of molecular species are still a subject of debate. There are two proposed models of molecular sputtering. The fragmentation model[1] assumes that the molecular species are emitted as complete fragments of the surface lattice. The recombination model[2] assumes that only atomic species are emitted and molecules are formed through the attractive interaction between the neighboring sputtered atoms during the same sputtering event. From the present experiment, we find that, firstly, both emission mechanisms can exist simultaneously on the same target surface, and, secondly, the emission mechanisms can be different for different charge states of a sputtered molecular species.

We have studied the emission of oxide ions from Ti and Nb surfaces, with 1 to 10 Langmuirs of oxygen exposure, during static mode 500 eV Ar^+ or Ne^+ bombardment in an ultrahigh vacuum system. The key idea of this experiment is that, if these oxide ions are emitted by the recombination process, their ionization probabilities (α) should show a predictable correlation with those of O and the metal atoms. In this experiment, the changes in α were achieved by the deposition of submonolayers of Cs or Li on the sample surfaces. We observed the following:

A) At low oxygen coverages, the emission of TiO^+, TiO_2^+, TiO_3^+, NbO^+, and NbO_2^+ all follow the predictions of the recombination model. However, higher oxygen coverages were observed to promote the formation of oxide ions by fragmentation. This occurs first with the dimers TiO^+ and NbO^+. The emission of Nb_2^+ deviates from the recombination model at all oxygen coverages investigated.

B) All the negative ions studied: TiO^-, TiO_2^-, TiO_3^-, NbO^-, NbO_2^-, and NbO_3^- failed to comply with the predictions of the recombination model. Instead, at all oxygen coverages used, these ion yields vary exponentially with the change of work function $\Delta\phi$ resulting from the deposition of Li and Cs:

$$Y^- \propto \exp(-\Delta\phi/\epsilon_0)$$

with different values of ϵ_0 for different ion species. This behavior is similar to that for negative atomic ions[3] and suggests the formation of such molecular ions by fragmentation. This phenomenon holds even at the lower oxygen coverages where the positive counterparts are formed by the recombination of atomic species.

(1) A. Benninghoven, SIMS II, Springer Series in Chemical Physics **9**, 116 (1979).

(2) B. J. Garrison, N. Winograd, and D. E. Harrison, Jr., Phys. Rev. **B18**, 6000 (1978).

(3) M. L. Yu, Phys. Rev. Lett. **40**, 574 (1978).

Resonant Ionization of Short-Lived Neutral Molecules as a Mechanism for Sputtered Molecular Ion Creation

K. J. Snowdon and W. Heiland

Fachbereich Physik, Universität Osnabrück, Osnabrück F.R.G.

E. Taglauer

Max-Planck-Institut für Plasmaphysik, Garching F.R.G.

Studies of the electronic, rotational, vibrational and translational energies of N_2^+ ions sputtered from nitrogen implanted Si have recently led to the identification of a new mechanism for molecular ion formation (two-body associative ionization with diabatic curve crossing[1]). The mechanism invokes formation of the corresponding neutral via inverse predissociation, followed by the Franck-Condon ionization of this unstable intermediate. The electron tunnels either to a vacant state in the solid, or to the vacuum continuum, depending on its energy with respect to the neutral molecule first ionization limit.

Emission spectra (optical and infrared) and translational kinetic energies and angular distributions of sputtered molecular ions created via this mechanism are calculable for species whose potential energy curves and predissociation behaviour are known. Examples discussed in detail in this paper are N_2^+ and CO^+. The possibility that the broad band spectra emitted during the sputtering of many heavy metals could arise from the recombination of a neutral metal atom with an O^- ion, followed by its ionization and subsequent deexcitation following formally the same mechanism outlined above, is discussed.

1. K.J. Snowdon, W. Heiland, E. Taglauer: Phys.Rev.Lett. 46 (1981) 284.

MECHANISM OF EJECTION OF F^+ FROM LiF SURFACES BY ION NEUTRALIZATION. J. A. Schultz, P. T. Murray, Ranjit Kumar, and J. W. Rabalais, Dept. of Chemistry, University of Houston, Houston TX 77004.

The total sputtering yield of positive secondary ions from LiF bombarded with "inert" gas ions is known to be dependent on electronic structure effects at beam energies between 200 and 2,000 eV[1]. In our work we examine the yields of F^+ and Li^+ ions for their dependence on both the potential energy (PE) of the primary ion (He^+, Ne^+, Ar^+, Kr^+, Ar^{+2}, Kr^{+2}) and the kinetic energy (KE) of these ions. The appearance of F^+ is strongly suggestive of an Auger electronic process removing two electrons from F^- within either the solid or a sputtered cluster. In LiF solid this requires about 20 eV. The table below gives PE (approximated by the ionization potential of the neutral inert gas) which are available to the system when a primary ion is neutralized as it approaches the surface. Relative yields of F^+ and Li^+ (arbitrary units) measured at two different primary beam KE are representative of our data.

	~Neutral	Beam 400 eV		Beam 1,400 eV	
Ions	I.P.(eV)	F^+	Li^+	F^+	Li^+
He^+	24	16	u	20	300
Ne^+	21	3	300	27	1,700
Ar^+	16	b	400	3	3,400
Kr^+	14	b	100	1	2,300

[u] unknown
[b] background is ± .2 units

The results are summarized as follows:

1) At beam energies <400 eV the yield of F^+ correlates with the PE contained in the primary ion hole.
2) At beam energies >400 eV the yield of F^+ from the primary ion neutralization starts to be masked by an F^+ yield which depends on the KE of the primary ion. The change in yield with primary energy roughly correlates with the KE tranfered to F-F recoil collisions.
3) The yield of F^+ is not an insignificant portion of the positive secondary ion yield.

The results at low energies are consistent with surface neutralization of the incoming ion, removal of one or two electrons from the solid, and desorption of F^+ by Coulomb repulsion[2]. At higher energies neutralization still occurs; however, recoil of F^+ with F^-, F° with F°, or F^- and F° is postulated to result in electron promotion by collisionally induced curve crossing which further ionizes the material. We speculate that the F^+ comes only from the surface because it is likely to be neutralized before it can escape from the bulk. From the literature on ion bombardment of ionic solids it is apparent that the processes described here are not unique to lithium fluoride.

[1] S. N. Morozov, O. D. Gurich, and T. U. Arifov IAN SSSR 43 (1979) 612 and references therein.
[2] E. S. Parilis, "Atomic Collisions in Solids:, North Holland (1970).

TRANSMISSION ELECTRON MICROSCOPE STUDY OF ION BEAM INDUCED INTERFACIAL REACTIONS IN MOLYBDENUM THIN FILMS ON SILICON

L.J. Chen[†], L.S. Hung[††] and J.W. Mayer
Department of Materials Science and Engineering
Cornell University
Ithaca, NY 14853

Transmission electron microscopy has been applied to study interfacial reactions in molybdenum thin films on silicon. Polycrystalline molybdenum film, 500 Å in thickness and 500-1500 Å in grain size, was chemical vapor deposited on (001) oriented, n-type silicon substrate heated to 650-700°C in hydrogen ambient. The samples were then implanted with 150 keV Ar^+ to fluences $3x10^{15}$ - $1x10^{16}/cm^2$ with the dose rate about $2.4x10^{14}/cm^2$sec. Thin foils for transmission microscope study were prepared by chemical polishing samples from silicon side. The deposited side of the sample was covered with an electronic wax for protection during chemical polishing. Transmission electron microscopy was then performed with a JEOL 100B microscope equipped with a ±60° side entry specimen stage. Hexagonal $MoSi_2$, tetragonal $MoSi_2$ and hexagonal Mo_5Si_3 were found to form mainly along grain boundaries. Similar results were obtained for in-situ annealing of the thin foil at 700°C for two hours in the electron microscope. The observations provide direct evidence of the important role of grain boundary diffusion in the formation of silicides.

† Permanent address: Department of Materials Science and Engineering, National Tsing Hua University, Hsinchu, Taiwan, Republic of China.

†† Permanent address: Institute of Nuclear Research, Shanghi, China.

Anodization and Rutherford Backscattering Measurements of Superimposed Metal Film - GaAs Structures

J.D. Canaday and C.W. Fischer

Physics Department, University of Guelph

Guelph, Ontario, Canada N1G 2W1

This paper reports the growth of composite anodic Nb or V oxide and GaAs oxide films on GaAs and a study of resulting films using Rutherford scattering. The deposited metal films having thicknesses ranging from 10 to 100 n m and a fraction of the underlying GaAs where anodized galvanostatically in an acid-glycol-water electrolyte. The resulting voltage time graphs of the composite anodic metal/GaAs system will be presented and compared with those measured on the elemental V, Nb and GaAs systems. Measurements of oxide thickness versus oxide voltage are used to determine the anodization constant and oxide field. Plots of oxide thickness versus charge will be presented and are used to obtain a measure of the anodic efficiency which is compared with similiar measurements on the elemental V, Nb, and GaAs systems.

Rutherford backscattering measurements using 1.6 MeV He^{+} ions are used to measure the composition and the fraction of the composite oxide formed by oxygen ion transport. To measure the latter quantity we ion implant a Xe^{136} layer into the GaAs substrate. The position of the Xe^{136} layer and its distribution is measured using Rutherford scattering. The fraction of oxide formed by oxygen ion transport is computed from the measured position of the Xe^{136} prior and subsequent to anodization. The results of these measurements are that 84 ± 2% of oxide thickening is due to oxygen transport and the remaining 16% is due to Ga and As transport. This is comparable with the oxygen transport measurements on the pure V and Nb systems where it is found to be 72% and 76% respectively. Oxide composition measurements show that both Ga and As are present at the surface of the composite oxide. This finding is consistent with the statement that both metal and oxygen ions are mobile during oxide growth.

SURFACE PRE-TREATMENT DEPENDENT FORMATION OF MOLYBDENUM NITRIDE BY LOW ENERGY N_2^+ ION BOMBARDMENT. N.Shamir*, D. A. Baldwin, and J. W. Rabalais, Dept. of Chemistry, University of Houston, Houston, TX 77004

Thin layers of molybdenum nitride were formed on a molybdenum sample by the reaction of low energy, mass selected and intensity controled N_2^+ beams with the Mo surface. AES was used for determination of the relative amounts of nitride formed, by measuring the $N(KL_2L_2)$ Auger peak intensity. A family of intensity vs. bombardment dose curves for energies 7.5 - 100 eV was obtained after pre-cleaning of the sample by a series of flashes to ~1,500°C and an equivalent family was obtained after a pre-cleaning by 3 keV Ar^+ ion sputtering.

The two families of curves show the following differences:

1. The "flashed surface" (FS) curves exhibit higher intensity than the "sputtered surface" (SS) curves (except for the 100 eV curve).
2. The FS tends to saturate for high exposure doses before the SS saturates; The saturation level of the SS (which was not reached in this experiment) is apparently higher than for the FS (again with the exception of the 100 eV nitride).
3. The initial slope of the low dose curve is about the same for both the FS and SS.

The differences are explained by the following effects:

1. The layer formed on an SS is thicker than that formed on an FS due to radiation damage enhanced diffusion. Thus, for a pre-saturation dose the N concentration on the upper layers is larger for the FS and hence the stronger AES signal. This assumption is supported by the interpretation of a depth profile for the same energy bombardment formed a layer on both FS and SS.
2. The thicker layer and the rough surface for the SS account for a higher dose needed for saturation of an SS compared to an FS and the higher saturation AES signal level.
3. The higher efficiency of a rougher surface for ion capture is compensated by is higher efficiency for Auger electron capture, thus giving about the same low dose slope.
4. The 100 eV beam is assumed to form a nitride layer that for both the FS and SS is comparable to or greater than the AES sampling depth and to the radiation damaged layer, thus giving about the same level of saturation for both surfaces. The sputtering of the N_2^+ beam (especially the N prefferential sputtering), which starts to be significant at this energy, tends to cause a steady state saturation level at a lower bombardment dose.

*On sabbatical leave from the Nuclear Research Center - Negev, Beer-Sheva, Israel.

MOLYBDENUM NITRIDE FILM GROWTH UNDER N_2^+ AND N^+ IMPACT ON A MOLYBDENUM SURFACE: ENERGY & DOSE DEPENDENCE. D. A. Baldwin, N. Shamir*, and J. W. Rabalais, Dept. of Chemistry, University of Houston, Houston, TX 77004

Aspects of nitride film formation on an annealed polycrystalline molybdenum surface under N^+ and N_2^+ ion impact have been studied. AES measurements have been made of nitrogen concentration in the surface layer resulting from exposure to nitrogen ions in the dosage range of 10^{12} - 10^{17} ionscm^{-2} and at impact energies ranging from 0 to 100 eV. Ion beams of controlable current density were used, produced with a m/e analysed , differentially pumped ion source.

For nitridation by N_2^+, curves showing AES nitrogen signal versus ion dose at constant impact energy, for a range of energies, have shapes characteristic of saturation of the surface layer with nitrogen. True saturation of the AES signal occurs when a film with maximum nitrogen-content stoichiometry has a thickness greater than the AES sampling depth (i.e. λ, the mean electron escape depth). This condition is apparently achieved in our experiments at N_2^+ impact energies <60 eV since saturation doses at 60 and 100 eV yield approximately the same AES nitrogen signal intensity. Below 50 eV impact energy, saturation doses of N_2^+ yield films with AES nitrogen signals smaller than the escape depth limited signal. This is interpreted as being characteristic of forming either thinner nitride films or films of less than maximum nitrogen concentration when energies below 50 eV are used. By taking reasonable values for λ and for N atom concentration in the 100 eV N_2^+ saturated film, estimates can be made of the efficiency of nitridation or sticking probability from the experimental results. This efficiency increases strongly with impact energy and decreases strongly with previous nitrogen concentration in the film for nitridation by N_2^+. By contrast, for nitridation by N^+, the efficiency appears to be nearly constant with respect to impact energy above 10 eV but shows trends similar to N_2^+ with respect to pre-existing nitrogen concentration in the film.

The efficiency of nitridation by N_2^+ at low pre-coverages is controlled mainly by the dissociation probability of the diatomic upon impact with the surface. N^+ reacts to form the nitride even at ≈0 eV impact energy whereas the N_2^+ must have >4 eV in order to react at all. The known chemical inertness of N_2, together with the above measurements, strongly suggest that the N_2^+ must be collisionally dissociated in order to react to form the nitride. The N^+ data allows extraction of the reaction cross section as a function of energy. The N_2^+ data represent a convolution of the dissociation probability and the reaction cross section, hence, the dissociation probability can be extracted from a knowledge of the N^+ reaction cross section.

*On sabbatical leave from the Nuclear Research Center - Negev, Beer-Sheva, Israel.

FORMATION OF N-LAYERS IN SILICON BOMBARDED BY LOW-ENERGY OXYGEN IONS

V.A.Labunov, V.E.Borisenko

Minsk Radioengineering Institute
Podlesnaya 6, 220069 Minsk, USSR

Appearance under-surface n-layers in silicon crystals bombarded by 400 eV oxygen ions is reported.

Oxygen free silicon crystals (111) oriented, uniformly doped by boron ($1,4 \times 10^{15}$ atoms/cm^3) were used for the investigation. Ion bombardment was carrying out at current density 1 mA/cm^2 for 10-30 min. Sample temperature was fixed in the range 100-600°C. Sheet resistance, layer depth and concentration distribution of electrons in the layer were measured.

It was found out that n-layers were formed only after bombardment at the temperature higher than 350°C. The layer depth increases with the rise of the bombardment temperature and reaches 1,0-1,5 μm. Electron distribution in the layer measured by spread resistance method is characterized by surface concentration 10^{16}- 10^{17} e/cm^3 and well approximated by $n=n_o \exp(-x/L)$, where L = 0,24 μm.

Formation of n-layer is supposed to be due to vacancy - oxygen complexes introduced by ion bombardment. The model of generation and migration processes of these complexes is based on the concept of radiation-enhanced diffusion under low-energy ion bombardment.

DYNAMIC SIMULATION OF CHANGES IN NEAR SURFACE COMPOSITION DURING ION BOMBARDMENT

M.L. Roush, T.D. Andreadis and F. Davarya
Chemical and Nuclear Engineering Department
University of Maryland
College Park, Maryland 20742, USA

and

O.F. Goktepe
Naval Surface Weapons Center
White Oak, Maryland 20910, USA

A Monte Carlo based computer code, called EVOLVE, is used to simulate the concentration changes which develop as a consequence of the incident beam atoms and the resulting cascades of recoil atoms. The target is treated in slab geometry, with the elemental composition of each slab initially specified in order to represent the system of interest. Arrays of integers which specify composition in the layers, are incremented to account for the reduction in concentration at the point of origin of a recoil atom and the increase of concentration at the point at which a particle stops. This program considers atomic mixing of all species including the implanted beam atoms during the simulation of ion bombardment. Incident ions as well as the recoil atoms of the cascade produced in the medium are followed until either they escape from the solid or their energy falls below a low cutoff value (1.2 eV). This code is being used to simulate the evolution of concentration changes which result from the response of the solid to incident beam atoms in a number of cases of current interest.

EVOLVE is used to simulate systems which have displayed dose-dependent sputtering yields under ion bombardment. Simulations are utilized to examine several hypotheses of plausible causes of the observed increasing sputtering yield. Another dynamic system examined is that of a binary alloy which displays preferential sputtering under ion bombardment. The altered composition near the surface of such a solid is explored by examining sequences of depth profiles under differing conditions. Finally, simulation results are presented for the sputtering of a sample composed of alternating layers of two different metals.

STAINLESS-STEEL OXIDATION INVESTIGATION, USING NUCLEAR TECHNIQUES FOR SURFACE STUDIES, WITH AN AUTOMATED SCANNING PROTON MICROBEAM: EXPERIMENTAL SYSTEM AND RESULTS

J. M. Calvert
Phys. Dept., Schuster Lab., Univ. of Manchester, Manchester M13 9PL,U.K.

L. F. Requicha Ferreira
Departamento de Física, Universidade de Coimbra, 3000 Coimbra, Portugal

A number of detailed measurements have been carried out using an automated scanning proton microbeam on a stainless steel sample oxidized for 1036 hours in $^{16}CO_2$ and 45 hours in $^{18}CO_2$ at 640° C. The sample after being oxidized was tapered. This way, an amplification to the depth of the oxide scale has been obtained. The distribution of ^{18}O in the scale, which gives information on the oxidation mechanism was determined by measuring the yield of α-particles in the $^{18}O(p,\alpha)\,^{15}N$ reaction at the bombarding proton resonance energy of 1.763 MeV, when the tapered section was scanned by the microbeam. Averaged information about Fe and Cr distributions have been determined using PIXE techniques.

The automated proton microbeam system has been designed and built for the accomplishment of the studies above mentioned. It is based on the Harwell microbeam apparatus (slightly modified) but facilities have been added to this for automatic repetitive scanning of the microbeam over the sample. A special chamber was built having accurate two-dimensional positioning of the sample using stepping-motors. Also a microcomputer was built specially for controlling the complete operation of data collection and adjustment of experimental conditions such as scan size and position. Some other features have been included in this system, e.g., variable number of steps per scan, ADC size, time per step, local and remote control, etc.

Microbeam spot sizes of a minimum of 10 microns have been obtained. Scanning distances for proton beams of 2.0 MeV could be set for 100 microns. These values have been optically measured using a quartz disc with an engraved scale 127 microns long (5 thou) divided into 50 equal divisions of 2.54 microns, mounted on the sample holder and observed by an optical microscope.

The automated scanning microbeam system proved to be reliable, time-saving, accurate and reproducible as far as data collected in different ocasions from the sample were concerned.

The system demonstrated its value of collecting a large amount of data in a very systematic way and showed in the case of the steel in study:

i) Significant penetration of ^{18}O through the outer oxide layer thus showing that cation transport is not the only oxidation mechanism.

ii) The distribution of ^{18}O can only be explained by oxidation within the spinel layer. It cannot be explained by isotopic exchange.

iii) Growth within the spinel layer is not restricted to the oxide - alloy interface but occurs through the major part of the layer.

iv) No direct evidence of the effects due to trace elements such as build up at interfaces.

Sputtering Yield Calculations for Light Ions Incident on Wall in Tokamak

Xu Ting-wei (Sichuan Univ.)
Fan Zheng-tang (Anhui Institute of Plasma Physics)
He Qi-chao (Sichuan Univ.)

In tokamak reactor, the sputtering yields of wall materials, for example Fe, bombarded by light ions, for example H^+, from plasma are so small that it is difficult and expensive to calculate in terms of direct Monte Carlo method. A new method has been introduced which combines roulette and splitting technique with statistical estimate for accelerating convergence in Monte Carlo simulation. The main points of the method are as follows.

At first, when a primary ion is going to move in the inward direction under conditions of both incidence and cascade process, we game a roulette. We produce a pseudorandom number R and compare it with a given parameter q=0.1--1. If R q, we win the game and the ion goes on its travel with a new weight which is q^{-1} times as large as before; on the contrary, we fail in the game and consider that the ion has died and start a new ion history.

Secondly, when a target atom is going to move in the outward direction within target after a collision with a particle in the cascade process, we split the atom into n=1--3 pieces. They separately go on their travels with a new weight which is reduced n times.

All of new displaced atoms have the same weights as that of incident particles.

Thirdly, when Jth displaced atom in cascade caused by Ith incident ion travels in the outward direction within target after Kth collision, its probability through the surface into plasma is given by

$$P_{ijk} = \exp\left[-\Sigma(E_{ijk})\frac{x_{ijk}}{\cos\alpha_{ijk}}\right]$$

and its contribution to sputtering yield supposing that W_{ijk} is its weight

$$y_{ijk} = W_{ijk}P_{ijk}$$

The unbiased estimate of sputtering yield on condition that the sample size N is large enough is given by

$$Y = \frac{1}{N}\left(\sum_i\sum_j\sum_k y + \sum_i\sum_j \xi\right)$$

Where

$$\xi_i = \begin{cases} W_{ijk}, & \text{if displaced atom acrosses the surface} \\ 0, & \text{otherwise} \end{cases}$$

Sputtering yields of the wall materials in tokamak bombarded by light ions from plasma have successfully and economically been calculated by above method and compared with present results.

TUESDAY MORNING, JUNE 9, 1981

Plenary Session

Main Auditorium

Chairman: R. KAPLAN

9:00 Interaction of Metals with Semiconductor Surfaces.
L. J. BRILLSON

9:45 Subband Physics: Energy Bands and Transport Properties of an Interfacial Charge Layer
F. KOCH

10:30 Electronic Surface States of II-VI Compound Semiconductors.
T. TAKAHASHI and A. EBINA

11:15 Atomistic or Molecular Processes on Clean Surfaces: Recent Advances
R. UEDA

INTERACTION OF METALS WITH SEMICONDUCTOR SURFACES

L.J. Brillson
Xerox Webster Research Center, 800 Phillips Rd. W-114
Webster, NY 14580

Metal films on semiconductor surfaces produce strong atom and charge rearrangement at their microscopic interface. Using soft x-ray photoemission spectroscopy (SXPS) to study atomic thicknesses of metal evaporated on semiconductor surfaces cleaved in ultrahigh vacuum, we have characterized the chemical and electronic structure of the interface region on a monolayer scale. For III-V and II-VI compound semiconductors, the presence of a metal film induces a substrate dissociation and diffusion of cation and anion into the metal. The magnitude of this diffusion scales proportionally with bulk heats of formation for both semiconductor families. Depending on the strength of bonding between metal and semiconductor atoms, the stoichiometry of anion vs. cation outdiffusion varies systematically over several orders of magnitude. The interaction between most metal films and III-V compound substrates is dominated by "chemical trapping" due to metal-anion bonding; it leads to a mixed metal-anion interface region whose width scales linearly with interface heat of reaction. Charge redistribution induced by metal chemisorption alters the interdiffusion of weakly bonding interfaces via electromigration. Metal films on II-VI compound substrates exhibit reactive interdiffusion and both metal-anion and metal-cation bonding. For these compound semiconductor substrates, SXPS and XPS core level features establish that metal indiffusion can also take place at monolayer or lower coverages. In addition we have used monolayer thicknesses of reactive metals ("interlayers") at metal film-semiconductor substrate interfaces to modulate the relative composition of outdiffused species within the metal film. From the strength of interface chemical bonding on a microscopic scale, it is possible to control not only the chemical but also the electronic properties of the macroscopic metal-semiconductor interface.

L.J. Brillson, Phys. Rev. Lett. 40, 260 (1978).

Subband Physics
Energy Bands and Transport Properties of an Interfacial Charge Layer

F. Koch

Physik-Department, Technische Universität München
8046 Garching, FRG

An interfacial charge layer is built up in a semiconductor surface region in a number of different ways. The MOS transistor with its insulated gate configuration is a commonly used example. Other possibilities are semiconductors covered with a low work-function metal (e.g. Cs on Si), a semiconductor interface with another semiconductor of lower electron affinity (e.g. remote doping in GaAs-GaAlAs), or a semiconductor with an adsorbed gas layer (e.g. atomic H on ZnO). Optically tunable charge layers can be created with special molecules or atoms separated by a potential barrier from the semiconductor (e.g. MNOS devices, or dye molecules on ZnO).

The two-dimensional, electronic states of the charge layer are known as electric subbands. The investigation of their physical properties is subband physics.

After a discussion of the subband concept, we give an account of the experimental investigation of subband-structure by tunneling, infrared emission and absorption spectroscopy, inelastic light scattering, and magnetoconductance studies.

We conclude the review of subband physics with a look at the transport-related properties of the charge layer. Experimental research on the oscillatory magnetotransport, on cyclotron resonance, plasmon excitation, on minigaps, on carrier localization and metal-insulator transition, etc., etc., etc. ... has served to complete the characterization of the interfacial charge layer.

Electronic Surface States of II-VI Compound Semiconductors

Tadashi Takahashi and Atsuko Ebina
Research Intitute of Electrical Communication
Tohoku University, Sendai 980, Japan

We will survey recent studies on 2-6 compounds performed by a combination of techniques of photoemission spectroscopy, electron-energy-loss spectroscopy, LEED, AES, contact-potential difference, and optical reflectivity. There is a wide variety of ionicity in chemical bonding of 2-6 compounds, i. e., ZnTe and CdTe are rather covalent, ZnSe may be intermediate, and ZnO, CdSe, and CdS are ionic. Thus, it may be possible to study the effects of ionicity on the electronic structure of the clean surface and the surface with adatoms.

Photoemission results of the cleaved (110) or $(10\bar{1}0)$ surface of ZnSe (and ZnTe) and ZnO are compared with theoretical calculations in order to determine the energy position of the occupied surface states. An attempt will be made to obtain information on the empty surface states from ELS data.

Surface atomic structures of the nonpolar (110) or $(10\bar{1}0)$ surface deduced from LEED intensity analyses will be described.

From AES and ELS results, we have found that there is no differences in chemical composition and electronic structure between the cleaved and Ar^+-bombarded-annealed (110) surfaces of ZnTe, but in the case of ZnSe and CdTe loss spectra is different between the two differently prepared surfaces, indicating some defects may exist on the annealed surface.

The chemical composition of the polar 111 surface of ZnTe and CdTe is stoichiometric, while in more ionic compounds of ZnSe and ZnO a great deviation from stoichiometry was detected on the polar surfaces of $\{111\}$ and $\{0001\}$.

A band bending at the surface starts on adsorption of a very small amount of oxygen (far less than 1% coverage of a monolayer) for the cleaved (110) surface of ZnTe and ZnSe, while in the case of CdTe the pinning of the surface Fermi level tends to release on adsorption of oxygen.

Schottkey barrier formation on ZnTe, ZnSe, CdTe, CdSe, and CdS surfaces are summarized.

ATOMISTIC OR MOLECULAR PROCESSES ON CLEAN SURFACES: RECENT ADVANCES

Ryuzo Ueda

Department of Applied Physics,
School of Science & Engineering,
Waseda University

3-4-1 Ohkubo, Shinjuku-ku, Tokyo, 160 Japan

Recent developments in studies on atomistic or molecular processes on clean solid surfaces are reviewed. In a collision between atomic or molecular beams and solid surfaces, the processes such as scattering (elastic or inelastic), adsorption (physical or chemical), desorption, migration or random walk and association or dissociation of molecules on the surfaces are possible. Recent advances in analytical methods including electron spectroscopy, mass spectroscopy, in-situ observation using electron diffraction could contribute to characterize the surface processes.

Molecular beam epitaxial (MBE) method which was recently developed for device-oriented research, is also successful for fundamental research in surface processes. Reaction kinetics on residence time, correlation between incident and reflection flux, sticking coefficient etc. can be estimated by this method.

The role of surface imperfection in adsorption and heterogeneous catalysis has been of interest for surface reactions. Defects, steps and other irregularities on the surface are responsible for nucleation and growth of thin overgrowth. Diffusing molecules cause a supersaturation in a sharply limited region. The width of this region gives a value for the path of diffusion which can be estimated experimentally. In multiply oriented deposits, grain boundaries are formed and diffusion at internal surfaces controls the recrystallization kinetics. These deposits finally reach to the oriented overgrowth—epitaxy.

Tuesday afternoon, June 9, 1981

Session Tu-A: Deposition and Properties of Thin Films

(Room 0123)

Chairman: J. E. ROWE

1:40 Film and Surface Studies by MEED. G. SHIMAOKA

2:00 Electrical Properties of Sputtered RuO_2 Films. M. TAKEUCHI, K. MIWADA and H. NAGASAKA

2:20 Preparation and Characterization of Thin Dielectric Films. V. S. DHARMADHAKARI

2:40 Substrate Biased R.F. Sputtering of Zinc Oxide Films. D. K. MURTI

3:00 Production and Properties of Sputtered Thin Films for Solar Selective Absorbing Surfaces. G. L. HARDING and S. CRAIG

3:20 Carbon Thin Films Obtained by Means of R. F. Plasma-Decomposition of Hydrocarbon. Y. ONUMA, Y. KATO and K. HORI

3:40 Characterization of Plasma Nitride. H. KOYAMA

4:00 The Surface Temperature of a Substrate during the Vacuum Evaporation. Y. H. SHEN

4:20 Polarization in Dielectric Films due to Uncompensated Mobile Charge. V. P. ROMANOV

4:40 Structure of Thin Film Ag-O-Cs Photocathode and its Dark Current. Q.-D. WU

FILM AND SURFACE STUDIES BY MEED

Goro SHIMAOKA
Research Institute of Electronics, Shizuoka University
Johoku 3-5-1, Hamamatsu 432, Japan

LEED (energy range about 10~200eV) and RHEED (energy range above about 10 keV) are usually used for the study of the structure of solid surfaces. Due to the strong atomic scattering cross-section LEED is particularly suitable for the observation of two dimensional surface layers, but to visualize its diffraction pattern one must accelerate the diffracted beams through a grid. Such post-acceleration of the diffracted beams is not necessary for RHEED, but it is very sensitive to the roughness of the surface since the angle of incidence of the electron beam is very small. Therefore, very flat surface is necessary for RHEED, and if there are any small protuberances transmission diffraction pattern is involved. In the present study we have designed a new electron diffraction apparatus which is possible to examine very thin surface layers of a crystal using an intermediate energy range of 0.2~3keV to fill the gap between LEED and RHEED. Vacuum system of the apparatus is oil free and can be evacuated to a pressure better than 10^{-7}Pa. Fig. 1 shows schematic arrangement of the specimen (S) to the incident electron beam. Using an electron gun, G_1 or G_2, reflection diffraction patterns with low (~3°) or high (about 50~90°) Bragg angle produced on a screen (F_1, hemispherical; F_2, flat plate painted with a fluorescent material, which is sensitive to low-energy electrons) are clearly visible through a viewing window (V_1; V_2). This technique makes precise measurement of orientation and interplanar spacings of very thin surface layers possible, and has various advantages over both LEED and RHEED. Figs. 2 and 3 show examples of MEED patterns from a MgO (001) surface, which are taken at 720 and 220eV respectively. The former indicates more three dimensional character while the latter represents more two dimensional structure.

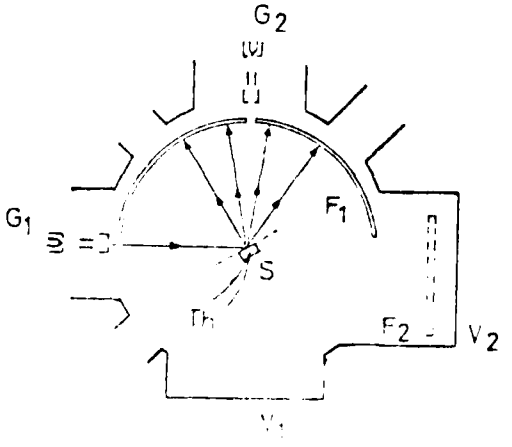

Fig.1 Schematic [illegible] experimental arrangement.

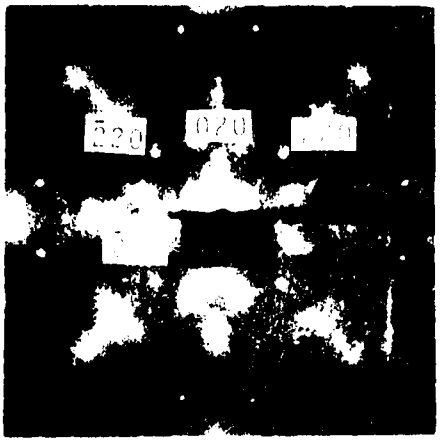

Fig.2 MEED pattern of MgO (001) at 720eV.

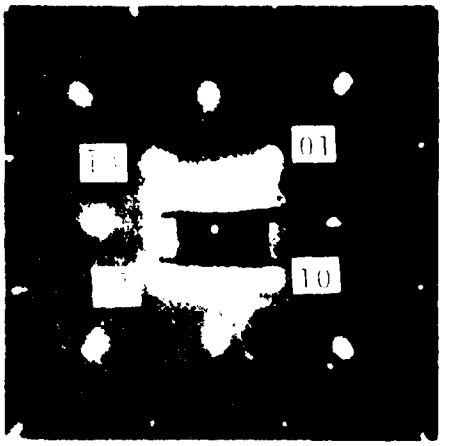

Fig.3 MEED pattern of MgO (001) at 220eV.

Electrical Properties of Sputtered RuO_2 Films

M. Takeuchi
Department of Physics, University of Alberta, Edmonton, Alberta, Canada

and

K. Miwada and H. Nagasaka
Department of Electrical Engineering, Faculty of Engineering, Ibaraki University, Hitachi, Ibaraki, Japan

RuO_2 is known to show metallic conduction. RuO_2 films about 400 - 6000 A thick were prepared by r.f. sputtering from a RuO_2 powder target in an atmosphere of argon, and the electrical properties and the crystal structure of the sputter deposited films were investigated. Effects of the addition of oxygen to the sputtering gas argon on the properties of the films were also studied. Corning 7059 glass slides were employed as substrates. The sputtering power density was from 1.6 to 4.7 Wcm^{-2}. The substrate temperature depends on the sputtering power density and is about 70 °C and 190 °C at the power density of 1.6 and 4.7 Wcm^{-2}, respectively.

The crystallinity of the sputtered RuO_2 films, examined by X-ray diffraction, were found to depend on both the film thickness and the sputtering power density. At the power density of 3.1 Wcm^{-2}, the films with thickness less than about 1000 A did not show any X-ray diffraction peaks, while the films with thickness of above 1100 A showed diffraction peaks corresponding to RuO_2 (110) and (211) planes and their intensity increased with an increase in their thickness. The crystallinity of the sputtered films increased with an increase in the sputtering power density, too. The addition of 5 % oxygen to the sputtering gas argon also improved the crystallinity of the sputtered films.

The electrical resistivities of the sputtered RuO_2 films decreased from 3×10^{-4} ohm-cm to 1×10^{-4} ohm-cm with an increase in the sputtering power density from 1.6 to 4.7 Wcm^{-2}. In other words, the RuO_2 films with higher crystallinity tend to have lower resistivities. Temperature dependences of the resistivities were also measured in the temperature range of -180 to 160 °C. It was found that the specimens prepared at higher power density showed positive temperature coefficient of resistance (TCR). This is consistent with results on bulk RuO_2. The specimens prepared at low power density showed negative TCR, while the specimen prepared at the sputtering power density of 2.3 Wcm^{-2} showed a TCR of zero. These results can be explained by a model in which the sputtered films consist of microcrystalline RuO_2 grains dispersed in amorphous RuO_2 matrix. Crystalline RuO_2 has a positive TCR value, while amorphous RuO_2 is considered to have a negative TCR value. The amorphous RuO_2 makes the film resistivity high. This model can also explain the high resistivities in the RuO_2 films prepared at low power density. Hear-treatment of sputtered RuO_2 films decreases their resistivity and increases their TCR values. This can also be explained by the increase in the crystallinity in the sputtered films due to the heat-treatment.

The authors wish to thank Professor F. L. Weichman of the University of Alberta for his helpful advice.

Preparation and characterisation of thin dielectric films

Vineet S. Dharmadhakari*

Thin Film Division, National Chemical Laboratory, Poona-32 (INDIA)

Abstract: - Thin dielectric films of bismuth oxide and neodymium flouride were prepared by thermal evaporation. However heating of these compounds in vacuum resulted in their dissociation. An X-ray photoelectron spectroscopy study of as-evaporated bismuth oxide films clearly showed the presence of a lower suboxide along with some pure bismuth metal. A linear relation was found to exist between the binding energies and oxidation states. Chemical shift analysis in binding energy of F(1s) level in NdF_3 film matrix also showed the presence of lower valence state. X-ray and electron diffraction techniques were used for the structural analysis of the films. Scanning Electron Micrographs of as-evaporated bismuth oxide films revealed that they were composed of loosely packed grains which were approximately spherical where as the oxidised films showed the evidence of platelet characteristics of γ-Bi_2O_3. Effect of film thickness (d) on dielectric constant (ε) and capacitance (C) at 1KHz, at liquid nitrogen and room temperature for as-evaporated bismuth oxide and neodymium flouride films and for thermally oxidised bismuth oxide films is presented. The relative performance of thin film capacitors fabricated from these structures is discussed.

Present address: Dept. of Electrical Engineering and Computer Engineering, University of New Mexico, Albuquerque, NM 87131, U.S.A.

SUBSTRATE BIASED R.F.SPUTTERING OF ZINC OXIDE FILMS

D. K. MURTI
Xerox Research Centre of Canada, 2480 Dunwin Drive, Mississauga, Ontario, L5L 1J9, CANADA

Zinc oxide has been extensively studied in recent years and finds use in such applications as solar cells, surface acoustic wave devices and varistors. Piezoelectric quality films are characterized by their high resistivity and the preferential orientation of their fibre grains while applications of ZnO in solar cells require films with low resistivity and high optical transmittance.

The objective of the present study was to prepare and control the structural and electrical properties of zinc oxide films. The preparation and control of the properties of zinc oxide films was achieved by substrate biased r.f.sputtering technique. Thin films of ZnO were sputtered from a zinc oxide target in an argon atmosphere onto Corning 7059 glass and NESA (transparent conducting glass) substrates. Zinc oxide films with thicknesses ranging from 0.3 μm to 1.5 μm were deposited at deposition rates ranging from 0.03 nm/s to 0.3 nm/s with and without the application of a bias voltage to the substrate.

It was found that zinc oxide films were semiconducting when prepared with a substrate bias voltage and insulating when deposited without a bias voltage to the substrate. Resputtering at the substrate due to bias voltage induced ion bombardment, can cause the film composition to be different from the target composition. The changes in the electrical properties could be due to changes in the stoichiometry of ZnO films. Investigations are currently underway to monitor the changes in the surface compositions of the ZnO films prepared under various conditions.

The preferred orientation of the ZnO films was determined by x-ray diffraction techniques. It was found that the preferred orientation is controlled primarily by the deposition rate and is independent of the film thickness. In addition, there was no change in the orientation between ZnO films deposited on amorphous (Corning 7059 glass) and crystalline (NESA) substrates. At relatively low deposition rates (0.03 nm/s) the ZnO films had a preferred (002) orientation which changed to (110) with increase of deposition rate. Finally, at higher deposition rates the films had a (100) preferred orientation. The films had an optical absorption edge at 390 nm corresponding to an energy gap of 3.2 eV which is in agreement with that for single crystal ZnO.

PRODUCTION AND PROPERTIES OF SPUTTERED THIN FILMS FOR SOLAR SELECTIVE ABSORBING SURFACES

G.L. Harding and S. Craig

School of Physics, University of Sydney, 2006 Australia

Solar selective surfaces are necessary for solar photothermal conversion in order to maximise the heat extraction efficiency of solar collectors. Selective absorbing surfaces must have high absorptance (α) over the solar spectrum and low emittance (ε) for thermal infrared wavelengths. Thin film selective absorbing surfaces for all glass tubular evacuated collectors must have high stability at temperatures up to 400°C in vacuum and the film deposition technology must be compatible with the requirement of the uniform coating of ~1.5 m long glass tubes in mass production.

At Sydney University selective surfaces are produced by non-reactive and reactive dc magnetron sputtering in a prototype production system which coats batches of twenty 1.5 m long glass tubes, with a turn around time of less than one hour. The selective surfaces consist of a metal base layer with high infrared reflectance (~ 300 nm thick Cu, Ni, Al or stainless steel) sputtered onto the glass, overlayed by an absorbing film consisting of a reactively sputtered stainless steel or chromium-carbon cermet. The absorbing layer is graded from almost pure metal at base layer to almost pure carbon at the top surface. Solar absorptance $\alpha \geq 0.94$ and emittance $\varepsilon \leq 0.05$ at 120°C are routinely obtained for surfaces having a copper base layer.

Recent research and development will be described under the following headings -

(a) Construction and operation of the prototype tube coating system and possible designs for high volume production tube coaters.

(b) Optical and electrical properties of the metal base layer with emphasis on the temperature dependence of emittance.

(c) The relationship between composition and optical properties (including refractive indices) for the metal-carbon film.

(d) Degradation of the optical properties of the selective surfaces at high temperature and the corresponding degradation mechanisms as determined by Auger electron spectroscopy.

(e) Enhancement of absorptance of the selective surfaces by incorporating a textured copper base layer produced by sputter depositing in high argon pressures or by introducing small partial pressures of oxygen or nitrogen during deposition.

Carbon Thin Films obtained by means of R.F. Plasma-decomposition of hydrocarbon

Yoshiharu Onuma, Yoshitake Kato and Kuniuki Hori
Shinshu University, Faculty of Engineering
500 Wakasato, Nagano City, Japan

Abstract

For many years carbon films have been investigated by many workers in chemical and physical points of view. But there has been no carbon films prepared by means of plasma-decomposition of hydrocarbon.

In this experiment, carbon thin films have been obtained by means of R.F. assisted decomposition of benzen vapour in order to obtain conductive thin films and to apply to electronic devices.

The surface morphology, structure, IR absorption and electrical properties of the carbon thin films have been investigated.

The conclusions of this investigations may be summarized as follows.

1) It is easy to obtain carbon thin films at comparatively low temperatures by means of R.F. plasma decomposition of benzen vapour.

2) Carbon thin films have the higher conductance of about 5[illegible] Ω^{-1}cm^{-1} than that having been obtained ordinarily at 1200°C in atmosphere.

3) Electron transmission microscopy and electron diffraction analysises show that carbon thin films consist of micro fine particles

4) From the results of I.R. absorption analysis, it can be seen that thin films have content of hydrogen and its content does not depend on the substrate temperatures.

5) Carbon thin films thus obtained may be applicable to various electronic devices.

Characterization of Plasma Nitride

Hiroshi KOYAMA

Computer Development Laboratories
4-1 Mizuhara Itami Hyogo, 664 Japan

Plasma enhanced silicon nitride offers excellent properties as an encapsulant and an interlevel dielectric in silicon integrated circuits. It can be deposited over the metallization at a relatively low temperature by the reaction of silane and ammonia in a glow discharge. The physical and electrical properties of the plasma nitride are dependent on a variety of deposition parameters and it is necessary to evaluate exact composition for a better control of the deposition process.

Auger electron spectroscopy (AES) is a promissing method in analyzing the elemental composition of silicon nitride. To evaluate the bulk composition, however, it is necessary to carry out ion sputtering which results in breaking of the Si-N bonds. The composition is, therefore, altered significantly and the film is found to be extremely silicon rich using the Ar ion sputtering Auger analysis.

The present experiment aims to evaluate the composition of the plasma nitrides by Auger electron spectroscopy coupled with nitrogen ion sputtering. Correlation factors for optical absorption are also given which are to be related to the variation of the new Auger spectra.

In the Auger spectrum from Ar sputtered plasma nitride the main peak occurs at ~90 eV (Peak I) with a characteristic shoulder at ~83 eV (Peak II). On the other hand in the new Auger spectrum from nitrogen sputtered plasma nitride Peak II becomes dominant with increasing nitrogen content. The ratios of Peak II to Peak I for plasma nitrides with refractive indices of 2.12, 1.96 and 1.87 are measured to be 0.54, 1.05 and 4.85, respectively after 25 seconds of 5 keV nitrogen sputtering.

The ratios of the N-H and Si-H bond concentration (N-H/Si-H) of these plasma nitrides, which are quantified from the absorption spectra, are estimated to be 0.37, 1.07 and 5.83, respectively. And they are close to the AES data mentioned above. Peak I and Peak II in the Auger spectrum from silicon nitride have been attributed to free silicon and silicon/SiN, respectively. However the presence of bonded hydrogen should not be ignored for further consideration of electron states in plasma nitride.

It is thus clear that the Auger electron spectroscopy coupled with nitrogen sputtering is quite sensitive to the compositional variation of plasma nitrides. The in-depth profiles of nitrogen and free silicon in plasma nitride on an actual silicon integrated circuits is now able to be measured by the present method. Changes in energy of Auger and absorption peaks with increasing nitrogen content are also helpful in view of the characterization of plasma nitride.

THE SURFACE TEMPERATURE OF A SUBSTRATE DURING THE VACUUM EVAPORATION

Y. H. Shen
(Modern Physics Institute, Fudan University, Shanghai, P.R.C.)

Abstract

The method for non-contact temperature measurement by the interference of laser beams has been improved so that the surface temperature of a substrate during vacuum evaporation can be monitored. Experimental results show that if the substrate temperature increases slowly (about 1° C/min), the surface temperature will be about the same as the average bulk temperature. But if the substrate temperature increases rather fast (about 10 ° C/min), the surface temperature will be obviously higher. The difference could be in the order of ten degrees.

Moscow Institute of Electronic Technology, Moscow, USSR

POLARIZATION IN DIELECTRIC FILMS DUE TO UNCOMPENSATED MOBILE CHARGE

By V.P. Romanov

Theoretical investigation has been carried out of polarization effects in dielectric films containing mobile ions. It has been established that drift-diffusion and drift mechanisms of polarization take place.

From a joint solution of the Poisson equation and the equation for the density of a charged particle flow, with regard of diffusion (J_{diff}) and drift electric ($J_{drift}^{electric}$) and elastic ($J_{drift}^{elastic}$) flows, analytical expressions are derived for spatial distributions of the ion concentration N(x), the intensity E(x) and potential $\varphi(x)$ of the electric field. It is shown that in the case of high ion concentration the distributions N(x), E(x), and $\varphi(x)$ are considerably influenced by elastic interaction between charged particles and the dielectric medium ($J_{drift}^{elastic} \gg J_{diff}$, the drift polarization). In the limiting case of low ion concentration ($J_{drift}^{elastic} \ll J_{diff}$, the drift-diffusion polarization) the dependences for N(x), E(x), and $\varphi(x)$ agree with the known ones [1]

Analysis of experimental studies (for example, [2]) on the sodium ion distribution in a silicon dioxide layer in the light of the suggested theory has shown that the role of elastic interaction between charged particles and the dielectric medium is important in this case. The calculated dependences N(x) for sodium ions in a silicon dioxide layer are in good agreement with the experimental ones.

References

[1] V.P. Romanov, and Yu.A. Chaplygin, Phys. Stat. Sol. (a), 53, 493 (1979).

[2] T.M. Buck, F.G. Allen, J.V. Dalton, and J.D. Struthers, J. Electrochem. Soc., 114, 862 (1967).

Structure of Thin Film Ag-O-Cs Photocathode and Its Dark Current

Wu Quan-de
Department of Radio-Electronics, Peking University, Beijing, China

A semitransparent Ag-O-Cs cathode is a thin film with silver colloidal particles and silver granules dispersed in a film of Cs_2O. The structures of silver colloidal particles and granules were studied by means of replica method and direct transmission observation in electron microscope/1/. We come to the conclusion that the photoelectric emission of this cathode above wavelength 4000Å comes from small silver colloidal particles in the film of Cs_2O/2/. It was found that for long wavelength response the equivalent diameters of small colloidal particles are about 31 Å/3/.

Typical values of the thermionic emission current of this cathode at room temperature lie in the range from 10^{-11} to 10^{-14} A/cm². Using the model given in Ref.3 Fig.2, we can explain the dark current of this cathode at room temperature theoretically. Components of thermionic emission may be produced by the following mechanisms:

(a) the diffusion of electrons, thermally excited in the small silver colloidal particles with potential barrier about 1.06 eV, to the surface. It is assumed that the total volume of these colloidal particles in unit volume is only a small fraction of the volume. The estimated value of this component is about 10^{-13} A/cm².

(b) the diffusion of electrons, thermally excited from the surface states of silver colloidal particles and from Cs atoms in interfaces of colloidal particles and the film of Cs_2O, to the surface. From the results of photoemission/4,5/, we may assume this component is of the same order of magnitude as for case (a).

(c) electrons generated in the depletion regions around silver colloidal particles via trapping centres. Its mechanism is similar to the discussion in Ref./6/, where it is shown that for the expected values of electron lifetime, surface state densities and trapping cross sections, emission from the Cs_2O layer is likely to dominate the emission from the III-V substrate/6/.

(d) electrons generated in the semiconductor film of Cs_2O from Cs donors. Since Ag donors are situated in deep level, the contribution of these donors can be neglected. When volume fraction of silver colloidal particles and silver granules and volume fraction of depletion regions around silver particles and granules have increased due to additional silvering process, the volume fraction of Cs_2O layer must decrease. The result is that the electron density in the conduction band of Cs_2O layer must decrease, and its dark current decreases also. The other cause of decrease of dark current is the disappearance of Cs_2O layer between the depletion region around the silver colloidal particle and the surface of the cathode, then the work function should increase.

(e) electrons generated from filled surface states. This kind of thermionic emission can be neglected.

Some experimental facts stated in Sommer's book/7/ about the thermionic emission of Ag-O-Cs photocathodes can be explained.

/1/ Wu Quan-de, ACTA PHYSICA SINICA, 28(1979),553. /2/ ditto, 28(1979), 599. /3/ ditto, 28(1979),608. /4/ G.Hincelin et al., Proc. 7th Intern. Vac. Congr. and 3rd Intern. Conf. Solid Surfaces, (1977),1209. /5/ G.Chabrier et al., Phys. Rev. B, 13(1976),4306. /6/ R.L.Bell, Solid-State Electronics, 13(1970),397. /7/ A.H.Sommer, Photoemissive Materials, 1980.

Tuesday afternoon, June 9, 1981

Session Tu-B: Semiconductor Surfaces and Heterostructures

(Room 1105)

Chairman: F. KOCH

1:40 On the Electronic Properties of Ge-GaAs (110) Heterostructures. H. GANT, R. MURSHALL and W. MÖNCH

2:00 Intermixing and the Mechanism for Schottky Barrier Formation. W. E. SPICER, P. SKEATH, C. Y. SU and I. LINDAU

2:20 Field Effect Spectroscopy of Fast Surface States at Oxidized GaAs Surfaces. E. W. KREUTZ and P. SCHROLL

2:40 Surface Studies of InP by Electron Energy Loss Spectroscopy and Auger Electron Spectroscopy. C. W. TU and A. R. SCHLIER

3:00 Unified Theory of Intrinsic States, Core Excitons, and Defect-Induced States at Semiconductor Surfaces. R. E. ALLEN and J. D. DOW

3:20 Angular Resolved Photoemission Measurements on Clean and Hydrogen Covered Ge(111) Surfaces. R. D. BRINGANS and H. HÖCHST

3:40 Interface State and Oxide Charge Generation in the Si-SiO_2 System Photoinjection of Carriers. E. W. KREUTZ

4:00 Charge Transport and Storage in Ion Implanted Metal-Oxide-Semiconductor Structures. L. AUGULIS and L. PRANEVIČIUS

4:20 On the Acceptor Nature, Formed in the Surface Layer at Silicon Thermal Evaporation. L. N. ALEKSANDROV, R. N. LOVYAGIN and L. N. SAFRONOV

4:40 Relationship between the Polar Surfaces of CdS Crystals and some Properties of CdS-Cu_2S and CdS-CdTe Heterojunctions. A. KOBAYASHI

5:00 Development and Characterization of a Monochristalline Silicon Solar Cell. N. KESRI

2nd International Conference on Solid Films and Surfaces

ON THE ELECTRONIC PROPERTIES OF Ge:GaAs(110) HETEROSTRUCTURES

H. Gant*, R. Murschall, W. Mönch*
Laboratorium für Festkörperphysik der Universität Duisburg,
D-4100 Duisburg, Germany

The electronic structure of epitaxial Ge overlayers grown by molecular beam epitaxy on clean, cleaved GaAs(110) surfaces was followed in situ by ELS, ARUPS, and work function studies using the Kelvin method. The Ge coverage Θ was variied from the submonolayer range up to about 20 monolayers. For coverages below half a monolayer of Ge changes in work function are measured of opposite sign with p- and n-type GaAs. Since the ARUPS measurements show the ionization energy to remain constant up to $\Theta \approx 1$ the changes observed in work function are caused by an increase in band bending the sign of which indicates that depletion layers are formed for both p- and n-type substrates. These space charges are balanced by the excess charge in two chemisorption-induced surface states. From the measured temperature dependance of the work function it follows that below substrate temperatures of 250°C the surface potential is determined by a donor-type surface state on p-type and by an acceptor-type surface states on n-type substrates while it is pinned by both states for higher temperatures. The analysis of the band bending as function of the Ge coverage yields the energetic position of both Ge-induced surface levels as $E^A_{ss} - E_v = (0.75 \pm 0.1)$eV for the acceptor and $E^D_{ss} - E_v = (0.42 \pm 0.1)$eV for the donor at a sample temperature of 320°C. The density of both states was found to increase with the Ge-coverage as $N_{ss} = (0.06 \pm 0.04)\sigma_{110} \times \Theta$.

With further increasing Ge coverage up to $\Theta \approx 5$ the work function and the ionization energy decrease by 0.1 eV and 0.3 eV, respectively. The electron energy-loss peaks remain at the same position up to $\Theta \approx 1$ but were found to shift, too, in the range up to $\Theta \approx 5$. For thicker Ge films all properties were found to remain constantly and therefore the electronic structure of the growing Ge(110) film is now observed.

The well known 20 eV energy-loss peak of the clean GaAs(110) surface, up to now attributed only to transitions from Ga(3d) to Frenkel-type excitons of dangling-bond surface states, was found to persist up to coverages of 80 monolayers at a slightly shifted position at 19.7eV. However, no Ga was detected at the growing Ge(110) surface with AES and ELS. By comparison with surface state calculations [1] this energy loss may be attributed - at least for the Ge-film - to excitations from bonding to antibonding back-bond surface states.

Finally, the previously reported arsenic surface enrichment [2] is found with ELS, too, since loss peaks involving excitations from As(3d) core levels are still observed at the highest Ge coverages.

[1] I. Ivanov, A. Mazur, and J. Pollmann, Surface Sci. 92 (1980) 365.
[2] W. Mönch, H. Gant, J. Vac. Sci. Technol. 17 (1980) 1094.

*Present address: Department of Materials Science & Engineering,
Stanford University, Stanford, CA 94305

Intermixing and the Mechanism for Schottky Barrier Formation+

W. E. Spicer, P. Skeath, C.Y. Su, and I. Lindau
Electrical Engineering Department
Stanford University, Stanford, CA 94305

Considerable insight has been obtained on the interdiffusion and defect formation at the interface between 3-5's and metal or oxide overlayers. One result is the unified model for the onset of Schottky barrier pinning and formation of MOS interface states.[1] However, there still seems to be considerable question as to the optimum method of measuring of the surface or interface Fermi level position, the nature and cause of observed intermixing between metal ad-atoms and the column three and five atoms, the effect of molecular dipoles on Schottky barrier heights and the movement of atoms, the importance of activation barriers, and other aspects of the interface problem.[1,2] These will be critically reviewed in an attempt to define areas of general agreement or disagreement. Above all, an attempt will be made to clarify the mechanism for intermixing of metals with the elements of the 3-5's on which they are deposited. New data will be presented for Au deposited on GaAs which shows that, when the GaAs, is free of oxygen (oxygen forms diffusion barrier), the defect mechanism dominates at Au coverages below a few monolayers. At larger Au coverages, a new mechanism of Fermi level pinning enters which is related to levels directly induced by the Au. Implications for practical Schottky barriers will be mentioned.

+ Work supported by DARPA and ONR.

Stanford Synchrotron Radiation Laboratory is funded by NSF.

1. W. E. Spicer, et al, Phys. Rev. Lett. 44, 420 (1980) and ref. therein.
2. L. J. Brillson, et al, Phys. Rev. Lett. 42, 397 (1979); Proc. of the Int. Conf. on Phys. of Semicond., Kyoto, Sept. 1980, pub. by Japanese Phys. Soc.

FIELD EFFECT SPECTROSCOPY OF FAST SURFACE STATES AT OXIDIZED GaAs SURFACES

E. W. KREUTZ and P. SCHROLL
Institut für Angewandte Physik, Technische Hochschule Darmstadt,
Schloßgartenstraße 7, D 6100 Darmstadt, Fed. Rep. Germany

The fast surface states at the GaAs/oxide interface are probed by field effect spectroscopy[1] as a function of substrate doping and of surface charge state. Thin single crystalline n (100) substrates (9×10^{15} to 8×10^{16} cm^{-3}) are chemically etched and subsequently storaged in laboratory air originating in a homogeneous natural oxide layer in the 20 - to 30 Å thickness region. Integral field effect is measured with a conventional circuit minimizing the effect of the displacement current. Differential field effect is performed with common Lock-in technique at suitable modulation frequencies and amplitudes. Changes in the charge state are accomplished by illumination with light, variation of temperature, and external electric fields. The surface potential and the spectrum of fast surface states are evaluated under the assumption of completely diffuse surface scattering as confirmed by the dependence of Hall coefficient and electrical conductivity on temperature.

The sign, the magnitude, and the kinetics of the electric field induced changes in surface conductivity are interpreted by depletion layers with an upward band bending of about half the gap. The density of fast surface states per energy interval consists of a U-shaped continuous distribution in the upper half of the substrate gap with a minimum about 0.5 eV below the conduction band edge. Above and below the minimum the density of states is about 2 to 4 orders of magnitude higher than at the minimum ($\simeq 10^{12}$ cm^{-2} eV^{-1}) separating two bands of states: An unoccupied surface state band (S1) above and an occupied surface state band (S2) below the minium. The increase of S2-density towards midgap is strongly correlated to the substrate doping indicating the contribution of point defects to the surface state density. The increase of S1-density towards the conduction band edge is nearly independent of the substrate doping. In analogy to the III-V compound semiconductior InSb[2] the S1-states may be associated with the lattice mismatch at the interface and the S2-states with subsurface point defect, in the space charge region.

1) E. W. Kreutz and P. Schroll, Surf. Sci. 37(1973) 410
2) E. W. Kreutz, E. Rickus, P. Schroll, and N. Sotnik, Surf. Sci. 86(1979)794

Surface Studies of InP by Electron Energy Loss Spectroscopy and Auger Electron Spectroscopy

by

C. W. Tu and A. R. Schlier

Bell Laboratories
Murray Hill, New Jersey 07974

ABSTRACT

We have used Auger Electron Spectroscopy (AES) and Electron Energy Loss Spectroscopy (ELS) to study the effect of argon ion bombardment on the structural and electronic properties of InP (110) surface, and the effect of different surface preparation techniques. The ELS spectra are taken in the second derivative mode to facilitate the peak identification.

We find that with an argon ion dose of $\sim 3\times10^{16}/cm^2$ at an ion energy of 2kV, the first 2 to 3 layers of vacuum cleaved InP (110) become almost all In, as evidenced by the appearance of In bulk and surface plasmons (BP and SP) and the extinction of the BP and SP of InP. Even at a low dose ($1.5\times10^{15}/cm^2$) and at low energy (250 eV) argon ion bombardment on an oxidized InP (110) surface, the surface contains InP, indium oxide, In islands and oxygen, but no phosphorus oxide.

Since the effect of argon ion bombardment on InP is so great, ELS spectra are obtained on various InP (100) surfaces without argon ion bombardment. We find that the InP (100) after HCℓ etch for 3 minutes shows In microclusters on the surface as indicated by a shoulder at the In BP position in the ELS spectra, whereas InP (100) with Br-methanol etch shows no In microclusters within our experimental sensitivity. However, the AES spectra for both samples are similar.

Unified Theory of Intrinsic States, Core Excitons, and Defect-Induced States at Semiconductor Surfaces*

Roland E. Allen and John D. Dow
Loomis Laboratory of Physics, Materials Research Laboratory,
and Coordinated Science Laboratory
University of Illinois at Urbana-Champaign
Urbana, Illinois 61801

Three types of electronic states are prominent in experimental studies of semiconductor surfaces: intrinsic surface states, surface core excitons, and defect-induced surface states. We present a unified theory of these states, with application to relaxed (110) surfaces.

Of nine III-V semiconductors, we find that only GaP has intrinsic surface states definitively within the fundamental gap, in agreement with the available data. The bottom of this intrinsic surface state band in $GaAs_{1-x}P_x$ is predicted to lie within the gap for $x \gtrsim 0.05$.

Our results for surface core excitons are in agreement with the available experimental data for the Ga-V and In-V compounds. We predict that these previously observed Frenkel excitons do not preclude other excitations to the intrinsic surface states, and we suggest renewed attempts to observe the intrinsic states.

Our theory of surface defects implies that the ubiquitous pinning states[1] responsible for Schottky barrier formation in III-V's are due to surface antisite defects. This assignment explains the donor-acceptor behavior, stability, etc. of the pinning defects. Furthermore, the results of our calculations are in quantitative agreement with the measurements.

*Work supported in part by ONR under contract N00014-77-C-0537.

[1]W. E. Spicer, I. Lindau, P. R. Skeath, C. Y. Su, and P. W. Chye, Phys. Rev. Lett. 44, 420 (1980).

ANGULAR RESOLVED PHOTOEMISSION MEASUREMENTS ON CLEAN AND HYDROGEN COVERED Ge(111) SURFACES

R.D. Bringans and H. Höchst

MPI für Festkörperforschung, Heisenbergstr. 1, 7000 Stuttgart 80, Federal Republic of Germany

The angular resolved photoemission technique provides a direct probe of the dispersion in momentum space of the electron energy bands of solids. In this study of the clean and hydrogen covered (111) surface of germanium, both the bulk band structure and surface states were investigated.

The possible technical applications of amorphous Si-H and Ge-H have stimulated a considerable amount of work on these materials and it has become clear that the effect of hydrogen atoms on the electronic properties of Si or Ge surfaces (either internal or external) should be investigated for a full understanding of these materials. Angular resolved photoemission can be used to provide information about the symmetry of the physical environment of the adsorbed hydrogen atom and about the bonding of the atom to the host lattice. Results are presented for hydrogen adsorbed on Ge (111) and show a strong hydrogen induced peak which has considerable angular dispersion. A comparison is made with recent photoemission results of amorphous Ge-H.

In addition to the interest in hydrogen adsorption, a prototype material such as Ge provides a good testing ground for many of the unresolved questions about the photoemission process. Angular dependent measurements made on the clean Ge (111) surface will be discussed in this context and compared with band structures.

INTERFACE STATE AND OXIDE CHARGE GENERATION IN THE Si-SiO_2 SYSTEM BY PHOTOINJECTION OF CARRIERS

E. W. KREUTZ
Institut für Angewandte Physik, Technische Hochschule Darmstadt,
Schloßgartenstraße 7, D 6100 Darmstadt, Fed. Rep. Germany

The generation of interface states and of oxide charge in the Si (substrate) /SiO_2 (film) heterojunction system are examined during X-irradiation and during illumination with visible and UV light. Samples under investigation are oxidized single crystalline wafers and MOS capacitors. In both the cases substrates of p(100) Si (carrier concentration 7 x 10^{14} cm^{-3}) are thermally oxidized in dry oxygen resulting in oxide films in the 500 to 5000 Å thickness region. Semitransparent or thick Al electrodes have been used as field plates. The interface state density and the oxide charge are evaluated from combined measurements of surface conductivity, internal photoemission[1)], and thermal annealing as a function of external electric fields.

The spectral response and the temperature dependence of the internal photoemission data follow in the oxide shallow levels below the oxide conduction band minimum, deep levels above the oxide valence band maximum, and centers about midgap. The kinetics of the photoemissive processes involve that charging and discharging of these states are accomplished by the excitation of carriers over or tunneling of carriers through the internal potential barriers and by the creation of electron-hole pairs with subsequent trapping. The sign, the magnitude and the location of the photon induced oxide charge depend on the excitation mechanism, the exposure time, the oxide thickness, the oxide electric field, and the temperature. The interface state density is effected by the midgap oxide states close to the interface which are generated by the photon injected current. The changes in the interface state density are governed as the oxide charge changes.

1) E. W. Kreutz, phys. stat. sol. (a) 29 (1975) 195

Charge Transport and Storage in Ion Implanted Metal-Oxide-Semiconductor Structures

L. Augulis, L. Pranevičius

Polytechnic Institute of Kaunas, LITHUANIA, U.S.S.R.

Charge storage and memory characteristics of metal-implanted SiO_2-Si structures have been investigated. The ion implantation have been used to create strictly localized and controled concentration of trap centers in SiO_2 which have been charged or discharged by electrical pulses. To achieve memory effects the trap centers have to be situated in SiO_2 as possible as near to the Si-SiO_2 interface to allow an effective tunneling process which is the basic requirement for electrical operation.

It is very important that the tail of defects distribution in SiO_2 would not effected the properties of Si-SiO_2 interface. If the Si-SiO_2 interface is damaged by ion implantation the density of fast surface states increases. Increasing surface states density debase the electrical properties of devices.

These contradictory requirements have been fulfilled by proper implantation. The charge effects and memory characteristics have been observed in MOS structures implanted by Ar, Ti and Sn ions with energies 50-100 keV and doses 10^{13} ions·cm^{-2} and less.

The memory characteristics of implanted MOS devices are similar to MNOS but simpler in fabrication. The switching characteristics were measured during 10^6s. The discharge was not observed over an investigated period.

The charge transport mechanism in the implanted MOS structures has been investigated. It is found that at doses of the order of 10^{13} ions·cm^{-2} the conduction mechanism proposed by Fowler-Nordheim changes to Poole-Frenkel mechanism. To observe memory effects the MOS structure have to include SiO_2 layer with differing conduction mechanism along it thickness. It is achieved technologically using ion implantation. The conductivity through the upper surface layer of SiO_2 with the high concentration of defects is determined by Poole-Frenkel mechanism and conductivity through the SiO_2 layer situated near the Si-SiO_2 interface with the low concentration of defects is determined by the Fowler-Nordheim mechanism.

The physical nature of defects which act as trap centers created by ion implantation in SiO_2 is discussed.

ON THE ACCEPTOR NATURE, FORMED IN THE SURFACE LAYER AT SILICON THERMAL EVAPORATION.

L.N.Aleksandrov, R.N.Lovyagin, L.N.Safronov.
Institute of Semiconductor Physics, Siber.Branch.
of the USSR Academy of Science, Novosibirsk, USSR.

For the preparation of atomically clean Silicon surface before epitaxy or heterojunction formation the thermal evaporation of surfacial layer at temperatyre 1200-1350^{0}C is used. It is known that this action results in the formation of surface p-type layer conductivity in Silicon of n-type or to the high charge carrier concentration near surface in Silicon of p-type.

For the ascertation of acceptor nature the spectrum of low temperature ($\leq$6K) photoluminescence of this layer were studed. It was discovered, that the spectrum of photoluminescence of the plate surface layer after thermal evaporation in ultra high vacuum ($<10^{-6}$ Pa) are the superposition of several bands stipulated for exciton annigilation. They are connected: 1) with single unionized Boron atoms in substitutional position in Silicon lattice; 2) with pairs or more large clusters of substitutional Boron atoms in the layer, that has thickness of 1μm and high acceptor concentration (near 10^{18} cm^{-3}).

The processes, that results in narrow concentration profile of Boron atoms near Silicon plate surface formation are discussed. Accumulation of Boron is a result of considerable difference (to 60-100 time) of the Boron and Silicon atoms evaporation rate in the nonsteady-state diffusion condition. The receiption of impurity atoms is possible both from the residual atmosphere and from the monocrystalline specimen volume, for example, because of the electrically non-active boron-contained complexes desintegration.

[illegible] L.N.Aleksandrov, R.N.Lovyagin, V.Novik, A.I.Suprikin. Proceed. AS USSR, [illegible] Materials, 15 (1980) 1148; (in Rus).

[illegible], I.S.Smirnov. Proceed. 6th Intern. Summer School on Latti- [illegible] Sal, Poland, 1980.

[illegible], N.Lovyagin. ICVGE-4, Preprints, Nagoya, 1978, p.270.

Relationship between the polar surfaces of CdS crystals and the properties of CdS-Cu_2S and CdS-CdTe heterojunctions.

Akihiko Kobayashi
Dept.of Applied Physics, The Univ.of Tokyo.
Bunkyo-ku, Tokyo 113, JAPAN

The single crystals of II-VI semiconducting compounds have polar surfaces consisting of metallic and or non-metallic constituent elements of the compounds, and it is known that there is difference in the chemical activity of the respective polar surfaces. I report here the effects of the polar surfaces of CdS crystals on the formation of the transition region of CdS-Cu_2S and CdS-CdTe heterojunction diodes.

CdS-Cu_2S heterojunctions prepared by chemically converting CdS surfaces into Cu_2S have p-n step structure at the transition region of the heterojunction diodes. But the different diffusion potentials are obtained for these diodes, that is, the potential is about 0.8 V for the samples in which Cu_2S is grown on the S-face of the CdS (S-face sample) and the potential of about 0.5 V for the Cd-face samples.

The junction capacitance of the S-face samples increases gradually as the temperature rises, while the junction capacitance of the Cd-face sample begines to decrease at about 100 K and to increase around 200 K. This capacitance decrease is considered as the presence of an interface layer between CdS and Cu_2S, because CdS is an n-type semiconductor and the presence of the interface layer decreases the fiffusion potential. The penetration of Cu-element into the CdS side of the Cd-face samples is shown by EPMA measurments and the presence of the interface layer is caused by the penetrated Cu and understood by the fact that the Cd-face of the CdS is more chemically stable than the S-face is.

CdTe layer is grown on the polar surfaces of the CdS by LPE from Cd-solution and the grown layer is also shown to be strongly dependent on the polar surface of the CdS crystals. The red-brown layer is grown on the S-face and the penetration of Te is shown in the CdS side by EPMA measurments, so the penetrated Te is considered to cotribute to the formation of the red-brown layer. The brack layer, however, is grown on the Cd-face and the layer is identified as CdTe by comparing the photoluminescence spectra of the layer with those of CdTe single crystals. No penetration of Te is shown in the CdS side of these CdS-CdTe heterojunctions.

The electrical and optical properties of the transition region of thus prepared CdS-CdTe heterojunctions will be presented precisely at the conference together with the results obtained for the CdS-Cu_2S heterojunctions.

DEVELOPMENT AND CHARACTERIZATION OF A MONOCHRISTALLINE SILICON SOLAR CELL.

N. Kesri

Institute of Physics, University of Science and Technology Houari Boumediene, Alger, BP.9, ALGERIA

Abstract :

The following is a presentation of the work undertaken to develop and characterise a monochristalline silicon photovoltaïc cell, this being the first time that such a cell has been developed with in a research division of the Algiers University of Science and Technology and in conjunction with industrial laboratories.

On the basis of a wafer of monochristalline silicon of the p-type, 7.5cm in diameter and 375μ thick, the following successive stages led to the development of this cell: a) epitaxial growth of a layer p on a layer p^+, b) the bringing about of a p-n junction by the diffusion of phosphorus obtained from the thermal decomposition of $POCl_3$ in an nitrogeneous atmosphere, c) evaporation of aluminium on both surfaces followed by photomasking and deposition of a protective layer of silicon oxide on the front surface. Manipulation of a cell with p-n homojunction gave a short circuit current I_{sc} of about 0.5 amps and an open circuit voltage V_{oc} of about 0.5 volts, i.e. an effective signal of almost 90 watts per square metre. Tests were made on the cell obtained by epitaxial growth of a slightly doped layer on a substrate of the same type but strongly doped. Characterisation was related to the type and concentration of charge carriers and to resistivity, using the four-point method and Hall's effect. Characteristics I-V were determined. It can be seen a strong inverse current and the lacq of any significant difference between the efficiency of cells without an epitaxial layer ($p-n^+$) and these with epitaxy (p^+pn^+).

Tuesday afternoon, June 9, 1981

Session Tu-C: Core Level Spectroscopy

(Room 1123)

Chairman: R. N. LEE

1:40 A Quantum Effect in Surface Plasmon Excitation. P. LONGE and S. M. BOSE

2:00 Incident-Energy Dependence of the 3p Electron Energy-Loss Spectra of Nickel. T. JACH and C. J. POWELL

2:20 Absolute Core Level Binding Energies for 4d Transition Elements. Y. S. CHEE, B. SLAGSVOLD, J. F. MORAR, R. L. PARK and R. N. LEE

2:40 The Appearance Potential Spectroscopies of Evaporated Thin Lanthanum Films. J. ZHUGE, X. L. PAN and Z. Y. HUA

3:00 Soft X-Ray Appearance-Potential Spectra of Rare Earth Ho and Ho-Ni Alloy. D. CHOPRA and H. K. CHUNG

3:20 Resonant Photoelectron Appearance Potential Spectroscopy. Z. Y. HUA, J. ZHUGE and X. L. PAN

3:40 Appearance Potential Spectra of Semiconductors. J. F. MORAR and R. L. PARK

4:00 Evidence for Screening Effects in the Carbon KVV Auger Lineshape of Intercalated Graphite. B. I. DUNLAP, D. E. RAMAKER and J. S. MURDAY

4:20 Auger Line Shape Analyses for Expitaxial Growth in the Cu/Cu, Ag/Ag, and Ag/Cu Systems. R. W. VOOK and Y. NAMBA

4:40 Surface Chemical Characterization by Auger Signal Decomposition: Silicon Nitride. H. H. MADDEN and G. C. NELSON

5:00 XPS Studies of the Photodecomposition of AgCl. J. SHARMA, P. DiBONA and D. A. WIEGAND

5:20 Electron Spectroscopie Study of Phase Transition $V_2O_5 \rightarrow V_6O_{13}$. I. CURELARU, E. SUONINEN and E. MINNI

A QUANTUM EFFECT IN SURFACE PLASMON EXCITATION*

Pierre Longe
Institut de Physique B5 - Université de Liège
Sart Tilman, B-4000 Liège, Belgium

and

Shyamalendu M. Bose
Department of Physics and Atmospheric Science,
Drexel University, Philadelphia, PA19104.

An important quantum effect related to the uncertainty principle should modify the surface plasmon excitation rate in X-ray photoemission or other electron spectroscopies of metals (semi-infinite medium and thin films). It is shown that the total intensity of the surface plasmon satellite, compared to the main line intensity as a reference, depends quadratically on the inverse electron velocity and not linearly as suggested by the usual semiclassical model[1]. This modification of the surface plasmon excitation rate is essentially due to a quantum effect which seems to have been neglected up to now; this is directly related to the uncertainty principle. Indeed the interaction time Δt of the exciting electron with the surface mode is of the order of $(vq)^{-1}$, v being the electron velocity and q^{-1} the penetration depth of the surface wave ($\hbar q$ is the surface plasmon momentum). This finite Δt entails that the energy $mv^2/2$ of the exciting electron becomes uncertain within the range $\hbar/\Delta t \simeq \hbar qv$ with regard to the conduction electrons in the surface wave region, even when this energy is measured with the accuracy of the detector. The quantum character of the exciting electron may thus become important for high energies and one can no longer use the usual semiclassical model where this electron is treated as an 'external' potential exciting individual or collective modes of the conduction electron gas.

More precisely, using a formalism presented by Chastenet and Longe[2] for the bulk plasmon problem, the excitation probability of the surface plasmon, which is of the order of $e^2/\hbar v$ in the semiclassical approach, appears to be modified in the quantum approach by a factor of the order of $\hbar q/mv$. This quantum correction should be observable in experimental situations which are discussed.

*Research supported by FNRS, Belgium.

1. H. Raether in Springer Tracts in Modern Physics, Ergebnisse der Exakten Naturwissenschaften, ed. by G. Höhler (Springer, Berlin, 1965) vol. 38 p. 84.
2. D. Chastenet and P. Longe, Phys. Rev. Lett. 44, 91 (1980); 44, 903(E), 1980.

Incident-Energy Dependence of the 3p Electron Energy-Loss Spectra of Nickel

Terrence Jach and C. J. Powell

Surface Science Division, National Bureau of Standards, Washington, D.C.20234

Measurements have been made of the electron energy-loss spectra of nickel for incident electron energies in the range 150 eV to 2000 eV. These measurements have been made using a double-pass cylindrical-mirror analyzer and with the scattered electrons retarded to a pass energy of 100 eV. Attention has been focussed on the 50-100 eV energy-loss range which includes features associated with excitations from the Ni 3p level.

At high incident electron energies (1-2 keV), the loss spectrum has three principal features. The most pronounced feature is the edge at about 67 eV energy loss corresponding to the threshold for 3p-electron excitation. Two much weaker features observed are a dip in the energy distribution just below the 3p edge and a satellite peak about 12 eV above the edge. The first of these weak features corresponds to a Fano-type interference which is more limited in extent than that found previously.[1] The second weak feature is a "satellite" which may correspond to atomic excitations found in nickel vapor.[2]

We have found that the intensities of the Fano feature and of the satellite relative to the main 3p edge decrease considerably as the incident energy is reduced from 1000 eV to 150 eV. We believe that the disappearance of the Fano dip is associated with an increase in the Fano-lineshape parameter q as the momentum change in the excitation increases. The disappearance of the satellite intensity may be associated with deviations from dipole scattering with increasing momentum transfer. Other possible interpretations will also be discussed.

[1] R. E. Dietz, E. G. McRae, and J. H. Weaver, Phys. Rev. B 21, 2229 (1980).
[2] R. Bruhn, B. Sonntag, and H. W. Wolff, J. Phys. B 12, 203 (1979).

ABSOLUTE CORE LEVEL BINDING ENERGIES FOR 4d TRANSITION ELEMENTS

Yong S. Chee, Bjorn Slagsvold,*
J. F. Morar, and Robert L. Park
Department of Physics, University of Maryland
College Park, Maryland 20742

and

R. N. Lee, Naval Surface Weapons Center
White Oak, Silver Spring, MD. 20910

APS has been used previously to determine the absolute core binding energies for the $2p_{3/2}$ level of the 3d transition elements. We have recently extended these measurements to include 4d transition elements. APS determines binding energies by measuring the threshold energy for promoting a core electron into an unfilled state; therefore the density of available states for the first few volts above the Fermi level will influence the shape of the spectrum and must be considered in the determination of binding energies. A small modulation was impressed on the incident electron energy so that lock-in techniques could be used to record a derivative spectrum. The moldulation broadening and the broadening caused by the thermal energy spread of the incident electrons have also been considered in the data analysis. Since the only absolute measurement made in determining these binding energies was the potential difference between the sample and the emitter this method avoids the many uncertainties of using electron momentum analyzers, as in XPS where the energy of an ejected core electron is inferred from its measured momentum. XPS should benefit from the availability of an accurate table of binding energies useful for calibration.

* Current Address: Fysikkseksjonen, NTH, 7034 Trodheim, Norway.

THE APPEARANCE POTENTIAL SPECTROSCOPIES OF EVAPORATED THIN LANTHANUM FILMS

J. Zhuge, X. L. Pan and Z. Y. Hua
(Modern Physics Institute, Fudan University, Shanghai, P.R.C.)

Abstract

The SXAPS and AEAPS of La are comparatively studied. A specially designed electron gun with a Wehnelt electrode is used for the AEAPS. Two types of cathode used in the gun are pure tungsten and LaB_6 coated on Ta. The latter also served as an evaporating source of La. Experimental results show that the peak shapes of AEAPS for La are different from those obtained by SXAPS. In AEAPS the La-M_5 and La-M_4 peaks are splitted. Furthermore, the height ratio of the splitted parts of M_4 peak for the thin evaporated La film (on stainless steel) are different from that of the La ingot. The work function of La measured by the AEAPS method is 3.8 eV with pure tungsten as the reference (4.52 eV).

Soft X-Ray Appearance-Potential Spectra of Rare Earth Ho and Ho-Ni Alloy*

D. Chopra and Hyo Ki Chung
Department of Physics, East Texas State University
Commerce, Texas 75428, USA

Soft x-ray appearance-potential spectra of $M_{4,5}$ and $N_{4,5}$ levels of metallic holmium (Ho) and Ho-Ni alloy have been obtained in the 140-1400 eV range. The spectra represent the differential excitation probability of the core levels and mirror the self-convolution of the density of unoccupied states of the surface atoms under the influence of alloy composition. The final states in Ho are localized or atomic f levels which split due to the exchange interaction of the f electrons and d vacancies. This splitting leads to considerable multiple structure in the spectra. The observed binding energies of the M and N levels of Ho-Ni alloy were determined to be lower than those of metallic Ho. The binding energy of Ni L_3 level in the alloy showed a shift of 0.8 eV to higher energy. The widths of Ho peaks also showed a corresponding decrease as a result of alloying. Both these measurements suggest the charge transfer from Ni to Ho is in variance with the observed greater electronegativity of Ni relative to Ho. The interpretation of the observed spectra has been attempted in terms of the common Fermi level of the alloy[1] adjusted according to surface concentrations of constituent atoms and their densities of states. This model predicts an increase in the core level binding energies in Ni and a decrease of those in Ho. The conclusion is consistent with the observations that Ni is nonmagnetic in most R-Ni compounds (R = rare earth) resulting from the transfer of electrons from R to Ni until the nickel d-band is filled.[2-3]

* Supported by the Robert A. Welch Foundation and East Texas State University

[1] G.K. Wertheim, J.H. Wernick and G. Crecelius, Phys. Rev. B 18, 1978

[2] J. Farrell and W.E. Wallace, Inorg. Chem. 5, 105 (1966)

[3] J.W. Ross and J. Crangle, Phys. Rev. 133, A 509 (1969)

RESONANT PHOTOELECTRON APPEARANCE POTENTIAL SPECTROSCOPY

Z. Y. Hua, J. Zhuge and X. L. Pan
(Modern Physics Institute, Fudan University, Shanghai, P. R. C.)

Abstract

The resonant photoelectron appearance potential spectroscopy (RPAPS) is a new core-level spectroscopy developed from the basic idea involved in the soft x-ray appearance potential spectroscopy (SXAPS) and the x-ray photoelectron appearance potential spectroscopy (XPAPS).

A solid sample is exposed to the soft x-rays generated from a build-in x-ray tube, where the material used for the tube anode is identically the same with that of the sample. When the anode voltage reaches the threshold value (appearance potential), the core-level electron of the sample may have a resonant absorption of the characteristic x-rays and be excited to a higher level, with a hole being created in the core-level and Auger electrons emitted through the deexcitation process. By measuring the total photoelectron yield with respect to the anode potential the RPAPS is obtained.

Comparing with SXAPS, RPAPS has the advantage of better sensitivity for the sub-peaks of principal elements and peaks for the impurities under the same operating condition. Results from pure nickel and nickel alloys are given for demonstration.

APPEARANCE POTENTIAL SPECTRA OF SEMICONDUCTORS*

J. F. Morar and Robert L. Park
Department of Physics and Astronomy
University of Maryland, College Park, Md. 20742

High resolution appearance potential spectra of the L and K levels for the (100) face of silicon have been measured with a new soft x-ray appearance potential spectrometer employing a field emission array electron source and nude surface barrier x-ray detector. The measured threshold for the silicon L and K levels were 95.5 and 1842.0 volts respectively. The relationship between these thresholds and the binding energies of the silicon L and K levels will be discussed. The greatest advantage of using APS for the determination of core level binding energies is that the incident electron energy is the only quantity measured absolutely. In conventional APS this energy is determined by measuring the potential difference between the cathode and sample, and correcting for the thermal energy distribution and work function of the cathode. In this spectrometer field emitted electrons tunnel directly from the Fermi level so there is no work function correction to be made; furthermore the energy distribution of the emitted electrons is well characterized by reliable theoretical calculations. Since field emission produces no light a nude surface barrier x-ray detector was used thus producing an instrument with high accuracy, resolution, and sensitivity.

* Work supported by the U.S. Office of Naval Research under Contract N00014-75-C-0292. Computer time and facilities provided by the University of Maryland Computer Science Center.

EVIDENCE FOR SCREENING EFFECTS IN THE CARBON KVV AUGER LINESHAPE OF INTERCALATED GRAPHITE

B. I. Dunlap, D. E. Ramaker, and J. S. Murday
Code 6170
Naval Research Laboratory
Washington, DC 20375

A symmetry resolved one-electron density of states (DOS) for graphite is extracted from existent XPS and XES data and used in conjunction with atomic matrix elements to construct a carbon KVV Auger lineshape for graphite which is in substantial agreement with experiment. In the absence of available XES data for C_8Cs and C_6Li, an additional peak is added to the graphite one-electron DOS near the Fermi energy; the energy and intensity of this peak is determined by fitting the C KVV Auger spectra of C_8Cs and C_6Li. The intensities of this peak are interpreted as screening charge surrounding the C 1s core. A fraction of an electron (1/4 and 1/3) resides on the core ionized carbon atom for the case of C_8Cs and C_6Li, respectively. This effective screening charge is examined in terms of recent screening models. The differential effects of this charge on the photoelectron and Auger lineshapes are also discussed.

AUGER LINE SHAPE ANALYSES FOR EPITAXIAL GROWTH IN THE Cu/Cu, Ag/Ag, and Ag/Cu SYSTEMS

R. W. Vook and Y. Namba

Department of Chemical Engineering and Materials Science
Syracuse University, Syracuse, N.Y. 13210

ABSTRACT

A new measure of the MVV doublet Auger line shape called the R-factor has been applied to homoepitaxial layer growth on (111)Cu and on (111)Ag as well as to the epitaxial growth of (111)Ag on (111)Cu. AES and TEM show that as thick (~ 1500Å) monocrystalline Cu and Ag films grow thicker, R oscillates with a period equal to one atomic layer. Polycrystalline films do not show such a periodicity. The changes in doublet line shape are interpreted as arising from the superposition of two sets of doublets slightly displaced in energy. One set is presumed to come from the flat areas of the film and the other from the edge areas of incomplete layers. The origin of the periodicity in R arises then from the atomic relaxations that can be expected at the edges of surface steps, whose density varies periodically during growth.

For the initial stages of (111)Ag growth on (111)Cu, an initially high R_{Ag} decreased to bulk values as the Ag thickened beyond one or two monolayers for both polycrystalline and monocrystalline films; but periodicities in R_{Ag} and R_{Cu} were detected only for monocrystalline growth. The high initial values of R_{Ag} are interpreted as arising from changes in the energy levels of the corresponding Auger transitions with changing interatomic spacing. Since the Ag overgrowth is compressed towards the smaller lattice parameter of the Cu substrate, energy levels in the valence band of Ag might be expected to become more widely separated. Consequently a more highly resolved MVV doublet for Ag would occur, resulting in a larger R_{Ag}. The effect is not observed in the MVV levels from the thick Cu substrate because of its structural rigidity.

The growth mode for (111)Ag on (111)Cu was shown to be of the Stranski-Krastanov type. Previous measurements using transmission electron microscopy and diffraction were combined with Auger amplitude and R_{Ag} factor studies to show that Ag grows initially as two-monolayer high islands (with some more complicated phenomena occurring at 50 coverage) until two complete monolayers have formed. On this Ag bilayer substrate, two-monolayer high Ag islands form to a coverage of approximately 50%. As more Ag is deposited, the coverage increases only slightly, but two-monolayer high islands nucleate on top of the islands that are already present, leading to a high, flat island surface topography, in agreement with previous TEM and coverage measurements.

The results show that by combining TEM, TED, and RHEED studies with AES amplitude and R factor line shape measurements, one can obtain highly detailed information on the structure, microstructure, and growth modes of epitaxial thin or thick films.

Surface Chemical Characterization by Auger Signal Decomposition: Silicon Nitride*

H. H. Madden and G. C. Nelson
Sandia National Laboratories†
Albuquerque, New Mexico 87185

In a recent study[1] of the silicon $L_{2,3}VV$ signal from plasma-deposited silicon nitride films the presence of elemental silicon and of silicon-hydrogen bonding could be inferred from an analysis of the shape of the Auger signal. By subtracting $L_{2,3}VV$ signals representing Si-Si and Si-H bonding from the plasma nitride signal a residual signal was obtained that agreed in shape with the signal from a stochiometric, chemical-vapor-deposited silicon nitride film.[2] All of the signals had been corrected for loss features by background subtraction and loss deconvolution, and were in the integral, N(E) mode. Subsequent analysis of the plasma nitride lineshape was performed by synthesizing the curve using a least-squares-fit computer routine and three component curves representing Si-Si, Si-H and Si-N bonding. This curve synthesis technique also indicated that for the plasma nitride Auger lineshape analysis can be used to detect differing states of chemical bonding. The Si-$L_{2,3}VV$ signal from a silicon oxynitride film was also analyzed using the curve synthesis technique and the results were found to be in contradiction to those of an earlier signal decomposition analysis.[2] A synthesized curve that agreed well in shape with the silicon oxynitride signal could be obtained using Si-Si, Si-H, Si-N and SiO_2 component curves. Meaningful use of these techniques of curve decomposition and curve synthesis for extracting chemical bonding information from Auger lineshapes depend strongly on working with all possible component curves and on the relative energy positions of the component curves with respect to the composite curve and with respect to each other. Methods for handling these potential "pitfalls" of the techniques will be discussed.

---

*This work sponsored by the U. S. Department of Energy under Contract DE-AC04-76-DP00789.

†A U. S. Department of Energy facility.

[1] H. H. Madden, J. Electrochem. Soc. 128, 625 (1981).

[2] H. H. Madden and P. H. Holloway, J. Vac. Sci. Technol. 16, 618 (1979)

AD-A130 495 INTERNATIONAL CONFERENCE ON SOLID FILMS AND SURFACES (2ND) (ICSFS-2) PROG. (U) MARYLAND UNIV COLLEGE PARK JUN 81 N00014-81-C-0039 2/2

UNCLASSIFIED F/G 7/4 NL

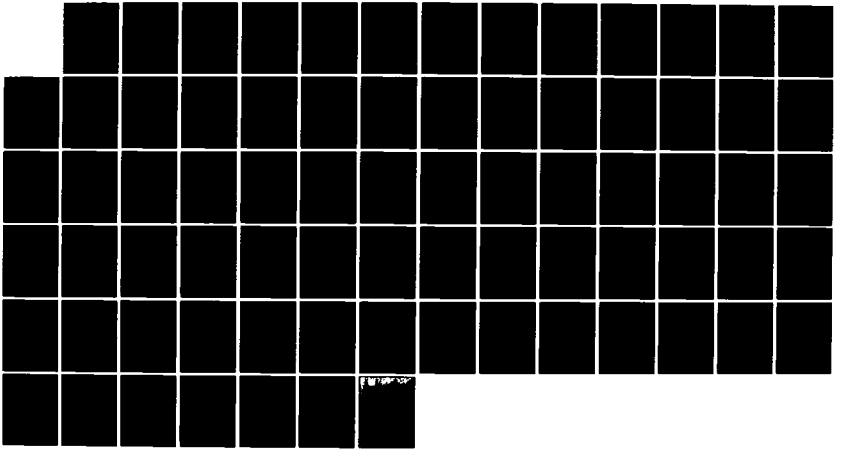

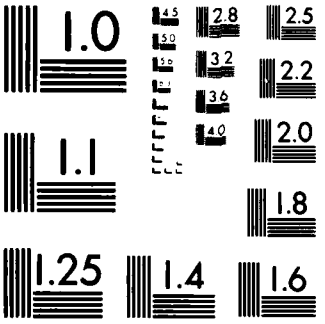

XPS Studies of the Photodecomposition of AgCl

J. Sharma*, P. DiBona** and D. A. Wiegand
Energetic Materials Division
LCWSL
ARRADCOM, Dover, N. J. 07801

The decomposition of AgCl due to ultraviolet and x-ray irradiation was investigated by X-ray Photoelectron Spectroscopy (XPS). Samples were prepared from freshly made AgCl powder either directly from the powder or by melting AgCl onto a platinum substrate, the latter giving significantly higher XPS intensities than the former. The AgCl was exposed only to weak red light prior to irradiation. The results after irradiation indicated a broadened Cl 2p doublet which was resolved into an unbroadened and unshifted Cl 2p doublet and a Cl 2p doublet shifted to a higher binding energy ($\sim$ 2 eV.). Similar results were found for the Cl 2s line. The results thus indicate the presence of a less electronegative form of Cl on the surface of AgCl after irradiation. The Ag lines were neither broadened nor shifted within the precision of the measurements ($\sim$ 0.2 eV.). With increasing time of irradiation the intensities of the Ag line decreased. Possible forms of this photo-induced Cl and the relationship to the photographic process will be discussed.

* Present address: Naval Surface Weapons Center
White Oak, Silver Spring, MD 20910

** Present address: Honeywell Inc.
Hopkins, MN 55343

I. Curelaru

Chalmers University of Technology, Department of Physics,
S-412 96 Göteborg, Sweden

E. Suoninen and E. Minni

University of Turku, Department of Physical Sciences,
SF-20500 Turku 50, Finland

ELECTRON SPECTROSCOPIC STUDY OF PHASE TRANSITION $V_2O_5 \rightarrow V_6O_{13}$

In previous studies [1,2], the phase transition $V_2O_5 \rightarrow V_6O_{13}$ was found to occur on the surface of multicrystalline V_2O_5 samples as a result of electron bombardment. The observations of the resulting XPS spectra [1] were, however, hampered by interference of the spectra from the indium substrate and possible surface reactions during the experiments. In the present study, a silver substrate was used to reduce interference due to substrate oxidation. The kinetic energy of the bombarding electrons was gradually raised to 5 keV. The pressure of the analyzer chamber was monitored during the bombardment. Composition of the residual chamber atmosphere was also observed.

The observed changes of the vanadium XPS emission confirm creation of V^{4+} ions in the surface layer as a result of the bombardment. The oxygen emission is seen to remain virtually unchanged. This shows that the VO_4 tetrahedra, which are the basic building block of all V-O compounds, are not effected. Onset of the transition is manifested by a short pressure peak caused by emission of gases due to the transition reaction. Analysis of the emitted gas is difficult because of the dynamic nature of the emission, but the main effect during the pressure rise seems to be increase in the emission of gases produced by catalytic reactions consuming the oxygen liberated in the transition reaction.

Subsequent heating of the sample after intense bombardment did not appreciably change the XPS spectrum. It is concluded that the depth of the transformed layer exceeded the escape depth of the electrons (< 1 nm) after bombardment with 5 keV electrons. Widely different values are observed for the critical electron energy needed to initiate the transition in different experiments (cf. data in [2] and [1]). Assuming the transition to be temperature controlled, this can be understood on the basis of varying surface heating conditions.

[1] E. Suoninen, E. Minni and I.M. Curelaru, J. de Microscopie et de Spectroscopie Electronique 6, no. 1 (1981).

[2] I. Curelaru, Solid State Communic. 34, 729 (1980).

WEDNESDAY MORNING, JUNE 10, 1981

Plenary Session

Main Auditorium

Chairman: R. E. GLOVER, III

9:00 Order in Two Dimensions
L. D. ROELOFS

9:45 LEED Studies of Surface Imperfections.
M. HENZLER

10:30 Clean Surface Reconstruction of BCC{001} Metals.
A. J. MELMED and W. R. GRAHAM

11:15 Epitaxy of Metal Films
E. BAUER

12:00 Misfit Accommodation at Interface by Dislocations.
J. WOLTERSDORF

Order in Two Dimensions

Lyle D. Roelofs

Physics Department

Brown University

Providence, RI 02912

Recent developments in the study of phase transitions in surface layers and overlayers are reviewed. In particular we outline the types of order which can occur in 2-d systems with emphasis on the effects of the (3-d) substrate. We also discuss the effects of various types of disorder inherent in real substrates and phase transitions of the substrate itself on both ordering properties and critical behavior. The current status of critical phenomena studies in chemisorbed and physisorbed layers is discussed and compared.

LEED Studies of Surface Imperfections

M. Henzler, Universität Hannover, Germany

The diffraction of low energy electrons is mostly used either for qualitative informations (e.g. existence of superstructures) or for determination of atomic positions within unit mesh via intensity evaluation assuming a strictly periodic surface. A lot of additional information is available as soon as besides existence and intensity of a spot its profile on the screen (in general profile in k-space) is used. In this way all kind of deviations from simple periodicity, periodic or non periodic may be derived quantitatively and qualitatively without much computations. For a qualitative evaluation a set of basic structural elements and their representation in the reciprocal space is discussed, so that a lot of imperfections like steps, islands, domains, point defects and some elements of their arrangement (like random or regular) are easily observed just by visual inspection of the LEED pattern. For quantitative evaluations the limitations due to the instrument have to be considered. They are described by the average quantity "transfer width", the maximum distance of surface atoms for a coherent diffraction. New instruments show transfer widths of more than 100 nm so that the maximum resolvable defect distance is a multiple of that length. For quantitative evaluation of non constant island sizes, terrace widths and so on assumption or informations on distributions (random or correlated) are needed together with a low computation effort. Out of the so far not high number of examples some typical ones are selected giving structural informations which are not available by other means, like surface cleaning procedures, chemical reactions with reconstruction, island formation during adsorption or epitaxy. A wide field is open for further use of the LEED beam profile evaluation.

ABSTRACT

Clean Surface Reconstruction of BCC{001} Metals

A. J. Melmed
Surface Science Division
National Bureau of Standards
Washington, D.C. 20234
and
W. R. Graham
Department of Materials Science
and Engineering
University of Pennsylvania
Philadelphia, Pennsylvania 19104

During the past decade, it has become known that the atomic structures of clean BCC{001} metal surfaces are not always the same as their bulk relatives; that is, sometimes they are reconstructed. W{001} was reported to be reconstructed below room temperature, evidenced by LEED, in 1971 and this was subsequently shown to be a clean surface phenomenon. Clean Mo{001} below room temperature and later Cr{001} and V{001} below about 630K were reported to be reconstructed and most recently, clean Nb{001} and clean Ta{001} were reported to be unreconstructed, e.g. normal, over wide ranges of temperature. An impressive array of surface probing techniques has been applied to various aspects of the reconstruction question, including LEED, AES, UPS, FIM, PLEED, MeV helium ion scattering and electron work function measurement, and a considerable amount of theoretical effort has been applied.

Among the BCC{001} metals reported to be reconstructed, there are substantial differences in the observed phenomena and differences regarding the correct theoretical description such that it is not appropriate, at present, to draw general conclusions. Even with W, which has probably been studied most extensively, there remain significant differences in the published conclusions of several authors. For these (and other) reasons, emphasis will be given in this presentation to the details of W{001} reconstruction.

It is generally agreed by LEED investigators that clean W{001} undergoes a reversible structural phase transition, going from a simple (1X1)structure above 300-400K to a reconstructed phase characterized as $(\sqrt{2}x\sqrt{2})R45°$ at lower temperatures, although all authors do not agree on the structural details. FIM studies have challenged the validity of the phase transition concept and have apparently lent support to some, but not all, of the LEED structural conclusions. The various LEED-derived and FIM-derived conclusions will be discussed and compared, and an attempt will be made to give a description of clean W{001} reconstruction which is consistent with most of the available data.

Epitaxy of Metal Films

E. Bauer, Physikalisches Institut,
Technische Universität Clausthal, D-3392 Clausthal-Z.
und SFB 126 Göttingen-Clausthal, Germany

The use of surface analytical methods such as LEED, AES, ISS, thermal desorption spectroscopy (TDS), work function change ($\Delta\phi$) measurements and the improvements of traditional thin film analysis techniques such as transmission and reflection high energy electron microscopy have lead to renewed interest in the epitaxy of metal films in recent years. In contrast to the older work which was mainly concerned with epitaxy via three-dimensional nucleation ("Volmer-Weber growth mode") on ionic crystals, the recent work concentrated more on growth modes in which at least initially an adsorbed monolayer is formed ("Frank-van der Merwe and Stranski-Krastanov modes"). These occur predominantly on metals but also on semiconductors. The results obtained in recent years in this field will be reviewed with special emphasis on the early stages of the condensation and on the interface structure.

MISFIT ACCOMMODATION AT INTERFACE BY DISLOCATIONS

J. Woltersdorf
Institut für Festkörperphysik und Elektronenmikroskopie
Akademie der Wissenschaften der DDR
Halle/Saale
German Democratic Republic

The great number of the existing dislocation concepts in interface theory, the different experimental observations of interface dislocations in the last decades, and the open questions of their interpretation and applicability form a complex of problems which can only be treated fragmentarily in this lecture. Thus we will restrict ourselves to a few selected topics which may be able to outline our subject.

The lecture is divided into the following parts:

a) Some introductory remarks are given, containing definitions as well as information on principal difficulties and open questions;

b) A short treatment on the relation between epitaxy and misfit is presented because the knowledge of the mode of growth and the extent of pseudomorphism is important for predictions concerning the generation and motion of misfit dislocations at interface;

c) The third part contains some features and results of the Frank-van der Merwe-model in connection with a characterization of some other interface models; the aim of this third part is to elaborate the physical and the mathematical background of the dislocation concept in the interface theory;

d) Fourth, some experimental observations of interface dislocations in various systems and different degrees of interaction strength are presented and discussed;

e) The last part, then, contains some selected summarizing theses.

Wednesday afternoon, June 10, 1981

Session W-A: Semiconductor Films

(Room 0123)

Chairman: L. J. BRILLSON

2:00 Dopant Incorporation Studies in Silicon Molecular Beam Epitaxy (Si MBE). F. G. ALLEN, S. S. IYER and R. A. METZGER

2:20 On the Nature of Electron Irradiation Damage in Hydrogenated Amorphous Silicon. H. SCHADE

2:40 Optical and Electrical Properties of Hydrogenated Amorphous Silicon Films Deposited by Tetrode RF Sputtering. Y. GEKKA, Y. KIMURA and T. MATSUMORI

3:00 Coupled Electron-LO Phonon Modes of GaAs-$A\ell_xGa_{1-x}As$ Multilayer Systems. S. DAS SARMA

3:20 The Substrate Heating Effects on Ion-Beam Sputter-Deposited $CuInS_2$ and GaP Thin Films. J.-R. CHEN, C.-C. NEE, N.-L. HWANG, L. LU and Y.-C. LIU

3:40 Recent Studies of ZnS Films: Evaporation, Growth and Laser Irradiation Effects. T. N. CHIN, O. W. O'NEILL and P. E. HOUSER

4:00 Multi-Layer Film Structure for Light Sources. L. N. ALEKSANDROV and A. S. IVANZEV

4:20 Field Effect Studies on MIS Structures on PbTe Films. A. L. DAWAR, O. P. TANEJA, P. KUMAR, S. K. PARADKAR and P. C. MATHUR

4:40 Electrical Effect of Na, Ag, and Tℓ Impurities on Lead Telluride Thin Films. A. L. DAWAR, O. P. TANEJA, S. K. PARADKAR, P. KUMAR and P. C. MATHUR

5:00 Electrical Effect of Hydrogen on SnTe Thin Films. A. L. DAWAR, O. P. TANEJA, B. K. SACHAR, A. O. MOHAMMED, P. KUMAR, S. K. PARADKAR and P. C. MATHUR

DOPANT INCORPORATION STUDIES IN SILICON MOLECULAR BEAM EPITAXY (Si MBE)

F. G. Allen, S. S. Iyer and R. A. Metzger
Department of Electrical Sciences and Engineering
University of California, Los Angeles 90024
(Tel: 213 - 825-1123)

ABSTRACT

We have studied dopant incorporation mechanisms in Si MBE via a model that allows for a steady state build-up of dopant on the host surface as a result of the incident flux, the desorbing flux and the incorporation rate. Application of this model to gallium on silicon will be discussed. Using isothermal desorption spectroscopy and Auger analysis we determine the activation energy for gallium desorption from silicon to be $\sim$ 2·88 ev. The activation energy for incorporation is deduced to be $\sim$ 1·20 ev. The time for achieving steady state conditions after abrupt changes in flux may be equivalent to several hundreds to a few thousands of angstroms of grown film at normal growth temperatures and rates. A technique has been developed by which the desired steady state value of the accumulation of dopant is pre-adjusted, such that, the smear is reduced to negligeable values (< 200 A°). The saturation of the Sticking coefficient at high fluxes has been measured.

ON THE NATURE OF ELECTRON IRRADIATION DAMAGE IN HYDROGENATED AMORPHOUS SILICON *

H. Schade
RCA Laboratories
Princeton, NJ 08540, U.S.A.

Recently we have found the threshold energy for electron damage in undoped hydrogenated amorphous silicon (a-Si:H) to be over a factor 100 smaller than in crystalline silicon (i.e., about 1 keV vs. 100 keV). This result was obtained from damage profiling, a technique that is based on a resistivity increase of the electron-irradiated area, presumably due to the creation of dangling bonds. The increased resistivity leads to a shift of the Auger energies, due to electrical charging of these areas under the primary electron beam used to generate Auger electron emission. Scanning Auger micrographs then reflect areal non-uniformities in resistivity, and thus reveal the area of prior electron irradiation. By combining scanning Auger microprobing and sputtering (damage profiling), the depth of damage can be determined, and has been found to compare well with the calculated electron range.

In order to determine the role of hydrogen in defect generation, we have studied samples with different hydrogen content, deposited from silane in a dc glow discharge onto stainless steel substrates at different temperatures. The depth of damage depends not only on the electron energy, but also on the electron dose, and more importantly, on the hydrogen content of the a-Si:H. The depth tends to reach a saturation value that requires smaller doses at high energies; this behavior stems from the energy dependence of the cross section for defect generation. As for the hydrogen content, at a given energy and dose, the depth of damage is distinctly larger for a higher hydrogen content. Since SIMS profiles and annealing have shown no loss of hydrogen as a possible cause for the electron damage, we must conclude that hydrogen is linked to the nature of the damage. Two explanations may account for the observed dependence on the hydrogen content: a) With more breakable bonds in films of higher hydrogen content, a smaller dose is required to generate the same number of defects and thus the same depth of damage. b) Different types of defects exist, requiring smaller formation energies with higher hydrogen content. Hence, at a given energy and dose, the depth of damage is larger in films with higher hydrogen content. We have further evidence for different defect centers from photoluminescence measurements.

Since we have observed quantitatively very similar electron irradiation effects also in deuterated amorphous silicon (a-Si:D), an atomic displacement of hydrogen or deuterium can be ruled out as the cause for electron damage. Instead, Franck-Condon-type processes are suggested as the cause for bonding changes and defect generation which conceivably require similar energies in both a-Si:H and a-Si:D.

* Research reported herein was supported by Solar Energy Research Institute, under Contract No. XJ-9-8254, and by RCA Laboratories, Princeton, NJ 08540.

OPTICAL AND ELECTRICAL PROPERTIES OF HYDROGENATED AMORPHOUS SILICON FILMS DEPOSITED BY TETRODE RF SPUTTERING

Yasuo GEKKA, Yutaka KIMURA* and Tokue MATSUMORI

Department of Electronics, Faculty of Engineering
*Department of Physics, Faculty of Science
1117, Kitakaname, Hiratsuka, Kanagawa, 259-12 Japan

The effect of argon (Ar) on deposition and hydrogenation of amorphous Silicon have been studied. There have been many recent studies on the propertiies hydrogenated amorphous silicon (a-Si:H) films deposited under high Ar pressure in the range 10^{-2}-10^{-1} Torr, using diode sputtering technique. However,in order to study the effect of Ar, the properties of films deposited under low Ar pressure is still tobe investigated.

In this work, the deposition of a-Si:H was carried out in a mixed gas Ar and hydrogen(H_2) using a tetrode RF sputtering technique which is operative under low Ar pressure in the range 10^{-4} to^{-3} Torr. The tetrode RF sputtering apparatus has two pairs of electrodes,establishing a stable plasma state between the thermionic cathode and anode under a certain anode voltage even if the atmosphere is in a low pressure less than 10^{-3} Torr. The stability of the plasma state was verified by constant anode current. The a-Si:H was deposited on the top of a substrate by the application of RF power between the Si-target and the substrate which were placed and faced each other in the plasma gas. The most stable plasma were obtained at the Ar pressure of 1×10^{-3} Torr. The substrate temperature and RF power were maintained at 250°C and 150W, respectively.

The pressure ratio of H_2 / Ar in the sputtering process, ξ, was chosen as a experimental variable factor. The deposition rate, the dependence of the optical absorption coefficient α on wave length λ and the dependence of the electrical conductivity σ on temperature T were measured on a-Si:H films deposited at various values of ξ. The experimental results were indicate that the deposition rate of a-Si:H decreases as the value of ξincreases. As ξ is raised from 0 to 0.1, α decreases and approaches to that of crystaline Si. In spite of this, α tends to increase again at ξ=0.3. Optical band gap E_{opt}, deduced from$\sqrt{\alpha h\nu}$ vs.hν characteristics, increases from 1.4ev to 1.85 ev as ξ is raised from 0 to 0.1, whereas the E_{opt} decreases again to 1.75 ev at ξ = 0.3. The dependence of σ on T which is characterized by ln σ vs. 1/T shows that a transition of conduction mechanism takes place as the value of ξ is raised from 0 to 0.01.

The large value of α and the small value of E_{opt} in the films deposited at ξ = 0 are ascribed to localized states resulted from dangling bonds of Si. The existence of the high density of the localized states was confirmed by thedetection of variable range hopping conduction. The variation of α and E_{opt} in the range of ξ from 0 to 0.05 appears to be due to the vanishing of localized states. The localized states vanish following the reaction of H atoms with dangling bonds of Si. It became clear that the formation of Si-H bonds is saturated at ξ = 0.05. Vanishing of localized state was confirmed by the detection of band conduction which takes place in the films deposited at ξ above 0.05. This is consistent with the results of α and E_{opt}.

During deposition at ξ above 0.1, Si=H_2 bonds are formed and excess H atoms form voids in the deposited film. Under α = 0.3, a phase transition takes place in the film, because of large mounts of Si=H_2 bonds and voids and existence of stress. The stress due to Ar atoms included in a-Si film has been known as an origin of shock crystalization. The characteristic values of α, E_{opt} and σ in the films deposited at ξ = 0.3 appear to be associated with such phase transition.

Coupled Electron-LO Phonon Modes of GaAs-$Al_xGa_{1-x}As$ Multilayer Systems

S. Das Sarma, Department of Physics and Astronomy, University of Maryland, College Park, Maryland 20742

Abstract

Resonant inelastic light scattering spectroscopy has recently been used to study selectively doped GaAs-$Al_xGa_{1-x}As$ multilayers grown by molecular beam epitaxy technique. Electronic single particle and collective intersubband excitations have been observed in the quasi two-dimensional systems in these experiments. The collective electronic excitations are coupled to the longitudinal optical (LO) phonon modes of GaAs. Within a simple model of electron-LO phonon coupling for these quasi two-dimensional systems, we show how the relative intensities of the coupled modes and the non-Lorentzian line shape of the Raman spectra can be understood. Comparison with experimental results clearly shows that the linewidth of the single particle intersubband transition is proportional to the energy difference between the two subband levels involved in the excitation process. Possible mechanisms (electron-electron interaction, electron-impurity interaction, inhomogeneous broadening, etc.) giving rise to this kind of linewidth will be discussed. Finally the effect of final state interaction between the excited electron in the upper subband and the hole left behind in the lower subband, on such intersubband transition will be discussed in details, with particular reference to LO phonon mediated electron-electron interaction.

Spin-flip light scattering experiment essentially probes the single-particle electronic excitations in the system and is proportional to Im X_{ij} where X_{ij} is the irreducible response function for transition from subband i to subband j. In the simplest approximation Im X_{ij} has a peak at E_{ji}, the single particle energy difference between the subbands i and j, with a linewidth of Γ_{ji}. Non-spin-flip light scattering on the other hand probes the collective excitation spectrum and is proportional to Im $\tilde{X}_{ij}$ where $\tilde{X}_{ij}$ is the reducible response function. We have calculated X_{ij} in this system including effects of resonant screening by Coulomb interaction and LO-phonon mediated electron-electron interaction. Due to hybridization of electron and LO-phonon modes Im $\tilde{X}_{ij}$ has two peaks at energies $E^{\pm}_{ji}$. The line-shape of the spectrum is found to be non-Lorentzian. Comparison between E_{ji} and $E^{\pm}_{ji}$ gives valuable information about the strengths of Coulombs and electron-LO phonon interactions in the system. There is excellent agreement between the theoretically calculated line-shape and the experimental data[1] if one takes $\Gamma \propto E_{ji}$. There is experimental evidence[2] indicating that this is indeed the case in these systems.

References:

1. Ch. Zeller, S. Das Sarma, and G. Abstreiter. Physical Review B (to be published).

2. A. Pinczuk et al., Surf. Sci. 98, 126 (1980).

THE SUBSTRATE HEATING EFFECTS ON ION-BEAM SPUTTER-DEPOSITED $CuInS_2$ AND GaP THIN FILMS

Jiann-Ruey Chen, Chi-Chen Nee
Department of Materials Science and Engineering
National Tsing Hua University
Hsinchu, Taiwan, Republic of China

Huey-Liang Hwang, Learong Lu
Department of Electrical Engineering
National Tsing Hua University
Hsinchu, Taiwan, Republic of China

and

Yuen-Chung Liu
Department of Physics
National Tsing Hua University
Hsinchu, Taiwan, Republic of China

The $CuInS_2$/GaP heterostructure is proposed for efficient photovoltaic conversion for the reasons: (1) the direct gap of 1.55 eV for $CuInS_2$, (2) the large gap of GaP (2.25 eV) can provide the window effect, (3) the lattice mismatch between $CuInS_2$ and GaP is small (1.3%). In this work, ion beam sputtering was employed to deposit $CuInS_2$ and GaP thin films on graphite and single crystal NaCl substrate, in which the substrate heating effects were studied. The crystallographic structures were examined by the transmission electron microscope (TEM), and the deposited film compositions and impurity contents were analyzed by the Rutherford backscattering spectrometry (RBS).

From the RBS spectra, the as-deposited GaP and $CuInS_2$ films were found to be near-stoichiometric. Oxygen was only detected in the GaP films, which might be explained by the strong affinity between Ga and O_2.[1] The phase transitions at various temperatures were summarized, and compared with the reported phase transitions of the Ge sputter-deposited films.[2-4]

1. J. J. Loferski et al., Tech. Report No. SERI-X1-9-8012-1-03, p. 5, Dec. 1979.
2. E. Krikorian et al., J. Appl. Phys. 37, 3665 (1966).
3. C. K. Layton et al., Thin Solid Films 1, 169(L) (1967).
4. I. H. Khan, J. Appl. Phys. 44, 14 (1973).

RECENT STUDIES OF ZnS FILMS: EVAPORATION, GROWTH AND LASER IRRADIATION EFFECTS

T. N. Chin and Owen B. O'Neill
Fire Control Div., FC&SCWS Lab., US Army ARRADCOM
Dover, NJ 07801
and Phillip E. Houser
Applied Science Div., LCWS Lab., US Army ARRADCOM
Dover, NJ 07801

Abstract

In the evaporation of II-VI materials, it has been found that II-VI compounds are dissociated at temperatures much lower than their melting-point temperature, and the column VI elements can exist in several forms depending upon temperature and pressure. Within the last few years, however, films of CdS, ZnS and ZnSe have been prepared through electron beam evaporation for studies of photoconductivity and luminescence. Since thermal accommodation of gaseous species, chemical reactions and film growth all take place on the deposited surface, the interfacial processes are complex and further investigations are required to elucidate the mechanisms involved. On the basis of the atomistic theory of surfaces, several principles are outlined for compound film growth with the vacuum evaporation method.

The experiments in this study are designed to identify the principal processing parameters and their role in the growth and structures of the deposited films. The accommodation coefficient is found to be a meaningful parameter to characterize the film growth. At a constant deposition rate, the growth rate of the compound film diminishes as the substrate is heated, approaching the equilibrated temperature. Results obtained from this investigation demonstrate that the equilibrated temperature in the film growth increases with the increase of deposition rate. A three-dimensional diagram is presented here to show the dependence between these three parameters, i.e., deposition rate, substrate temperature, and accommodation coefficient.

Several typical growth structures of the ZnS films are shown in the SEM micrographs. The columnar growth structures and relatively large grains are distinctly observed in these ZnS films. Initial results obtained here are not yet sufficient to evaluate the applicability of the three structural zones as proposed in the Movchan-Demchishin model. An attempt has also been made to explore the effects of laser irradiations with these materials. Some initial results are included to illustrate the laser-induced strong interactions with these ZnS films.

MULTI-LAYER FILM STRUCTURE FOR LIGHT SOURCES.

L.N.Aleksandrov, A.S.Ivanzev.
Institute of Semiconductor Physics, Academy of Sciences of the USSR, Novosibirsk; All Union Research Institute of Light Sources, Saransk, USSR.

The use multi-layer semiconductor film structure allow to change the emission Spectrum and the spectral concentration of a radiometric quantity for the visible radiation of the light sources. The principle operation of the multi-layer interference film filter, their preparation at vacuum deposition structure transformation in the high temperature conduction were shown.

At the deposition on the glass or silica substrates the films are polycrystalline or amorphous. Strain stresses results in film recrystallization and the changing of their optical properties. The data of thermal treatment of the Zinc Sulphide and Magnium films in vacuum, Argon, Nitrogen or air atmosphere effects on transmittance and recrystallization kinetic are given.

They are studed the optical properties of the multi-layer structure with buffer Chromium film on the glass. When the film deposition rate is small, the Oxygen and Nitrogen are captured and form Chromium Oxides, Chromium Nitride layers on the glass. By films heating the transmission spectrum displacement to the short-wave side to 15–20 nm at the every 100K was observed. Over 600K the films become muddy and cracked because of the crystallization and increasing of thermal stresses.

The increasing of the thermal stability of multi-layer structures during the transformation of amorphous glass sourface into polycrystalline after deposition of metal films (Chromium) or Silicon monooxide or Silicon dioxide is shown. The possibility of making of incandescent lamp with "cold" light or "sun" lamps with colour temperature to 5500K with help of film coatings is shown.

The perspectivity of using of Tin Dioxide or Indium Dioxide doped films for heat-protecting coatings and increasing of incandescent lamp light emission is shown.

1. L.N.Aleksandrov, A.S.Ivanzev. Lightteonique, 1971, N5,(15); 1972,N12 (19), (in Rus).
2. A.S.Ivanzev. Proceed. AS USSR, Neorganical Materials, 1978, 14(962), (in Rus).
3. L.N.Aleksandrov, A.S.Ivanzev. Multi-layer film structure for light sources. Nauka, Novosibirsk, 1981, (in Rus).

"FIELD EFFECT STUDIES ON MIS STRUCTURES OF PbTe FILMS"

by

A.L. Dawar, O.P. Taneja, Partap Kumar, S.K. Paradkar and
R.C. Mathur
Department of Physics and Astrophysics, University of Delhi,
Delhi-110007, India.

ABSTRACT

D.C. conductivity and Hall coefficient measurements have been made on MIS structures of thin films of p-PbTe grown on mica and glass as a function of gate field and temperature. The films grown on mica were epitaxial and the effect of negativegate field was found to a decrease the Hall coefficient, Hall mobility and defect scattering mobility. The effect of positive gate field was opposite and less significant. On the other hand, the films grown on glass were polycrystalline and the mobility of charge carriers was an order less than the value for epitaxial films. The dominant scattering mechanism in these films is grain boundary potential barrier. The effect of negative gate field has been observed to decrease the grain boundary potential barrier and to increase the Hall mobility. These results have been explained on the basis of accumulation and depletion of charges induced by the field at the surface.

"ELECTRICAL EFFECT OF Na, Ag, AND Tl IMPURITIES ON LEAD TELLURIDE THIN FILMS"

by

A.L. Dawar, O.P. Taneja, S.L. Paradkar, Partap Kumar and P.C. Mathur
Department of Physics & Astrophysics, University of Delhi,
Delhi-110007, India.

ABSTRACT

Thin epitaxial films of PbTe incorporating Ag and Tl impurities were fabricated by co-evaporating these elements with PbTe from two separate boats onto heated mica and saphire. Na doped films were prepared by coevaporating NaCl and PbTe. Careful control was exercised to monitor the rates of various constituents in order to have a wide range of concentration range. D.C. conductivity and Hall coefficient measurements have been reported on these films in the temperature range (100-700K). Various band parameters i.e. mobility, effective mass and population ratio for light and heavy holes have been estimated as a function of carrier concentration and temperature on the bases of two valence band model. All these impurities have been found to give p-type behaviour. For a given carrier concentration the mobility ratio of light to heavy holes ($\frac{\mu_l}{\mu_h}$ = b) for Ag-dope was more as compared to those doped with Na and Tl. It has been observed that the value of b for all these films decreased with the increase of carrier concentration. However this decrease is more in the case of Tl and Na-doped films. The effect of various dopants on the valence band separation (ΔE_v) has been found to be almost independent of dopant and its concentration. The Hall mobility has been observed to decrease with the increase of carrier concentration. The data on mobility-temperature variation has been analysed in terms of different scattering contributries.

"ELECTRICAL EFFECT OF HYDROGEN ON SnTe THIN FILMS"

by

A.L. Dawar, O.P. Taneja, B.K. Sachar, A.O. Mohammed, Partap Kumar, S.K. Paradkar and P.C. Mathur

Department of Physics & Astrophysics, University of Delhi, Delhi-110007, India.

ABSTRACT

Thin epitaxial films of SnTe were deposited on mica and were exposed to molecular hydrogen for different durations at different pressures upto 500 psi. The films exposed to hydrogen for less than two hours and pressures less than 100 psi regained their initial conductivity values within 48 hours. The time period of this desorption process was dependent on exposure parameters. The films exposed to hydrogen for more than 2 hours and pressure more than 200 psi were stable for more than a period of thirty days indicating that the adsorbed hydrogen had indiffused into the films. Hall coefficient and d.c. conductivity measurements are reported on the films in which the aging effect was negligible. The studies on the film as a function of pressure to which these were exposed indicated that the conductivity first decreased with the increase of pressure, reached a minimum and then again started increasing. The value of Hall coefficient, on the other hand becomes more positive with the increase of pressure, reached a maximum, then started decreasing and finally changed sign to negative for high values pressure. The results have been explained on the bases of donor action of hydrogen gas.

Wednesday afternoon, June 10, 1981

Session W-B: Surface Phases

(Room 1105)

Chairman: M. Henzler

2:00 Direct Measurement of Pair Energies in Adatom-Adatom Interactions on a Metal Surface. R. CASANOVA and T. T. TSONG

2:20 Correlation between Adatom-Adatom Pair Interactions and Adlayer Superstructure Formation: Si on W{110}. T. T. TSONG and R. CASANOVA

2:40 The Role of Three-Adatom Interactions in Two-Dimensional Phase Diagrams. N. C. BARTELT, T. L. EINSTEIN and P. E. HUNTER

3:00 Exact Solutions for Ising Model Multisite Correlations on the Honeycomb and Triangular Lattices. C. H. MÚNERA, J. H. BARRY and T. TANAKA

3:20 Theory of dc Conductivity for a Two-Dimensional Superionic Conductor on the Honeycomb Lattice. T. TANAKA, N. L. SHARMA, C. H. MÚNERA and J. H. BARRY

3:40 Observation of the Structural Transition Pt(100) 1×1→hex by LEED Intensities. K. HEINZ, E. LANG, K. STRAUSS and K. MÜLLER

4:00 Structures of Cs-Adlayers on Reconstructed Ir, Pt and Au Surfaces. K. MÜLLER, E. LANG, H. ENDRISS and K. HEINZ

4:20 Direct Determination of the Size Distribution of Adsorbed-Layer Islands from LEED Beam Intensity-vs-Angle Profiles. L. H. ZHAO, T. M. LU, P. K. WU and M. G. LAGALLY

4:40 LEED, AES, ELS, Surface Conductivity and Work Function Measurements Study of Reconstruction Modes of (110)SnO_2. E. DE FRÉSART, J. DARVILLE and J. M. GILLES

5:00 Phase Diagram of Oxygen on Nickel (100). D. E. TAYLOR and R. L. PARK

5:20 Hydrogen Atom Diffraction from Ordered Xenon Overlayers Adsorbed on the (0001) Face of Graphite. T. H. ELLIS, S. IANNOTTA, G. SCOLES and U. VALBUSA

Direct Measurement of Pair Energies in Adatom-Adatom Interactions on a Metal Surface*

R. Casanova and T. T. Tsong
Department of Physics
The Pennsylvania State University
University Park, Pa. 16802

Pair energies in adatom-adatom interaction on the W{110} plane were obtained for Re-Re, W-Re, Ir-Ir, and W-Ir pairs. Each set of pair energies was derived from an experimental pair distribution involving about 1,000 field ion microscope observations with exactly two adatoms on a W{110} plane, and a theoretical pair distribution calculated for two non-interacting atoms on a plane of similar shape and size. The Re-Re interaction exhibited an oscillatory tail beyond 10 Å. The amplitude was about 8 meV near the 10 Å range. A strong repulsive region existed near 5 Å. These results were completely different from existing data for Re-Re interaction on the W{112} plane, strongly indicating a crystal plane dependence of the adatom-adatom interaction. Since, of all the adatom-adatom interactions examined theoretically so far, only the indirect interaction exhibited an oscillatory tail, we believe that our results confirm the existence of such an interaction and also give quantitatively reliable data on it. The W-Ir interaction also clearly showed an oscillatory tail. However, our data on W-Re and Ir-Ir interactions, while giving some indication of oscillatory tails, did not exhibit these tails clearly. From the pair distributions, we also derived, for the first time, reliable values for the pair energy at the closest bond separation. They were 99.0 ± 0.7 meV, 82.0 ± 2.5 meV, and 53.2 ± 3.6 meV, respectively, for W-Re, Ir-Ir, and W-Ir pairs. This study represents one of those rare cases where atomic interactions over large distance ranges have been obtained in solid state and surface phenomena with a direct method.

*Supported by NSF-DMR 7904862.

Correlation Between Adatom-Adatom Pair Interaction and Adlayer Superstructure Formation: Si on W{110}*

T. T. Tsong and R. Casanova
Physics Department, The Pennsylvania State University
University Park, Pennsylvania 16802

Behaviors of single silicon adatoms on a metal surface have been successfully studied for the first time. Direct observations of migration of adatoms, adatom-adatom interactions, and adlayer superstructure formation are made in the field ion microscope. Diffusion parameters of Si adatoms are derived with one Si adatom deposited on an atomically perfect surface. They are $E_d = 0.70 \pm 0.07$ eV, and $D_o = 3.08 \times 10^{-4} \times 10^{\pm 1.28}$ cm^2/sec.

Pair binding energies for Si adatoms on the W{110} for several bond configurations have been obtained by measuring the relative frequencies of observing these bond configurations. It is found that maximum binding occurs when two Si adatoms are separated by $\sqrt{2}$ a with the bond aligned in the $[1\bar{1}0]$ direction, and maximum antibinding occurs at a distance a with the bond aligned in the [001] direction; a is lattice constant. From these data we are able to calculate the relative 2-dimensional binding energy of an adatom in an adlayer of various atomic structures. The $[2\sqrt{2}/\sqrt{3} \times 4\sqrt{3}]$ R 35.26° superstructure has the lowest energy. Our search for Si adlayer superstructure formation by thermal equilibration of deposited Si adatoms confirms this prediction.

The superstructure, in general contains nucleational growth defects such as the antiphase domains and the stacking faults. The adlayer can be melted around 260 to 280°K. The detailed atomic processes of the 2-dimensional melting can be directly observed. Experimental results of this ideal model system in 2-dimensional phase transformation phenomena, together with results from a computer simulation, will be presented.

*Work supported by NSF DMR-7904862.

The Role of Three-Adatom Interactions in Two-Dimensional Phase Diagrams

N. C. Bartelt,* T. L. Einstein,* and P. E. Hunter,†
Department of Physics and Astronomy, University of Maryland
College Park, Maryland 20742

The phase diagram of overlayers of chemisorbed atoms on single-crystal surfaces contain a wealth of information about the lateral interactions between these atoms. In fact, when the system is "closed" (no desorption or bulk absorption) and when no substrate reconstruction or relaxation occurs, these interactions completely determine the diagram; they are the parameters of a lattice gas Hamiltonian. The only reliable method to retrieve the interactions is to make assumptions about them, perform Monte Carlo simulation, compare with the experimental diagram, adjust parameters accordingly, and try again until adequate agreement is achieved.

In most experimental phase diagrams, asymmetries are found about half-monolayer coverage. For our discussion these asymmetries can be divided into two kinds: 1) higher temperature asymmetries of a phase boundary for a long-range ordered phase with saturation coverage of 1/2 and 2) low-temper-ature gross asymmetries in which some phase exists for fractional coverage θ but not for $1-\theta$. Both asymmetries are often attributed to three-adatom interactions, which break the particle-hole symmetry of the lattice-gas Hamiltonian. For the second kind of asymmetry, simple expressions for the ground state energies of the possible phases give magnitudes (or at least inequalities) for such "trio" interactions. Explicit computations for model systems produce numbers consistent with these magnitudes. These computations also show, however, that there are usually several three-adatom configurations of comparable energy, not just the one or two typically invoked to explain asymmetries.

For the first kind of asymmetry, it is not the ground state energy of the ordered state but rather the excitation energy which is relevant to determining the curve of transition temperature versus θ. Simple pictures for a c(2x2) overlayer on a square lattice show that the low energy excitations are symmetric about $\theta = 1/2$ when there are either linear or right-angle-triangle repulsive triads. (When both are present, the symmetry is lost.) Monte Carlo simulations verify that in these cases there is indeed very little if any high-temperature asymmetry. Mean field calculations, on the other hand, show pronounced asymmetries; this feature arises from their neglect of correlations, specifically, of the ability of adatoms to disorder near the defects in the c(2x2) pattern at $\theta \neq 1/2$. Generalizations to other overlayer symmetries are also discussed.

We finally discuss the square lattice gas problem with first- and second-neighbor interactions from the viewpoint that transition temperatures are intimately related to low energy excitations. The simple equation arising from this picture is a remarkably good approximation for the true transition temperature in the case of repulsive nearest neighbor and attractive second-neighbor interactions. It is better than some far more complicated schemes and resulting expressions that have appeared in the literature.

*Supported in part by U. S. Department of Energy under grant DE AS05-79ER-10427.
†Also at NAVSWC, Dahlgren, VA.

Exact solutions for Ising model multisite correlations on the honeycomb and triangular lattices

C. H. Múnera, J. H. Barry and T. Tanaka
Physics Department, Ohio University, Athens, Ohio 45701

Two-dimensional Ising models serve as appropriate representations for various critical systems, a more recent example being the adsorption of helium monolayers on krypton-plated graphite substrates.[1] For Ising (or classical) lattice systems, rigorous linear algebraic identities among multisite thermal averages can be derived where the coefficients depend upon the interaction constant.[2] Presently investigating the $S = \frac{1}{2}$ Ising ferromagnet having nearest-neighbor range of interactions simultaneously for the honeycomb and dual triangular lattices (thereby enabling use of star-triangle-type relationships), closed exact systems of linear algebraic equations are developed for odd- and even-number-spin correlations. Supplementing these systems with the known literature value of the spontaneous magnetization and a select few even-number-spin correlations calculated by Pfaffian techniques, the systems of equations then lead directly to exact solutions for the remaining multisite correlations upon both lattice structures, e.g., up to and including ten-site correlations on the honeycomb lattice. The method also proves the existence of degeneracies between various correlations and is capable of extending all exact solutions to a class of bond and site defect problems. Corresponding exact solutions for the Ising antiferromagnet upon the honeycomb lattice (equivalent to a lattice gas model having nearest-neighbor repulsive interactions) can next be easily obtained by merely changing the algebraic sign of the interaction constant within the former solutions.

(1) M. J. Tejwani, O. Ferreira and O. E. Vilches, Phys. Rev. Lett. 44, 152 (1980).

(2) M. E. Fisher, Phys. Rev. 113, 969 (1959); M. Suzuki, Phys. Letters 19, 267 (1965).

Theory of dc conductivity for a two-dimensional superionic conductor on the honeycomb lattice. T. Tanaka, N. L. Sharma, C. H. Múnera and J. H. Barry, Physics Department, Ohio University, Athens, Ohio 45701

In the superionic conductor Na β-alumina, the ionic conduction takes place in a two-dimensional honeycomb lattice perpendicular to the hexagonal c-axis.[1] Motions of mobile ions are well represented by a lattice gas model in which an ion can hop from one lattice site to another. The total Hamiltonian is made up of hopping terms and the nearest-neighbor repulsive interaction between the mobile ions. According to the fluctuation-dissipation theorem, the ionic conductivity is calculated from the imaginary part of the retarded Green's function, which in turn calculated from the thermal Green's function. As is formulated by G. D. Mahan[2], in the lowest order perturbation and in the half-filled lattice system, the thermal Green's function is expressed in terms only of the two-dimensional spin correlation functions. C. H. Múnera et al[3] calculated all the honeycomb and triangular Ising spin correlation functions necessary for the dc conductivity of two dimensional superionic conductor. These correlation functions enable us to find the temperature dependence of the dc conductivity of two-dimensional superionic conductors. Cur formulation is similar to the one by Mahan, which is for the two dimensional square lattice, however, there are some significant differences. Cur expression of the thermal Green's function in terms of the static correlation functions is rigorous because of the use of the idempotent properties of the occupation number operators, and we have all the necessary exact static Ising correlation functions calculated with an extensive use of the Suzuki identities.[4]

1. S. J. Allen, Jr., A. S. Cooper, F. DeRosa, J. P. Remeika, and S. K. Ulasi, Phys. Rev. B, 174, 4031 (1978).
2. G. D. Mahan, Phys. Rev. B, 14, 780 (1976).
3. C. H. Múnera, J. H. Barry and T. Tanaka (This conference).
4. M. Suzuki, Phys. Letters, 19, 267 (1965).

Observation of the structural transition Pt(100) 1×1→hex by LEED intensities

K. Heinz, E. Lang, K. Strauß and K. Müller

Institut für Angewandte Physik, Lehrstuhl für Festkörperphysik der Universität Erlangen-Nürnberg, Erwin-Rommel-Straße 1, D-8520 Erlangen, Germany

LEED intensities have been measured during the structural transition of Pt(100) 1×1→hex. The unreconstructed surface was established by NO adsorption at room temperature. Successive careful thermal desorption and hydrogen reduction allowed for the clean 1×1 surface. The transition to the reconstructed phase was performed either by rapid heating to a constant elevated temperature or by continuous temperature increase with constant heating rate beginning at liquid air temperature. The LEED intensities of some integer order spots as well as of superstructure spots, which develop continuously during the structure transition, have been taken in both modes, i.e. isothermal and temperature dependent. Also intensity-energy spectra corresponding to the reconstructed and unreconstructed phases have been measured for comparison. Using a fast computer controlled television method for the intensity measurements the profiles of the diffraction spots could be simultaneously recorded as well.

It turns out that the spot width is constant from the very beginning of the transition. So -in contrast to the phase transition of W(100) 1×1↔c(2×2)- no island growth is observed at least for dimensions below the instrumental transfer width. Moreover it appears that the considerable decrease of integer order beam intensities precedes the growth of broken order beams of the reconstructed phase. This favours the model of an order-disorder-order type transition. Its development is considerably influenced by residual NO. It is evident from the isothermal as well as from the temperature varied measurements that the reconstruction is an activated process. The activation energy can be extracted from the intensity measurements. The evaluation of intensities varying with temperature additionally makes possible to deduce information about the Debye-temperatures of both the reconstructed and unreconstructed surface as well.

Structures of Cs-Adlayers on Reconstructed Ir, Pt and Au Surfaces

K. Müller, E. Lang, H. Endriß and K. Heinz

Lehrstuhl für Festkörperphysik, Universität Erlangen-Nürnberg, Federal Republik of Germany

The clean (100) and (110) surfaces of Ir, Pt and Au each appear in two different structures representing a metastable bulk phase and a stable reconstructed surface mode. According to common experience the reconstructed surface undergoes a transition to the bulk structure mode upon the influence of an adsorbate. In the case of the above mentioned samples the reconstructed phases can be temperature stabilized against Cs adsorption so that a Cs film grows on top of a well defined non bulk like ordered substrate. A series of adsorption structures can be observed as a function of coverage. These LEED data are interpreted in terms of structural properties of the substrate surface. In such a way the information about the ordered overlayer can be used to support certain surface models of reconstruction. While adsorption on the bulk structure surfaces runs through several coincidence lattices eventually reaching a close packed stage of the Cs layer, adsorption on reconstructed surfaces takes place in troughs of a corrugated substrate surface.With increasing coverage the Cs atoms move along these troughs temporarily forming coincidence lattices with their hexagonal substrate. Again the final stage appears to be a close packed Cs layer. In the case of Ir(100) the details clearly favour a buckled quasi hexagonal surface layer of Ir atoms and therefore support the commonly accepted model. Similar conclusions can be drawn for Pt(100) and Au(100) although in these cases the "troughs" in the surfaces are not and - according to the hexagonal model- cannot be as well resolved as for Ir.

Even for the (110) surface we propose the hexagonal model for the reconstructed (3×1) surface and a quasi hexagonal model for the (2×1) superstructure. Cs seems to stabilize the (3×1) phase at high temperature and low coverage, and adsorption of Cs followed by complete desorption is a good method to prepare also the clean (3×1) structure. Support for the structure models can be drawn from LEED intensity analysis as well as from Cs adsorption studies.

Direct Determination of the Size Distribution of Adsorbed-Layer Islands from LEED Beam Intensity-vs-Angle Profiles*

L. H. Zhao, T. M. Lu, P. K. Wu, and M. G. Lagally**
University of Wisconsin, Madison, WI 53706

If net attractive interactions among adatoms exist, two-dimensional condensation may occur in adsorbed layers at low coverages, forming frequently ordered regions with a unit mesh larger than that of the substrate. This condensed phase may exist as a distribution of finite-size islands, due either to kinetic limitations or to the existence of substrate extended defects that limit the growth of the overlayer phase. The shape of the island depends on the overlayer adatom-adatom interactions.(1) The intensity of LEED superlattice reflections is, under fairly general conditions,(2) just the superposition of the intensities scattered by individual islands and thus the angular distribution in the LEED beam mirrors the size distribution of islands. However, even if one knows a priori the shape of the islands, it has not been possible so far to determine the island size distribution uniquely from the angular distribution of intensity. We present a new mathematical method with which it is possible to deduce the island size distribution directly from the superlattice beam intensity distribution with angle, at least for islands whose shape can be approximated by a parallelogram. This method can be applied to any system with a square or rectangular substrate unit mesh, and also to systems like W(110)p(2x1)-O. Determinations of size distributions using experimental results for the latter system are presented.

---

* Research Supported by NSF Grant No. DMR 78-25754
** H. I. Romnes Fellow
(1) T. L. Einstein, CRC Reviews in Solid State and Mat. Sci., 7, 261 (1978)
(2) J. C. Tracy and J. M. Blakely, in The Structure and Chemistry of Solid Surfaces, ed. G. A. Somorjai, Wiley, New York (1969)

LEED, AES, ELS, SURFACE CONDUCTIVITY AND WORK FUNCTION MEASUREMENTS

STUDY OF RECONSTRUCTION MODES OF (110) SnO_2.*

E. de Frésart**, J. Darville and J.M. Gilles
LASMOS, Département de Physique,
Facultés Universitaires N.D. de la Paix,
Rue de Bruxelles 61, B-5000 NAMUR - Belgium.

Upon progressive annealing up to 920 K after ion bombardment of very pure (110) SnO_2, the following surface reconstruction types successively appear : p(4x2) (500 K), p(4x1) (640 K), p(1x1) (740 K), then either p(4x1)-p(1x2) or p(1x2) (770 K), depending upon cleaning procedure. Above 870 K, only p(1x1) is observed. The onset of these structures corresponds to a progressive reoxydation of the surface, a decrease of the bulk plasmon intensity as well as of the surface conductivity and an increase of the work function. Results indicate that the modification of the work function essentially occurs when the structures are changing : + 0.30 eV from p(4x2) to p(4x1) and + 0.35 eV from p(4x1) to p(1x1). Surface conductivity is decreased slowly for the first transition and rapidly for the second. This proves that electron affinity is alone responsible for the first variation while band bending is also changing during the second one. Around 900 K the change of structure is due to loss of material by evaporation. Formerly proposed structural models will be discussed in terms of these findings. The influence of preferential sputtering as a function of ion mass and energy will also be considered.

---

* Work performed under the auspices of the IRIS program supported by the Belgian Ministry of Science Policy.

** Holder of a "Bourse I.R.S.I.A.".

PHASE DIAGRAM OF OXYGEN ON NICKEL(100)

David E. Taylor and Robert L. Park
Department of Physics and Astronomy
University of Maryland, College Park, MD. 20742

We have used LEED and AES to study the phases of chemisorbed oxygen on Ni(100) in the coverage range of 0.1 to 0.5 monolayer and the temperature range of 100°K to 900°K. The p(2X2) structure of oxygen on Ni(100) is observed to undergo a reversible order-disorder phase transition with hysteresis (T_c = 605°K at θ = 0.25 monolayer), but it is possible this hysteresis is not intrinsic to the transition. The oxygen overlayer begins dissolving into the bulk nickel at about the same temperature as that where the p(2X2) structure disorders, which necessitates heating and cooling the sample through the critical region very swiftly in order to see the transition without losing oxygen from the surface. The observed hysteresis may thus be a non-equilibrium effect, rather than an indication of a first order phase transition. The fact that bulk dissolution begins near the disordering temperature of the p(2X2) structure is not thought to be accidential, and is taken to mean that the highly mobile oxygen atoms of the disordered phase have a substantially increased probability of bulk dissolution as compared with those in an ordered phase. The p(2X2) structure is observed to initially form a short-range order, "island" phase at room temperature, as evidenced by broad half-order LEED beams. This island phase is seen to give way to the long-range order of the full p(2X2) structure upon annealing. The c(2X2) structure of oxygen on Ni(100) is seen to be very stable up to remarkably high temperatures, over 800°K, at which point the overlayer dissolves very rapidly into the bulk. An order-disorder transition similar to that of the p(2X2) structure is not seen.

Work Supported by DOE-AS05-79-ER 10427

HYDROGEN ATOM DIFFRACTION FROM ORDERED XENON OVERLAYERS ADSORBED ON THE (0001) FACE OF GRAPHITE

T.H. Ellis, S. Iannotta, G. Scoles* and U. Valbusa**
Guelph-Waterloo Centre for Graduate Work in Chemistry,
University of Waterloo, Waterloo, Ontario,
Canada N2L 3G1

Recently, there has been widespread interest in the physics of two-dimensional systems with particular emphasis on the structure and dynamics of gas overlayers adsorbed on crystal surfaces. The experimental techniques used to date have included LEED, RHEED, THEED, AES, x-rays, neutrons and specific heat measurements. We present results on the first atomic beam diffraction measurements of rare gas overlayers on graphite. Some of the advantages of this techniques are the use of single crystal samples and a lack of layer penetration. Furthermore, this is the only method for studying directly the atom-layer potential by carrying out both diffraction probability and selective adsorption measurements.

In our experiments, a layer of xenon was grown under a continuous flux of xenon on a natural graphite crystal, following which the flux was terminated and the crystal cooled to 25 - 30°K. The positions of the diffraction peaks indicate a $\sqrt{3}$ x $\sqrt{3}$ layer in registry with the substrate. The intensities of the peaks are well reproduced by a hard-wall scattering model, both with and without a correction due to the attractive part of the potential, yielding peak to peak corrugations of 1.08 ± .05 Å and 1.19 ± .05 Å respectively. This agrees rather well with a theoretical potential which is composed of the sum of gas phase H-Xe potentials and a simple H-graphite C_3/Z^3 attraction. The corrugation of this potential, which is taken to be the difference in classical turning points at the appropriate two positions on the surface, is 1.00 ± .05 Å.

* also Physics Department, University of Waterloo.

** Present address: Physics Department, University of Genova, Genova, Italy.

Wednesday afternoon, June 10, 1981

Session W-C: Metal Surfaces

(Room 1123)

Chairman: G. G. KLEIMAN

2:00 Temperature Dependence in UV Photoemission from Cu(111). H. MÅRTENSSON, P.-O. NILSSON and J. KANSKI

2:20 Reflection High Energy Diffraction by the Ag(001), Ag(111) and Ag(110) Surfaces. P. A. MAKSYM and J. L. BEEBY

2:40 Non-Adiabatic Scattering from Metal Surfaces. J. W. GADZUK

3:00 Ab-initio Atom Cluster Models of Carbon Surfaces. W. H. FINK

3:20 Magnetic Moments at the Surface of 3d Transition Metals. J. DORANTES-DÁVILA and J. L. MORÁN-LÓPEZ

3:40 A New Polarization Model of Changes in the Work Function for Bare and Covered Transition Metal Surfaces. E. SHUSTOROVICH and R. C. BAETZOLD

4:00 Interionic Interactions at Metallic Surfaces. R. N. BARNETT, C. L. CLEVELAND and U. LANDMAN

4:20 Method of Determination of the Electron Structure of Films. S. N. BEZRYADIN, Y. K. VEKILOV and V. D. VERNER

Temperature dependence in UV photoemission from Cu(111)

H. Mårtensson, P-O Nilsson, and J. Kanski
Department of Physics
Chalmers University of Technology
S-412 96 GOTHENBURG, Sweden

UV photoemission energy distributions from Cu(111) have been studied as a function of temperature in the range 300-700 K. Plots of the logarithm of the peak intensities as a function of temperature resulted in straight lines. The slope of these lines may define an effective Debye temperature. This quantity was found to vary strongly between different peaks and was in general considerably lower than the bulk value (343 K).

Detailed analysis of the experimental data is quite complicated for several reasons. Considerable deviation from the kinematical situation occurs because of strong contribution from multiple scattering, resulting in an increased or decreased effective Debye temperature. The presence of the surface complicates the scattering paths even more. Also, the phonon spectrum at the surface is different from that in the bulk, which should result in a lowering of the Debye temperature. Finally, the optical excitation probability could in principle also contribute with a temperature dependence, although we think this is small.

REFLECTION HIGH ENERGY DIFFRACTION BY THE Ag(001), Ag(111) AND Ag(110) SURFACES

P.A. Maksym and J.L. Beeby
Department of Physics,
University of Leicester,
University Road,
Leicester LE1 7RH,
England.

Elastic reflection high energy electron diffraction (RHEED) by the Ag(001), Ag(111) and Ag(110) surfaces is studied with the aid of model calculations of the RHEED intensities. The electron energies are taken to be in the range 10-40 keV and the incident beam azimuth is taken to be in a direction of high symmetry. The calculations are based on the use of a dynamical diffraction theory in which the electrons are taken to be diffracted by a potential which is periodic in the two dimensions parallel to the surface but need not be periodic in the dimension perpendicular to the surface. The results of the calculations are presented in the form of rocking curves which illustrate how the diffracted beam intensities depend on the glancing angle of the incident beam. It is shown that the rocking curves have similar features to a typical set of LEED I-V plots: these are series of primary Bragg peaks, secondary Bragg peaks and resonance peaks. The primary Bragg peaks are weak because the atomic layers parallel to the surface predominantly diffract electrons out of the incident beam. A consequence of this is that the secondary Bragg peaks are very pronounced. The procedure used to compute the RHEED intensities also gives the perpendicular dependence of the electron wave function and plots of the electron intensity as a function of depth into the crystal are used to explain the mechanisms causing the various peaks in the rocking curves.

NON-ADIABATIC SCATTERING FROM METAL SURFACES

J. William Gadzuk

Surface Science Division

National Bureau of Standards

Washington, D.C. 20234

A proper dynamical theory of molecular processes at metal surfaces must provide a means of treating transitions between the coupled quantum states of the nuclear motion and internal electronic states of the reactant and product as well as the electronic and phonon state of the substrate. The excitations of the solid can serve as a heatbath, thus introducing the necessary condition of irreversibility into a molecular process at a surface. Recent theoretical studies have modeled the substrate excitations (electron-hole pairs, plasmons, phonons) as a boson gas and have treated the reactant nuclear motion within a classical trajectory approximation. Within this model, calculation of the irreversible energy transfer to the substrate and thus the reaction rate is fairly straightforward. However, this approach is not without its problems since a crucial input ingredient is the reactant trajectories in the region of strong interaction with the substrate and it is here that the usual simple analytic forms used in model studies could be inadequate.

The present work will focus on the relationship between the vibrational states of an adsorbed particle and the quantum mechanical trajectories required in surface reaction theories. The basic philosophy will be illustrated within the framework of an elementary, but exactly soluble model for non-adiabatic scattering from metallic surfaces which has been adapted from the "X-ray edge folklore".

Ab-initio Atom Cluster Models of Carbon Surfaces

William H. Fink
Department of Chemistry, University of California
Davis, California 95616

Ab-initio techniques for obtaining a wavefunction which simulates an infinite or semi-infinite solid with a finite cluster of atoms have recently been applied to model the electronic structure of the naked surfaces of diamond and graphite and of hydrogen atom adsorption on the (100) surface of diamond. The wavefunction for the system is written in the form $\psi = \mathcal{A}\psi_I\psi_{II}$ where $\mathcal{A}$ is an antisymmetrizer, ψ_I is frozen and ψ_{II} is determined variationally. Use of a projector to obtain the best possible approximate representation of ψ_I from a calculation which has been variationally determined in an environment simulating connection to the extended solid, permits the reduction of so-called edge effects in finite clusters. Clusters containing up to eight carbon atoms have been considered in geometries assumed by simple termination of the known bulk structure. While surface reconstruction may be important, it is more difficult to activate in these materials than in metals and an idealized geometry was considered an adequate and in fact necessary first treatment of the problems. The most active H adsorption site on (100) diamond was found to be an overhead site. A bridging site was also modeled and the energy profile for diffusion along the zig-zag chains of the surface was also explored. An unusually high value for the heat of H chemisorption was calculated. The surface electronic structure is examined with the aid of population analyses and contour maps. Difference densities were found to be particularly valuable to bring out the detailed changes in structure. A perspective of the approach will be presented in view of all the calculations completed to date.

Magnetic Moments at the Surface of 3d Transition Metals. J. Dorantes-Dávila and J. L. Morán-López, Departamento de Física, CINVESTAV del IPN, México, and K. H. Bennemann, Institute for Theoretical Physics, F. U. Berlin. By using the Hubbard tight-binding type Hamiltonian and the cluster Bethe lattice approximation we study the conditions for the existence of localized moments at the surface of transition metals. The electronic structure is solved and the size of the surface magnetic moment is determined selfconsistently. The theory is applied to Fe, Co and Ni and the results are compared to existing data.

A New Polarization Model of Changes in the Work Function for Bare and Covered Transition Metal Surfaces

Evgeny Shustorovich and Roger C. Baetzold
Research Laboratories, Eastman Kodak Company,
Rochester, New York 14650

We suggest a new polarization mechanism for changes in the work function $\Delta\phi$ for transition metal surfaces as a result of the p-(sd) orbital rehybridization of the surface atoms. This mechanism has been tested for model metal (M) slabs, bare and covered by an adatom (A) monolayer, within both an analytical perturbation LCAO MO model and extensive Hückel-type LCAO MO calculations. The surface dipole moment (D) contributions to $\Delta\phi$ have been considered as functions of the film thickness, the Fermi energy E_F, the adatom orbital energy ε_A, the metal p-d energy splitting $\varepsilon_p-\varepsilon_d$, and some other parameters. The analytical model treated these contributions for the unit cell LCAO MO's of highly dense (hd) and loosely dense (ld) surfaces, while the Hückel calculations used explicit two-dimensional Bloch functions within the relevant Brillouin zones. The main conclusions are as follows: (1) For bare surfaces, the hd vs. ld differences in ϕ (anisotropy $\Delta\phi$) distinctly correlates with those in D, the dp contribution being predominant. For a given pair of surfaces, $\Delta\phi = \phi(\text{hd}) - \phi(\text{ld}) > 0$ decreases as $E_F - \varepsilon_d$ or $\varepsilon_p - \varepsilon_d$ increases, showing no crossover along the transition series. These results do not depend on the metal parameter sets used. (2) Under chemisorption, both external (electrostatic) D_{ext} and internal (polarization) $\Delta D_{int} = D_{int}^{cov} - D_{int}^{bare}$ dipole moments contribute to $\Delta\phi = \phi^{cov} - \phi^{bare}$. For electropositive A's (such as alkalis), $\Delta D_{ext} < 0$ seems to be always predominant. For electronegative A's (such as H or halogens), however, $\Delta D_{ext} > 0$ may be smaller (in absolute value) than $\Delta D_{int} < 0$. In this case, corresponding to the paradoxical change $\Delta\phi < 0$, the small differences in the A vs. M electronegativity will be favorable. The results obtained agree with experiment and permit some puzzling regularities of $\Delta\phi$ to be explained and predicted.

Interionic Interactions at Metallic Surfaces*

R. N. Barnett, C. L. Cleveland, and Uzi Landman
School of Physics, Georgia Institute of Technology
Atlanta, GA. 30332

We develope a psuedopotential theory for interionic interactions near the surface of a simple metal. This formulation is used to obtain pair-potentials and to investigate the interaction of defects such as vacancies and impurity atoms with the metal surface. It may also be employed to study surface structure, phase stability, and vibrational modes and thermal properties.

The system is modeled by a semi-infinite electron gas confined to $z<0$ by an infinite barrier in which the embedded ion cores are represented by local model psuedopotentials (PP's). The response of the electron gas to the PP's, including exchange and correlation within linear response, is evaluated in second-order perturbation theory, and the potential due to the inhomogenous unperturbed charge density is included to first order in energy. Thus, the total energy of the system is given by

$$E_T = E_{eg} + \sum_{\vec{k}} \langle \vec{k} | W + W^o | \vec{k} \rangle + E_{bs} + E_M$$

where E_{eg} is the energy of the electron gas if no ion cores are present, $W^o(\vec{r})$ is a sum over the bare ion PP's, $w_i^o(\vec{r}-\vec{r}_i)$, and $W(\vec{r})$ is the screened PP. E_M is the direct interaction between ion cores. E_{bs} is the usual band-structure energy expression involving matrix elements $\langle \vec{k}|w_i^{bs}|\vec{k}+\vec{q}\rangle$. These screened PP matrix elements are obtained as the solutions of an integral equation which must be solved separately for each value of Q, the magnitude of component of $\vec{q}$ parallel to the surface barrier, and for each z_i, the distance of the ion core from the surface.

Considering interionic displacements parallel to the surface only, the interaction can be described by a pair potential. These potentials for pairs of ions near the surface exhibit a strong dependence on the distance of each ion from the surface and differ markedly from the bulk pair potential in shape, and in location and depth of the potential minimum. Significant differences from bulk behavior exist until both ions are a distance of at least $4/k_F$ from the barrier (about the third layer of the (111) face or the second layer of the (100) face) in the simple metals we studied. These large deviations from bulk pair potentials result from the quantums interference term in the integral equation for matrix elements. The semi-classical approximation consists of neglecting quantum interference. The pair potentials which result from this approximation differ from the bulk behavior only for pairs of ions less than about $2/k_F$ from the barrier.

In addition to a sum over the pair potentials and terms involving only the bulk electron density, there are contributions to the total energy, E_T, which depend on the distance of a single ion from the surface barrier. Preliminary results indicate that these terms make a significant contribution to the interaction of impurities and vacancies with the surface and to the relaxed surface structure.

*Supported by U.S.DOE Contract No. EG-77-S-05-5489.

METHOD OF DETERMINATION OF THE ELECTRON STRUCTURE OF FILMS

S.N.Bezryadin, Yu.Kh.Vekilov*, V.D.Verner
Institute of Electronic Technology[1], Moscow, USSR
*Steel and Alloys Institute, Moscow, USSR

The method of determination of the electron structure of films, based on the numerical integration of the integral Schrödinger equation in the momentum representation, is developed. The model parameters - the weights and nodes of quadrature formulas - have been determined on the bases of convergenes of solutions for the jelly model.

The method is applied to a calculation of the electron structure of 8-layers aluminium film. The electron spectrum thus found is compared with the projection of the zone structure for infinit crystal. The surface states were found in the internal gap of the spectrum. The near-surface electron density distribution is determined. An influence of effects of surface atom relaxation on the electron spectrum is investigated.

A similar method was applied to investigation of nonreconstructed surface (001) of twelve-layers silicon film. The surface states in the lowest gap of the spectrum were found, in good agreement with the results of other methods.

---

[1] Moscow, 103498

THURSDAY MORNING, JUNE 11, 1981

Plenary Session

Main Auditorium

Chairman: C. R. ANDERSON

9:00 Vibrational Spectra of Adsorbed Atoms and Molecules.
A. M. BRADSHAW

9:45 Inelastic Tunneling.
J. KLEIN

10:30 Angular-Resolved Photoemission.
F. R. McFEELY

11:15 X-Ray Excited Auger Studies of Metals and Alloys.
G. G. KLEIMAN

Vibrational Spectroscopy of Adsorbed Atoms and Molecules

W. Brenig

Fritz-Haber-Institut der Max-Planck-Gesellschaft, Berlin, West Germany.

The molecular dynamics of adsorbates in the chemisorbed state are subject to very simple rules. An atom has three translational degrees of freedom which in the gas phase are the three translational modes. Following adsorption these are converted into three vibrational modes, one perpendicular and two parallel to the surface. A non-linear molecule has 3n degrees of freedom of which three are translational and three (or two, if the molecule is linear) are rotational. Upon the surface both the translational and rotational motions are hindered giving rise to six (or five) external vibrational modes, which may couple to both the substrate and the molecular modes of the same symmetry. The 3n-6 (or 3n-5) molecular, or internal, modes may be further modified in frequency due to the (chemical) interaction with the substrate and degeneracies may be lifted due to the lower symmetry of the surface site. At non-zero coverage further frequency shifts can occur due to lateral interactions. For probing these vibrational modes of adsorbates on single crystal metal surfaces essentially two methods are currently available to the surface scientist: electron energy loss spectroscopy (EELS) and infrared reflection absorption spectroscopy (IR). For most adsorbed molecules EELS can be applied in a wide spectral range, thereby encompassing enough of the 3n modes to carry out a structural analysis. Of particular advantage in this connection is the possibility of distinguishing between dipole and impact scattering mechanisms by performing angle-resolved measurements. In dipole scattering only those modes can be excited which involve a change in dipole moment perpendicular to the surface. This delivers important orientational information. Whereas the IR method is presently restricted in its spectral range, it has the advantage of an intrinsically high resolution. Thus the different frequencies of internal modes due to different adsorption sites can be easily distinguished. The best-known example is found in CO chemisorption where terminal and bridging adsorption sites as in the metal carbonyls can be identified. Furthermore, the shape, half-width and coverage-dependent shift of internal modes contain information on the lateral interactions in the adlayer and thus on adlayer growth and order-disorder phenomena. The IR method has the further advantage of being pressure-independent and can thus be used to study surface reactions in situ at high pressures.

INELASTIC TUNNELING

J. KLEIN
Groupe de Physique des Solides de l'E.N.S.
Université Paris 7, Tour 23 - 2 place Jussieu
75251 PARIS CEDEX 05 - FRANCE

Inelastic electron tunneling spectroscopy (IETS) has been developed recently as a powerful and sensitive tool for studying vibrational spectra of molecules adsorbed on the insulator of a planar metal-insulator-metal junction. In this review, we present the principles of IETS and discuss the results of the different theories that have been advanced to explain the amplitude of the peaks in the tunnel spectra. Then the characteristics of this spectroscopy are considered : spectral range, sensitivity, resolution, selection rules... A brief account of typical fabrication techniques, doping techniques and measurement methods is given.

Illustrations of the method are shown on various molecules and in particular, a detailed analysis of the chimisorption of carboxylic acids is presented, discussing the attributions of the peaks by isotopic studies. The influence of the counter-electrode on the strength of vibrational peaks is discussed.

Amongst the many applications actually under progress, we have restricted our detailed discussion to four areas which seem promising in the future. Successively :

1) Application to surface chemistry
2) Study of the transition from physical to chemical absorption
3) Observation of chemical reactions catalyzed by alumina
4) Adsorption and reactions on supported metal catalyst particles.

A comparison with other surfaces spectroscopies is made and the advantages and disadvantages associated with each of these techniques are given.

Angular-Resolved Photoemission

F. Read McFeely

Massachusetts Institute of Technology

For a number of years anguiar resolution has been employed to enhance the surface sensitivity of high energy photoemission experiments. These experiments have had numerous objectives, among these quantitative surface analysis and studies of surface electronic structure have figured prominently. In 1976 the shape of XPS valence band spectra of noble metal single crystals were shown to have a systematic dependence on the propagation direction of the outgoing photoelectron, which was clearly a bulk effect. Conflicting theories of the origin of this effect, their resolution, and the implications to the study of surface electronic structure will be discussed. Related work on polycrystalline metallic films will also be reviewed, as will other aspects of high energy photoemission, particularly those relevant to adsorbate surface structure determination.

X-Ray Excited Auger Studies of Metals and Alloys: George G. Kleiman, Instituto de Física, Universidade Estadual de Campinas, 13100 Campinas, São Paulo, Brasil.

Auger spectroscopy has played a fundamental role in the development of modern surface science. Its characteristics of speed and surface sensitivity permit, for example, its wide application to problems of chemical identification and concentration analysis. Basic to many of these applications is the assumption of "finger printing", or the insensitivity of the Auger lineshape to the chemical environment. Verification of the validity of this assumption requires understanding of the lineshape. We present a review of work on high resolution Auger lineshapes of metals and alloys. By appealing to basic physical arguments, we explain, for example, the nature of the process, the types of Auger spectra (i.e., "band-like" versus "quasi-atomic"), current theories and their relation to excited state electronic structure, some connections with photoemission, and the present level of understanding of available Auger data. Among the consequences of this understanding which we will discuss is the possibility of using the Auger spectrum of a noble metal constituent of an alloy to determine some important, previously unmeasured quantities: the relative Fermi energy and dipole barrier in an alloy with respect to those in the pure noble metal.

Thursday afternoon, June 11, 1981

Session Th-A: Epitaxy and Segregation

(Room 0123)

Chairman: E. BAUER

1:40 Investigation of Order-Disorder and Segregation Behavior on Cu_3Au(100) and (110) Surfaces by LEIS(TOF). T. M. BUCK, G. H. WHEATLEY and L. MARCHUT

2:00 First Stage of Au/Ag(111) Epitaxy using Ion Scattering, LEED and Auger Analyses. R. J. CULBERTSON, L. C. FELDMAN and P. J. SILVERMAN

2:20 Iron-Cobalt Alloys: The Importance of Iron Surface Segregation for the Order-Disorder Theory and for Catalysis Reactions. G. ALLIE, C. LAUROZ, P. VILLEMAIN, M. COULON and C. VANVOREN

2:40 Thin Silver Films on Al(100). W. F. EGELHOFF, JR.

3:00 Au, Ag and Cu-films on Si(111) Surfaces Studied by Auger Electron Spectroscopy. R. WEISSMANN, G. FISCHER and K. MÜLLER

3:20 Measurement of the Intrinsic Stress as a Method for the In Situ Investigation of the Structure and Growth of Thin Films. R. KOCH, H. P. MARTINZ and R. ABERMANN

3:40 A New Method for Metal Electroreflectance Measurements Using Metal-Insulator-Metal Structures. J. P. GOUDONNET, G. CHABRIER, G. NIQUET and P. VERNIER

4:00 Automodulation of Composition of Complex Semiconductor Epitaxial Films. S. K. MAKSIMOV, E. N. NAGDAYEV and L. A. BONDARENKO

4:20 Diataxial Growth of Semiconductors. E. I. GIVARGIZOV, N. N. SHEFTAL and V. I. KLYKOV

4:40 Defect States in a WO_3 Film Grown on a W(111) Surface. H. HÖCHST and R. D. BRINGANS

INVESTIGATION OF ORDER-DISORDER AND SEGREGATION BEHAVIOR ON Cu_3Au(100) AND (110) SURFACES BY LEIS(TOF)

T. M. Buck and G. H. Wheatley
Bell Laboratories
Murray Hill, New Jersey 07974

L. Marchut
Department of Materials Science and Engineering
University of Pennsylvania
Philadelphia, Pennsylvania 19104

The time-of-flight version of low energy ion scattering, LEIS(TOF), was used to study order-disorder and segregation behavior on Cu_3Au(100) and (110) surfaces. This technique collects scattered neutrals as well as ions. With Ne^+ beams incident at 5 keV energy and scattered through 90°, variations of polar and azimuthal angles of incidence permitted composition analysis of the 1st and 2nd atom layers and also identification of some scattering from the 3rd layer. Long-range order as manifested in layer composition, and also by LEED, was much stronger on the (100) surface than the (110), in accord with earlier LEED results.[1,2] On both surfaces we observed evidence of competition between ordering and surface segregation, the likelihood of which has been predicted.[3] Thus, after long annealing at 200°C, below the critical ordering temperature of 390°C, the 1st and 2nd layers of the (110) surface had similar compositions $\sim Cu_{.71}Au_{.29}$, while on the (100) surface the 1st layer composition was $\sim Cu_{0.46}Au_{0.54}$ and the 2nd layer $Cu_{0.9}Au_{0.1}$. In both cases perfect order would give $Cu_{0.5}Au_{0.5}$ (1st or 2nd) and $Cu_{1.0}Au_{0.0}$ (2nd or 1st). In both cases, annealing above the critical temperature caused enrichment of Au in the 1st layer. The ordering tendency evidently prevails over segregation below T_c; even in the (110) case there is probably short-range order. At the same time the segregation tendency is disrupting perfect long-range order even in the (100) case.

1) H. C. Potter and J. M. Blakely, J. Vac. Sci. Tech. 12, 635 (1975).
2) V. S. Sundaram, R. S. Alben and W. D. Robertson, Surf. Sci. 46, 653 (1974).
3) J.-L. Morán-López and K. H. Bennemann, Phys. Rev. B15, 4769 (1977).

FIRST STAGE OF Au/Ag(111) EPITAXY USING ION SCATTERING, LEED AND AUGER ANALYSES. R. J. Culbertson, L. C. Feldman and P. J. Silverman, Bell Laboratories, Murray Hill, N. J. 07974.

The first atom(s) in an ideal string of atoms parallel to an incident ion beam forms a shadow cone which reduces the probability of close encounters between the incident particles and subsequent atoms in the string. This shadowing effect is quantitatively determined by measurement of the surface peak (S.P.) in the (Rutherford) backscattering spectrum. The shadow cone may also be formed by an adsorbate atom which, if registered to the substrate lattice, reduces scattering from the substrate. We report the first systematic investigation of the adsorbate shadowing effect and describe the use of this phenomena in understanding the first stages of epitaxy.

The close lattice constant match and chemical activity of the Au/Ag couple makes it an ideal system for studies of crystalline epitaxy. We have measured the Ag S.P. and the Au-Au shadowing, χ_{min}(Au), as a function of Au coverage for the <111> and <110> crystal directions at 140°K and 300°K. The Au-Au shadowing is a measure of the registry of the second absorbate monolayer to the first adsorbate monolayer; the Ag S.P. is a measure of the registry of the crystalline overlayer to the substrate. The Au coverage dependence of the Ag S.P. and χ_{min}(Au) is in good agreement with models which employ monolayer-by-monolayer growth mode (Franck-van der Merwe growth) as opposed to islanding or other statistical growth patterns. The sensitivity of the ion scattering parameters to the growth modes will be illustrated.

We also describe the analyses of epitaxial Ag/Au/Ag sandwich structures by ion scattering and LEED techniques and measurement of Auger extinction lengths using ion scattering as a reliable quantitative measure of coverage.

IRON-COBALT ALLOYS : THE IMPORTANCE OF IRON SURFACE SEGREGATION FOR THE ORDER-DISORDER THEORY AND FOR CATALYSIS REACTIONS.

G. ALLIE and C. LAUROZ, Equipe d'Etude des Surfaces, Laboratoire de Spectrométrie Physique (associé au C. N. R. S.) Boite postale n° 53X, 38041 Grenoble Cedex, France

P. VILLEMAIN, DRF-Centre d'Etude Nucléaire de Grenoble, Boite postale n° 85 X, 38041 Grenoble Cedex, France

M. COULON and C. VANVOREN, Laboratoire d'Adsorption et Réaction de Gaz sur Solides (ERA CNRS), Ecole Nationale Supérieure d'Electrochimie et d'Electrometallurgie, Boite postale n° 44 X, 38041 Grenoble Cedex, France

Thanks to the "Laboratoire de Cristallogénèse, CNRS, Grenoble", we obtained excellent monocrystalline ingots of a 50-50 iron cobalt alloy. A bulk study of this alloy showed an order disorder (OD) transition at 730°C. Moreover the theoretical model pointed out the importance of the surface concentration and predicted a segregation of one of the components into the surface plane.
In the other hand, people involved in catalysis used industrial cold-rolled sheeets of iron-cobalt 49-49 alloy with 2 % vanadium, to catalyse the chemical reaction of dipropornation of carbon monoxyde ($2CO \rightarrow CO_2 + C$). People note the preferential reaction on (100) grains and study the importance of the temperature and of the operative conditions for carbon deposition.
Using Low Energy Electron Diffraction (LEED) and Auger Electron Spectroscopy (AES), we showed :

1. A high iron segregation at the surface
2. A large sensitivity of the chemical reaction : $2CO \rightarrow CO_2 + C$, to the surface chemical state.

In the first part of this study, we have developed a cleaning process of the surface of the monocrystal, which is not described in the litterature, and we have obtained a standard surface well characterized by LEED and AES.
At thermodynamical equilibrium for different temperatures above 300°C, we have found the iron to be the predominant species on the clean surface with a controlable rate. Sputtering depletes it to a limiting value while a thermal treatment restores iron segregation.
This result indicates a high diffusion rate at the surface in comparison with the bulk. Around the bulk OD transition temperature (730°C), we have found no influence of this bulk transition to the surface state.
In the second part, to estimate the quantitative composition of the surface, we have studied iron and cobalt monocrystals. The experimental conditions were the same as in the case of Fe-Co alloy (taking much care to minimize the anisotropy of the Auger excitation). The next result is that the concentration of the iron reaches 75 % and that the limiting value after iron bombardment is very close to the bulk concentration 50-50.
In the third part, thanks to the fundamental knowledge of an ideal monocrystalline surface, it was possible to study surface of industrial cold-rolled sheets of Fe-Co 49-49 with 2 % of vanadium, after the dispropornation of carbon monoxyde. The results obtained confirm the importance of the surface state and of the operative conditions during the chemical reaction.

Abstract Submitted for the

2nd International Conference on Solid Films and Surfaces

Thin Silver Films on Al(100)

W. F. Egelhoff, Jr.
Surface Science Division
National Bureau of Standards
Washington, DC 20234

Films of Ag from 0 to 10 monolayers thick have been deposited on Al(100) and studied by LEED and XPS. This is the first study by photoelectron spectroscopy of ordered overlayers of one metal on another. The XPS valence band data demonstrate the evolution of the 4d band structure with increasing Ag thickness. The LEED patterns indicate a 4 x 4 structure at low coverage and epitaxial growth of Ag(100) thereafter. The Ag core levels exhibit changes in both binding energy and linewidth with coverage. Similar data for Cu and Au on Al(100) will also be presented.

Au, Ag and Cu-films on Si(111) surfaces studied by Auger electron spectroscopy

R. Weißmann, G. Fischer and K. Müller

Institut für Angewandte Physik, Lehrstuhl für Festkörperphysik,
Universität Erlangen-Nürnberg, Erwin-Rommel-Straße 1,
D-8520 Erlangen

Auger electron spectroscopy measurements on very thin ($\leq$ 5 nm) noble metal films, deposited at room temperature on clean (111) surfaces of Silicon are carried out in order to study the Si/metal interface. For the systems Si/Au and Si/Cu the Si $L_{2,3}$ VV (92 eV) Auger peak shows splitting of two lines at 90 and 95 eV. No splitting is observed for the Si/Ag interface.

The growth of Au and Cu films on Silicon substrates is discribed as a surface compound mechanism. After the deposition of more than two metal layers a diffusion of Silicon atoms in the overlayer forming a metal-silicide is observed. Photoelectron valence band spectra indicate a bonding between the Si 3p level and the Au 5d or Cu 3d band. The splitting of the $L_{2,3}$ VV Auger transition results from the local structure of the electron density of states in the vicinity of the Silicon atom in the noble metal matrix. Au-Silicide is a metastable alloy phase which decomposes into an equilibrium Si and Au heterogeneous mixture. For the Si-Cu-alloy a stable homogeneous phase is established by partial segregation of Silicon. The diffusion length of Silicon is the same in both metal films (d = 2 nm).

Vapour deposited Ag forms three monolayers on the Silicon substrate. With higher coverages an island growth mechanism is assumed from the Auger signal-time plot. The interdiffusion between Ag and Si is much smaller than in the case of Copper or Gold. At room temperature no Silicide formation has been observed. The Auger spectrum is a linear superposition of the pure Silicon and Silver spectra.

MEASUREMENT OF THE INTRINSIC STRESS AS A METHOD FOR THE IN SITU INVESTIGATION OF THE STRUCTURE AND GROWTH OF THIN FILMS.

R. Koch, H.P. Martinz and R. Abermann (Institute of Physical Chemistry, University of Innsbruck, A-6020 Innsbruck, Austria).

In earlier papers (TSF, 80,219(1979); 70,127(1980)) we have described a sensitive stress measuring apparatus, based on the cantilever beam principle. With this technique the intrinsic stress of thin films can be measured continuously during deposition. Using our model for the origin of the intrinsic stress published earlier, the stress curves can be interpreted in terms of the TEM structure of the films as a function of film thickness. In this paper we shall present the results of recent experiments where we have used this technique to study the mechanical, hence structural properties of thin Cr and Ag films. In particular we have investigated the interaction of both metals with oxygen during as well as after the metal evaporation. A comparison of these two metals is particularly interesting since in contrast to Ag, Cr forms a stable bulk oxid under the experimental conditions used. The intrinsic stress of a Cr film is tensile from the very beginning of the film deposition. From the large tensile stress we conclude, that primarily the grain boundary relaxation mechanism contributes to the internal stress. Changes in the incremental stress during the early growth stage are interpreted to be due to annealing and recrystallization processes in the film. With increasing oxygen pressure the incremental film stress increases in the early growth stage. According to our stress model this indicates a decrease in grain size, an interpretation confirmed by TEM. As the film thickness increases further the tensile stress in the respective film is the lower the higher the oxygen pressure during the Cr evaporation. We interprete this to be due to an increasing amount of oxygen built into the Cr film. Above 3×10^{-5} Torr oxygen (2 Å Cr/s) transparent chromium oxid films are formed. The constant incremental stress indicates the absence of grain boundary annealing and thus columnar film growth. When Cr films, after evaporation under best vacuum conditions, are exposed to the ambient vacuum ($\sim10^{-7}$ Torr) the tensile film stress is lowered by about 10% over a 25 min period. Increasing the oxygen pressure during this exposure reduces these changes and eventually an increase in the tensile stress is found. Thereafter the films are not affected by further exposure to oxygen, indicating the formation of a chromium oxid protective layer on top of the Cr film.

In Ag films compressive as well as tensile stresses are measured as the film thickness increases. The small compressive stress during the initial growth stage we believe to be due to the "lattice expansion mechanism". Then the film stress becomes tensile and the growth stage at which the film is electrically conductive is reached at a mean thickness of 100 Å (1 Å Ag/s). The subsequent increase in incremental stress is again interpreted to be due to a noticeable grain boundary annealing. When the film is completely continuous at 200 Å, the tensile stress reaches its maximum value. As the thickness of the continuous film increases further, the film stress is again compressive, due to the then dominating influence of the "strain mechanism". Increasing the oxygen partial pressure during the Ag evaporation has a marked effect on the position of the tensile stress maximum as well as on the incremental film stress. As the oxygen pressure is raised to $\sim10^{-5}$ Torr, this maximum is shifted from 200 Å to about 80 Å mean thickness. On the basis of our stress model we conclude from the changes in the incremental stress and the size of the stress maxima that, due to the formation of an oxygen chemisorption layer, the average grain size of the Ag films decreases with increasing oxygen pressure. This interpretation is in agreement with the structure of the film seen in the TEM.

A NEW METHOD FOR METAL ELECTROREFLECTANCE MEASUREMENTS USING METAL-INSULATOR-METAL STRUCTURES

by J.P. GOUDONNET, G. CHABRIER, G. NIQUET and P. VERNIER

Laboratoire de Photoélectricité - Faculté des Sciences Mirande
21100 DIJON, France

We have measured for the first time polarized metal électroreflectance (E.R) in the metal-insulator-metal (M.I.M) structures Ag-Al_2O_3-Au, Au-Al_2O_3-Ag, Al-Al_2O_3-Ag and Au-Al_2O_3-Au. The applied voltage induces a modulation of the reflectivity of both interfaces metal I insulator and metal II insulator. In the calculation of the effective E.R signal we have shown that the contribution of these interfaces do not simply add but must be combined with phase factors taking into account the interference effects between the different reflected waves.

The major advantage of the symmetrical structure Au-Al_2O_3-Au is a smaller number of unknown parameters. For these structures our experimental spectra for both polarizations and different angles of incidence are quite consistent with our theoretical calculations and the experimental results obtained from electrolytic cells by Kolb and Kötz [1], Kofman and al [2].

This method will allow metal electroreflectance measurements in a larger range of temperature and studies of interfacial adsorption.

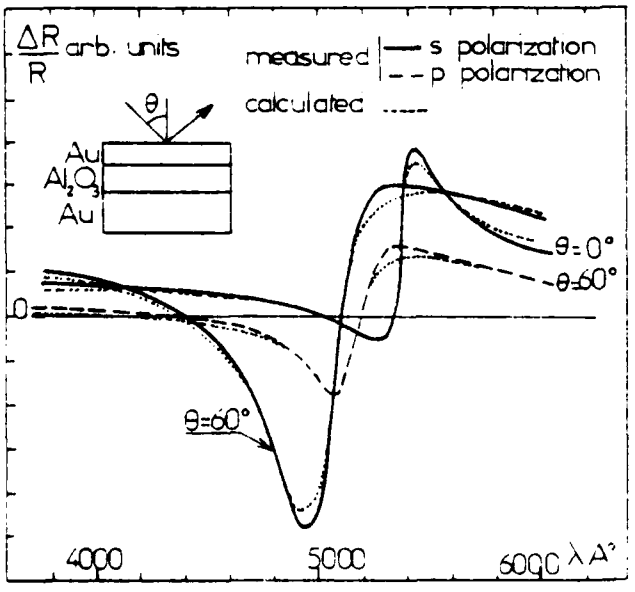

Measured and calculated E.R spectra of Au-Al_2O_3-Au structures

(1) D.M. Kolb and R. Kötz, Surf. Sci. 64 (1977) 96

(2) R. Kofman, R. Garrigos and P. Cheyssac, Surf. Sci. 44 (1974) 170

AUTOMODULATION OF COMPOSITION OF COMPLEX SEMICONDUCTOR EPITAXIAL FILMS

by S.K.Maksimov, E.N.Nagdayev, L.A.Bondarenko
Moscow, Institute of Electronic Technology

The composition of epitaxial GaAsP films grown from the gas phase under stable external conditions on the GaAs or GaP substrates exhibits periodic modulation along the [001] growth direction. In this paper we report on some new data relevant to this phenomenon.

A modulation of the composition has been studied using the method of transmission electron microscopy. The growth direction was in the foil plane. Computer simulated electron micrographs were used to optimize the electron microscope efficiency and to make a good use of the observed diffraction effects.[1,2]

By the example of GaInP films on the GaAs substrates it is shown that automodulation along the growth direction also occurs in films produced by LPE. Films of different origin differ in modulation peculiarities. During the gas-transport process modulation starts from the film-substrate boundary, whereas during the LPE process the boundary region contains "domains" of different composition, alongated in the growth direction. It seems probable that their presence is due to the non-uniformity of liquid phase composition. During the film growth a periodic modulation of the composition develops along the growth direction which suppresses the domain structure of the initial stages. The different peculiarities of modulation are likely to be due to a difference in the inertia of processes. This is an evidence for the modulation being the consequence of the crystallization process oscillatory character. The modulation appearence in case of $Ga_{0.5}In_{0.5}P/GaAs$ demonstrates that the phenomenon is not connected with minimization of elastic deformation energy caused by the substrate and film lattice misfit.

The oscillatory character of the crystallization process is found to result in a stepwise change of the composition on the boundaries of layers. Annealing results in the diffusion frontolysis which becomes continious. The stepwise character of the composition variations can be explained by N-like dependence of the growth rate on the process parameters and, presumably, is connected with phenomena on the front of crystallization.[3]

References.

1. S.K.Maksimov, E.N.Nagdayev, Doklady AN SSSR, 245, 6, 1369, (1979).
2. S.K.Maksimov, E.N.Nagdayev, VI-th International Conference on Crystal Growth (ICCG-6), Moscow, 1980, Abstracts, v.1, p.277.
3. A.A.Chernov, M.P.Ruzaikin, VI-th International Conference on Crystal Growth (ICCG-6), Moscow, 1980, Abstracts, v.1, p.284.

DIATAXIAL GROWTH OF SEMICONDUCTORS

E.I.Givargizov, L.N.Sheftal, and V.I.Klykov

Institute of Crystallography, USSR Academy of Sciences,
Moscow 117333, USSR

The term "diataxy", or "graphoepitaxy", is used for oriented crystallization on patterned amorphous substrates. This approach had been put forward several years ago [1], and has been successfully used recently for preparation of single crystal layers on fused quartz substrates [1,2].

One of the important factors in diataxy is the symmetry of the pattern. In general, the symmetry must correspond to the symmetry of the singular faces of the material to be crystallized, although patterns with other symmetries are sometimes suitable for the diataxy.

Experiments with CVD of Si and Ge on fused quartz substrates having different surface reliefs are described. Single crystal Si films as large as 15 mm^2 in area were grown. The Si films always had (111) orientation, while both (111) and (100) orientations were observed for Ge films.

Some results on the diataxial growth of A^3B^5 and A^2B^6 compounds will be presented.

---

1. L.N.Sheftal, in: Growth of Crystals (1976), Ed. L.N.Sheftal (Consultants Bureau, Plenum, New York), vol. 10, pp.185-210; also: L.N.Sheftal and V.I.Klykov, in: Rost Kristallov (Growth of Crystals) (1976), Ed. E.I.Givargizov (Nauka, Moscow), vol. 13, pp. 83-84 (Russian).

2. M.W.Geis, D.C.Flanders, and H.I.Smith, Appl. Phys Letters, 35, 71 (1979).

DEFECT STATES IN A WO_3 FILM GROWN ON A W(111) SURFACE

H. Höchst and R.D. Bringans

MPI für Festkörperforschung, Heisenbergstr. 1, 7000 Stuttgart 80,

Federal Republic of Germany

Tungsten trioxide has been found to be an effective catalyst for several chemical reactions and some early results show that it is a promising candidate for the photolysis of water. It is probable that most of these catalytic effects are related to the bulk and surface defects rather than to the intrinsic nature of WO_3. We have investigated WO_3 films which were epitaxially grown on a W(111) surface, with angular resolved photoemission spectroscopy. The dependence of the electronic structure of these films on their thickness is discussed. A comparison between the photoelectron spectra of the epitaxial grown films and amorphous films obtained by evaporation of WO_3 onto a stainless steel substrate shows that the amorphous films are quite different in their electronic structure. The band gap increases for the amorphous films and there are also states around the Fermi level. The states in the gap are related to oxygen defect states and can be increased or decreased in number by varying the growth conditions.

Thursday afternoon, June 11, 1981

Session Th-B: Electron Energy Loss Spectroscopy and Optical Methods

(Room 1105)

Chairman: A. BRADSHAW

1:40 EELS Study of Formic Acid on Pt(111)-O. N. R. AVERY

2:00 The Role of Electrodynamic Interactions on Energy Loss Intensities and Vibrational Frequencies of Adsorbed Molecules. B. I. DUNLAP and P. R. ANTONIEWICZ

2:20 Some Aspects and Results of Quantitative Electron-Loss Spectroscopy. Y. MARGONINSKI

2:40 Transmission of Monochromatic 0-15 eV Electrons Through Thin Films Organic Solids. L. SANCHE

3:00 Electron-Energy-Loss Electronic and Vibronic Spectroscopy of Matrix-Isolated-Benzene and Multilayer Benzene Films. L. SANCHE and M. MICHAUD

3:20 Electron-Spectroscopic Studies of $LiNbO_3$ and $LiTaO_3$ Surfaces. V. H. RITZ and V. M. BERMUDEZ

3:40 Surface-Enhanced Raman Scattering from Chemisorbed Pyridine on Ag(111): Dependence on Bonding Orientation. P. N. SANDA, J. E. DEMUTH, J. C. TSANG, J. M. WARLAUMONT and K. CHRISTMANN

EELS Study of Formic Acid on Pt(111)-O

Neil R. Avery
CSIRO Division of Materials Science
University of Melbourne
Parkville 3052 Australia

A cut-away view of the EELS apparatus is shown in the Figure. Although the instrument had a versatile in and out electron optical system to the monochromator hemispheres experience showed that the sensitivity and resolution (6meV) was most dependent on beam alignment which was controlled by the five sets of deflectors.

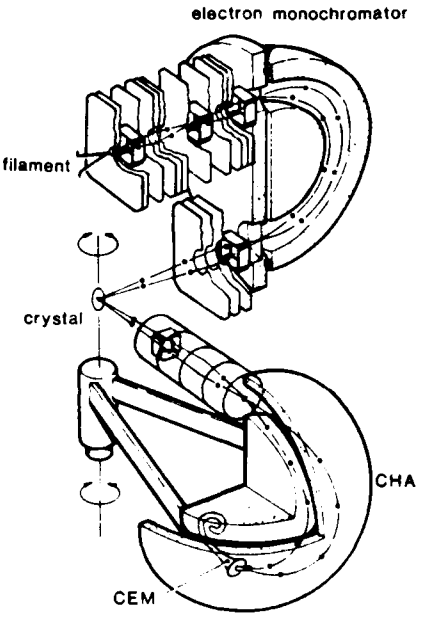

Adsorption of formic acid on Pt(111) was enhanced by increasing the Bronsted basicity of the surface with a chemisorbed layer of atomic oxygen. Excess formic acid on such a surface produced a layer of molecular formic acid which could be evaporated at -100°C. The remaining adsorbed layer was identified as an adsorbed formate species by the prominent bands at 360 cm^{-1} (νPt-O), ~880 cm^{-1} (δO-C-O), 1330 cm^{-1} (ν_s COO^-) and 2920 cm^{-1} (νC-H). The absence of a band near 1600 cm^{-1} due to screening of the ν_a COO^- mode (B_1 symmetry) indicated that the formate was adsorbed in the highly symmetric C_{2v} configuration. Whereas this procedure concealed the processes occuring at the adsorbate-metal interface during evaporation, titrating the Pt(111)-O surface at -150°C with submonolayer doses of formic acid revealed the ν_a COO band at 1620 cm^{-1}. Also the ν_s COO^- band was shifted to 1290 cm^{-1}. The tendency for these modes to be respectively more carbonyl and alcohol-like than in the free formate ion (1567 cm^{-1} and 1350 cm^{-1}) is indicative of a low symmetry monodentate linkage to the surface. Annealing the surface at -85° eliminated the $\nu_a COO^-$ mode and re-established the C_{2v} symmetry of the adsorbed formate ion.

THE ROLE OF ELECTRODYNAMIC INTERACTIONS ON ENERGY LOSS INTENSITIES AND VIBRATIONAL FREQUENCIES OF ADSORBED MOLECULES

B. I. Dunlap
Code 6171
Naval Research Laboratory
Washington, DC 20375

and

P. R. Antoniewicz
Department of Physics
University of Texas
Austin, TX 78712

The effect on energy loss intensities of the electrodynamic interactions with the substrate and neighboring adsorbed molecules is discussed. The experimentally observed large variations in the loss intensity from molecules adsorbed on various sites and as a function of coverage can be explained in terms of electrodynamic interactions.

SOME ASPECTS AND RESULTS OF QUANTITATIVE ELECTRON-LOSS SPECTROSCOPY

Y.Margoninski, Racah Institute of Physics, Jerusalem 91000 Israel.

In the course of an extended study of the electronic properties of polar ZnO surfaces, the influence of some surface treatments (exposure to atomic Hydrogen and O_2, heat treatments, Argon bombardment) on the Electron-Loss Spectrum (ELS) in the 3-30 eV was investigated. Initially, attention was focused only on the energy changes of the loss-peaks caused by the surface treatments, but later it was thought that additional information may be obtained from the amplitude changes, especially if these are correlated with changes in the surface conductivity.

During preliminary stages of quantitative measurements, we discovered that the amplitudes of peaks in the ELS and their resolution are much more sensitive to changes of instrumental parameters than the peak energies. The three most decisive factors were angle of incidence ϑ and the energy E_p of the primary electron beam, and the cancellation of the earth's magnetic field. For our spectrometer, a LEED optics analyzer, perpendicular incidence ($\vartheta=0$) was not the best choice and improved results were obtained with $\vartheta\simeq5°$. Selection of the optimal E_p was difficult, as here the question arose whether E_p could be chosen arbitrarily within a certain range, say any value between 50-65 eV, or should be selected to coincide with the maximum of the LEED intensity profile in this region. Another problem deserving attention and common to all forms of electron spectroscopy employing electronic differentiation techniques: should the spectrum be recorded in the first $dN(E)/dE$ or second $d^2N(E)/dE^2$ derivative mode? For amplitude measurements both modes are appropriate, but the second derivative could indicate spurious peaks that do not represent real electron transitions.

One of the most basic requirements of any quantitative study of ELS obtained from different surfaces is to measure the changes of the reflection coefficient α of the elastically reflected primaries, because they will directly affect the entire spectrum. We found that changes of α caused by the above mentioned treatments were surprisingly small, rarely exceeding 10%, but amplitude changes of peaks in the ELS of over 50% occurred quite frequently. The most puzzling results were observed on surfaces subjected to Ar bombardment. Here six of the eight recorded transitions decreased considerably by amounts varying between 40 - 60%, one decreased by only 20% and one, at 17 eV, did not change. The reflection coefficient decreased by only 3%, i.e., for all practical purposes was unaffected by argon bombardment. Judging from results published by Ludeke and Esaki in Phys. Rev. Lett. 33, 653 (1974), this strange attenuation of loss peaks following Ar bombardment is not confined to ZnO but occurs most probably also on Ge(111) surfaces.

TRANSMISSION OF MONOCHROMATIC 0-15 eV ELECTRONS THROUGH THIN FILMS ORGANIC SOLIDS

L. Sanche, Département de médecine nucléaire et de radiobiologie, Faculté de médecine, Université de Sherbrooke, Sherbrooke, Québec, Canada, J1H 5N4.

The transmission coefficient for monoenergetic electrons (0.04 eV FWHM) passing through thin films (~ 100 Å) organic solids has been measured in the range 0-15 eV. The apparatus consists of a high-resolution electron transmission spectrometer of the type devised by Sanche and Schulz[1]. Electrons exiting a trochoidal monochromator impinge on an organic film grown from the vapour on a metal substrate. The current transmitted to the substrate is recorded as a function of electron energy. The visibility of sharp structure can be enhanced by measuring the negative value of the second energy derivative of the transmitted current with respect to electron energy.

Spectra will be reported for films of benzene, pentane, n-hexane, 1-hexene, trans-2, trans-4, hexadiene, 1,3,5-hexatriene, cycloheptatriene, norbornadiene and norbornene. With these results and those previously published[2], the general properties of electron transmission spectra will be discussed in terms of the density-of-state of the "conduction band" and the formation of exciton and electron-exciton complexes. Broad maxima in these spectra are generally attributed to changes in the density-of-states or to an increase in transmitted current caused by a rise in the number of inelastically scattered electrons[2]. Sharp and weak features which are usually only apparent in the doubly differentiated transmission curves are believed to results from the formation of electron-exciton complexes[2] through the temporary capture of an injected excess electron by the field of a Frenkel exciton. The amplitudes and energies of the very-low-energy features ($E < 1.5$ eV) depend on the geometrical arrangement of the film constituents and on the nature of the metal substrate. These structures may possibly arise from strong energy variations in the structure factor.

1. L. Sanche and G.J. Schulz, Phys. Rev. A 5, 1672 (1972).
2. L. Sanche, J. Chem. Phys. 71, 4860 (1979).

ELECTRON-ENERGY-LOSS ELECTRONIC AND VIBRONIC SPECTROSCOPY OF MATRIX-ISOLATED-BENZENE AND MULTILAYER-BENZENE FILMS

L. Sanche and M. Michaud, Département de médecine nucléaire et de radiobiologie, Faculté de médecine, Université de Sherbrooke, Sherbrooke, Québec, Canada, J1H 5N4.

Electronic transitions near the surface of benzene multilayer films (50-100 Å) and in xenon matrices containing 2% benzene have been studied by high resolution (15-45 meV FWHM) electron-energy-loss spectroscopy (EELS) at primary energies between 5 and 14 eV. The apparatus consists of a pair hemispherical electrostatic deflectors and a closed-cycle refrigerated cryostat[1]. Condensed layers of benzene and benzene-doped matrices are grown from the vapour on a polycrystalline platinum substrate held near 20K with the cryostat. The film thickness is estimated from gas kinetic theory and work-function-changes measurements[2]. Electrons reflected from the film are analysed in energy and angle.

The three lowest electronic transitions exhibit a vibrational progression which can be ascribed to the $^3B_{1u}$, $^3E_{1u}$ and $^3B_{2u}$ free-molecule configurations. The energies of these states are the same for a benzene film or a benzene-doped xenon matrix. Compared to the gas-phase values, the $^3B_{1u}$ and $^3B_{2u}$ excitons are blue shifted by 10 ± 8 meV and redshifted by 100 meV, respectively, but the energy of the $^3E_{1u}$ is unchanged. On high resolution runs (15 meV FWHM) the $^3B_{1u}$ state splits into two vibrational progressions, 40 meV apart.

The other two electronic states observed are much broader than the instrument's resolution and do not exhibit any vibrational structure. The energies of these states are closed to those of the $^3E_{2g}$ and $^1E_{1u}$ gas-phase configurations. The energy width (2 eV) of the state $^1E_{1u}$ in pure benzene films decreases to 1 eV when benzene is embedded in a xenon matrix. This decrease in bandwidth may be due to a considerable decrease in autoionization for that state in the matrix.

The present studies demonstrate the ability of high resolution EELS to investigate electronic and vibronic surface properties of insulating films.

1. M. Michaud and L. Sanche, J. Vac. Sci. Technol. 17, 274 (1980).
2. L. Sanche, J. Chem. Phys. 71, 4860 (1979).

ELECTRON - SPECTROSCOPIC STUDIES OF $LiNbO_3$ AND $LiTaO_3$ SURFACES

Victor H. Ritz and Victor M. Bermudez
Optical Sciences Division
Naval Research Laboratory
Washington, D.C. 20375

A survey is presented of the Auger, UV photoemission and electron energy-loss spectra of lithium niobate and lithium tantalate single-crystal surfaces. Clean surfaces were prepared by fracture of insulating stoichiometric crystals in UHV. Results are reported for the clean surface before and after Ar^+-ion bombardment and for bombarded surfaces after exposure to O_2. Both Ar^+-ion and electron bombardment are found to remove surface oxygen, leading to characteristic changes in the low-kinetic-energy ($\sim$ 100 - 250 eV) Auger spectra. Some measurements were made in an oxygen ambient (5×10^{-6} Torr) to avoid disruption of the normal surface stoichiometry during AES and ELS. Both materials readily form surface carbides when carbon contamination is present. In UV photoemission, formation of oxygen-ion vacancies by ion bombardment produces a peak at about 2.5 eV above the valence-band edge in $LiNbO_3$ and at about 1.6 eV above the edge in $LiTaO_3$. Subsequent exposure to O_2 strongly attenuates the bombardment-induced photoemission. The UPS data are interpreted in terms of M^{4+} - (oxygen vacancy) complexes (M = Nb or Ta). ELS data in the 2 - 90 eV range of loss-energies show transitions from the valence band and upper core levels to states in the conduction band. The effects of variation of the primary-beam energy and of O_2 on the intrinsic ELS are examined. Evidence is found for the existence of surface states on $LiTaO_3$ (but not on $LiNbO_3$) prior to ion bombardment. Bombardment-induced surface defects are also observed in ELS but are not strongly attenuated by O_2. This suggests that the defects observed in ELS differ from those observed in UPS and may involve Li^+-ion vacancies. The effects of thermal annealing and of laser irradiation at λ = 488.0 nm on the surface defects are also examined.

Surface-enhanced Raman scattering from chemisorbed pyridine on Ag(111): dependence on bonding orientation+

P.N. Sanda, J.E. Demuth, J.C. Tsang, J.M. Warlaumont
and K. Christmann

IBM T.J. Watson Research Center
P.O. Box 218, Yorktown Heights, NY 10598

Coverage dependent UHV studies of surface-enhanced Raman scattering (SERS) from pyridine adsorbed on a clean Ag(111) crystal containing a weak periodic modulation will be presented. The Ag crystal has a nearly sinusoidal profile to allow optical coupling to surface plasmons which was necessary for us to observe SERS, yet the surface retains much of its (111)-character since the amplitude is small (~500Å) compared to its wavelength (1μm). The SERS experiments were performed in a UHV chamber (typical base pressure ~2×10^{-10}Torr) with in-situ facilities for LEED, Auger, and Raman spectroscopy. UV-photoelectron (UPS) and high-resolution electron energy loss-spectroscopy (EELS) were performed in separate vacuum systems and were used to characterize the adsorption of pyridine on Ag(111).

Chemisorbed pyridine demonstrates a large (~10^4) enhancement of the symmetric ring breathing mode at 990 cm^{-1} whereas the asymmetric ring breathing mode observed at 1034 cm^{-1} in the liquid phase is not observed (enhancement $\lesssim$ 500). This selective enhancement is consistent with a theoretical model by Jha, Kirtley, and Tsang[1] which considers the interaction between the molecular layer and the conduction electrons of the metal substrate. The coverage dependent Raman measurements show an onset of the 990 cm^{-1} peak at ~0.5 monolayers. This can be related to the occurrence of a compressional phase transformation for chemisorbed pyridine on Ag(111) at ~0.5 monolayers. Above this coverage pyridine is inclined ~55° to the surface (nitrogen lone pair-bonded) and below it, lies nearly flat on the surface (π-bonded).

+. This work was supported in part by the Office of Naval Research and the Cornell University Materials Science Center.

*. Present address: Institut fur Physikalische Chemie derUniversitat, Munchen, W. Germany

1. S.S. Jha, J.R. Kirtley and J.C. Tsang, Phys. Rev. B, 22 (1980) 3973

2. J.E. Demuth, K. Christmann, and P.N. Sanda, Chem. Phys. Lett., 76 (1980) 201

Thursday afternoon, June 11, 1981

Session Th-C: Adsorption

(Room 1123)

Chairman: L. D. ROELOFS

1:40 Kinetic Equations for Physisorption. H. J. KREUZER

2:00 Surface Potentials of Benzene Derivative Monolayers and Submonolayers at the Mercury/Nitrogen Interface. B. J. KINZIG

2:20 Alkoxy Complexes on Lithium-Identification and Geometry. S. GATES, J. A. SCHULTZ, L. G. PEDERSEN and R. C. JARNAGIN

2:40 Interactions of Lithium with Dry Air. C. R. ANDERSON and R. N. LEE

3:00 Evaluation of Surface Cleaning Procedures. R. G. MUSKET, C. A. COLMENARES, D. M. MAKOWIECKI, W. McLEAN, R. G. MEISENHEIMER and W. J. SIEKHAUS

3:20 H_2O Interaction with Ni(110): Auto-catalytic Decomposition in the Temperature Range from 400-550 K. C. BENNDORF, C. NÖBL, M. RÜSENBERG and F. THIEME

3:40 Hartree-Fock Theory of Multilayer Physisorption. H. J. KREUZER, P. SUMMERSIDE and R. TESHIMA

4:00 Ion Formation from Solid Surfaces due to very rapid Energy Transfer. F. R. KRUEGER

4:20 A Study of Gas Conduction in Evacuated Solar Energy Thermal Collectors. B. WINDOW and G. HARDING

Kinetic Equations for Physisorption

H.J. Kreuzer

Department of Physics, University of Alberta

Edmonton, Alberta, Canada, T6G 2J1

In gas-solid systems in which the surface potential of physisorption develops many bound states one finds (Z.W. Gortel, H.J. Kreuzer and R. Teshima, Phys. Rev. B22 (1980) 5655) that the desorption kinetics are quite insensitive to details of the surface potential, allowing one to approximate a system with many discrete bound states by a quasi-continuum (for the gas particles) ranging from the bottom of the surface potential up. The adsorbing or desorbing gas particle will then perform a random walk through the quasi-continuum of bound state energies which is controled by a (continuous) master equation which we derive from the set of rate equations for the bound state occupation functions. The kernel of the master equation is explicitly calculated for phonon-mediated adsorption and desorption in a Morse potential. We give the equivalent Smoluchowski-Chapman-Kolmogorov equation for which we find the Kramers-Moyal expansion. Identifying van Kampen's large parameter Ω for such gas-solid systems, we establish explicit criteria for the validity of a Fokker-Planck equation governing physisorption kinetics. With explicit numerical results we demonstrate that the time evolution of the adsorbate during the desorption process, as calculated from the rate equations, maintains quasi-equilibrium only at low temperatures, i.e. for $kT \ll 2U_o/(\hbar^2\gamma^2/2mU_o)^{1/2}$ [U_o and γ^{-1} are depth and range of the surface potential and m = mass of gas particle]. Perturbation theory of the master equation yields $t_d = t_d^c \exp[Q/kT]$ with $Q = U_o$ and $t_d^o = \omega_D^{-1}(M_s/m)(\hbar\omega_D/U_o)^4(2mU_o/\hbar^2\gamma^2)^{5/2}$ at low T with ω_D = Debye frequency of solid; M_s = mass of a solid particle. At intermediate temperatures $5(U_o\hbar^2\gamma^2/2m)^{1/2}/2 \ll kT \ll 3U_o/5$ we derive another simple expression from the Fokker-Planck equation with $t_d^o = \omega_D^{-1}(M_s/m)4m^2(\hbar\omega_D)^5(U_o\hbar^2\gamma^2)(*kT/72\pi)$. These results allow a critical assessment of classical "equilibrium" theories of desorption. Lower limits for the pre-exponential factor t_d^o which can be as low as 10^{-14} secs, are derived as $t_d^o \geq (M_s/m)(4\hbar/9\pi)(\hbar\omega_D/U_o)$ at low T and $t_d^o \geq (M_s/m)(2\hbar/9\pi)(kT/U_o)$ in the above intermediate temperature region. The emergence of several transient time scales in gas-solid systems with many surface bound states will be demonstrated, and the usefulness of the mean first passage time assessed.

Surface Potentials of Benzene Derivative Monolayers and Submonolayers at the Mercury/Nitrogen Interface

by

B. J. Kinzig
Naval Research Laboratory
Optical Sciences Division
Code 6510
Washington, D. C. 20375

ABSTRACT

Surface potentials of physisorbed organic adsorbates were studied as equilibrium monolayer films and as a function of coverage from solution-deposited adsorbates. The equlibrium film surface potential, denoted ESV, is a new class of measurement that enables comparison of experimental values with those calculated from the MacDonald-Barlow theoretical representation for contact potential differences due to adsorption on a metal surface. In the present study with small, rigid asymmetric aromatic molecular adsorbates, their anisotropic molecular properties were introduced into the calculations to account for orientation effects in the molecular adsorbate layer. Excellent agreement of experimental with theoretical values permitted assignments of orientation to be made to the adsorbates in equilibrium films. Limitations of homogeneous adsorbate theory for molecular adsorbate systems are discussed.

ALKOXY COMPLEXES ON LITHIUM-IDENTIFICATION AND GEOMETRY

Steve Gates, J. Al Schultz, Lee G. Pedersen and R. C. Jarnagin

The William Rand Kenan, Jr. Laboratory of Chemistry
The University of North Carolina at Chapel Hill
Chapel Hill, North Carolina 27514

The results of an experimental and theoretical investigation of the binding of the monohydric alcohols methanol, ethanol, n-propanol and n-butanol to metallic lithium are reported. The formation at room temperature of alkoxy type surface species of submonolayer to saturation exposures is evident from the UPS spectra obtained by reaction of 0.1L to 5L of the alcohols with clean polycrystalline evaporated thick films of lithium.

The evident absence (low abundance) of ROH/Li(s) species among the surface complexes formed is totally consistent with results of *ab initio* Hartree-Fock type molecular orbital calculations using as models of the surface species clusters of Li_n; $1 \leq n \leq 10$ where ROH, RO and RO-separated H were situated as admolecules. The calculations not only provide supportive evidence for the identity of the complexes formed but also provide a realistic "measuring probe" of changes in molecular geometry on adsorption as well as information concerning the geometrical attitude of the sorbed species in significant binding sites.

Minimal basis sets have been used for most of the calculated geometries but double zeta quality sets have been used for the ethoxy and methoxy species in several models. The simulated and experimental spectra compare favorably.

Extensive calculations for the methoxy complex on clusters of 6 to 9 lithium atoms constructed from the (111), (110), and (100) crystal faces of bulk lithium (CH_3O/Li_n n = 6, 8, or 9) show that a bridge site, with oxygen of CH_3O participating in an effective 3 center bond with 2 near neighbor lithium atoms, is favored on all clusters examined. A tendency for the O-C direction to lie normal to the Li-Li axis of the bridges was found, a condition that can result in O-C lying perpendicular or inclined to the "surface plane", dependent on the local structure.

INTERACTIONS OF LITHIUM WITH DRY AIR

Ch. R. Anderson and R. N. Lee

Naval Surface Weapons Center

White Oak, Silver Spring MD 20910

XPS studies have been made of the reaction product layers formed on lithium foils as a result of exposure to dry air. Exposures were made in a dry-room (0.5% R.H.) and transfer made to the XPS instrument (base pressure 10^{-10} Torr) without exposure to uncontrolled atmosphere. Comparison of the reaction product spectra with spectra of standard samples of Li_2CO_3 , LiOH and Li_2O showed that the reaction layer consists primarily of Li_2CO_3 and Li_2O. Formation of the LiOH previously reported (1) did not occur. Particular care was taken with instrumental calibration, and discrepancies between the previously reported (2, 3, 4) 1-s binding energies for Li and O in these compounds will be discussed.

1) M. M. Markowitz and D. A. Boryta; J. of Chem. and Eng. Data, 7, 586 (1962).

2) J. P. Contour, et. al.; J. Microsc. Spectrosc. Electron.; 4, 483 (1979).

3) S. P. S. Yen, D. Shen and R. B. Somoano; 158th Electrochem. Society Fall Meeting, Hollywood, Fla., 5-10 Oct. 1981.

4) K. M. Black, R. J. Bennett, S. Lachmansingh-Kruchten and P. A. Lindfors; Pittsburgh Conf. on Anal. Chem. and Appl. Spectrosc., 9-13 March 1981, Atlantic City, NJ.

EVALUATION OF SURFACE CLEANING PROCEDURES

R. G. Musket, C. A. Colmenares, D. M. Makowiecki, W. McLean,
R. G. Meisenheimer and W. J. Siekhaus

Lawrence Livermore National Laboratory
Livermore, California 94550

ABSTRACT

Surface cleaning procedures documented in the open literature for solid, elemental materials have been evaluated. The main emphasis has been on in-situ cleaning in a UHV chamber using one or more of several approaches (eg, sputtering with or without heating, heating in vacuum or in a gaseous atmosphere, cleaning or fracturing, and machining or polishing). Cleaning procedures for a total of 74 elements having vapor pressures below 10^{-9} Torr at room temperature were reviewed. Only those procedures documented with element-specific surface characterization techniques were included in the recommended procedures for each element. Appropriate characterization techniques included AES, XPS, SIMS, ISS, and SXAPS, which all have detection limits of about one atomic percent (or better) for contaminates. For some elements a variety of procedures have been found to be acceptable. Any differences in the procedures for polycrystalline and single crystal surfaces of the same element have been detailed. The written paper references all the documented original papers used to establish the recommended procedures. For the oral presentation, a discussion of the procedures for a few representative elements will be given.

*"Worked performed under the auspices of the U. S. Department of Energy by the Lawrence Livermore Laboratory under contract number W-7405-ENG-48."

H_2O INTERACTION WITH Ni(110): AUTO-CATALYTIC DECOMPOSITION IN THE TEMPERATURE RANGE FROM 400-550 K

C. Benndorf, C. Nöbl, M. Rüsenberg and F. Thieme

Universität Hamburg, Institut für Physikalische Chemie, Laufgraben 24, 2 Hamburg 13, West Germany

The interaction of H_2O vapour with clean and oxygen covered Ni (110) surfaces has been investgated with UPS, XPS, AES and work function change ($\Delta\Phi$) in the temperature range from 150-550 K.

The molecular adsorption on the clean Ni(110) at 150 K is characterized by three H_2O induced maxima in the UPS (He I and He II) 6.8, 9.4 and 12.7 eV below E_F, attributed to the π, σ_x and σ_x orbitals of water and an oxygen 1s B.E. of 533.6 eV.

At room temperature, H_2O adsorption is found to be possible only on oxygen precovered Ni surfaces, leading to the formation of a hydroxyl species with quite different features in the UPS and XPS.

At higher temperature (400-550 K) on the clean Ni(110) surface a decomposition of H_2O is detected, following the reaction scheme:

$$H_2O_{gas} \rightarrow O_{ads} + H_{2gas}$$

The amount of released O_{ads} -with an XPS determined B.E. of 529.8 eV- is measured with AES and $\Delta\Phi$ and compared to the well known data of O_2 adsorption and reaction on or with Ni(110) [1, 2,3]. Contrary to the molecular adsorption of H_2O at 150 K or the adsorption and reaction at room temperature with preadsorbed oxygen on Ni -leading in both cases to a lowering of $\Delta\Phi$- the reaction with Ni(110) at higher temperature, similar to the adsorption of oxygen on Ni(110) [2,3], is accompanied by an increase of the work function. The maximum value of $\Delta\Phi$ is$\simeq$ 0.5 eV, nearly independent from the crystal temperature and comparable to the work function change due to oxygen adsorption on Ni(110) ($\Delta\Phi \simeq$ 0.5 eV, O(2x1) LEED structure at 0.6- 1 L [2]). But in contrast to the adsorption of oxygen on Ni(110), which follows at low exposures ($\leq$ 1 L) a Langmuir kinetic [1] nearly independent of temperature, the reaction rate of H_2O with Ni(110) first increases with increasing oxygen coverage, slowing down at higher coverage. The reaction rate, determined from $\Delta\Phi$ and AES measurements decreases with increasing temperature, accompanied by a shift of the inflection point of the s-shaped $\Delta\Phi$-exposure curves (as well as the $O(KLL)_{p\text{-to-}p}$-exposure curves) from 0.8 L at 400 K to 4 L at 550 K.

The dependence of the reaction rate on the surface oxygen concentration and the significant dependence from crystal temperature will be discussed on the basis of an auto-catalytical process, involving surface oxygen as promotor.

1 P.H. Holloway and J.B. Hudson, Surface Sci. 43(1974) 123, 141

2 T.N. Rhodin and J.E. Demuth, Japan.J.Appl.Phys.Suppl. 2(1974) 167

3 C. Benndorf, B. Egert, C. Nöbl, H. Seidel and F. Thieme, Surface Sci. 92(1980) 636

Hartree-Fock Theory of Multilayer Physisorption

H.J. Kreuzer, P. Summerside and R. Teshima, Department of Physics, University of Alberta, Edmonton, Alberta, Canada T6G 2J1

The quantum statistical theory of phonon-mediated physisorption is extended from zero to multilayer coverage by including the two-body interaction between gas particles in the Hartree-Fock approximation. This retains the intuitive picture of an effective surface potential in which the energies of the bound states become nonlinearly dependent on their occupation and thus on the temperature. For fermionic gas particles one typically finds the behaviour depicted in the figure for ^{3}He adsorbing on solid argon. Starting at high temperature T we note that the ^{3}He-Ar system has a static (Morse) surface potential of depth $U_o/k_B = 160$ K and range $\gamma^{-1} = 2$ Å that develops 10 bound states. Keeping the pressure P = .8 Pa fixed we lower T thus raising the chemical potential μ. To avoid that more than the lowest bound state gets occupied (if this happened in the static surface potential then more than one gas particle would occupy the same adsorption site !) the energies of the higher bound states move up (upper panel) due to the increasing contribution from the (nonlinear) Hartree-Fock potential. As the occupancy of the lowest bound state approaches one (center panel) at T ~ 7.0 K, the upward motion of the second bound state energy stops, because by now the effective surface potential has changed so drastically that the wavefunction of the second bound state no longer has its peaks in the original surface potential well but some 4 Å further away from the surface where a second layer starts to develop. This is illustrated in the lower panel where we follow the mean position of a gas particle trapped in the lowest bound state (first adsorption layer), in the second bound state for T <7K (second adlayer) etc. Note that the third layer does not form completely due to the weak He-He interaction. After completion of the first adlayer, i.e. for T < 7.0 K the effective Hartree-Fock surface potential has a deep potential well close to the wall followed further out by a high repulsive barrier on the outside of which a second well develops to trap gas particles into a second adlayer etc. Whereas for Fermi-Dirac gas particles the ground state, and thus the heat of adsorption stays for most systems constant as a function of coverage up to multilayer coverage and then depending on the ratio of the ranges and depths of surface to 2-body interaction also go down or up for the second and third layers one finds for Bose gas particle that the ground state and the heat of adsorption must go up drastically as the first monolayer forms. The coverage dependence of adsorption and desorption rates are calculated.

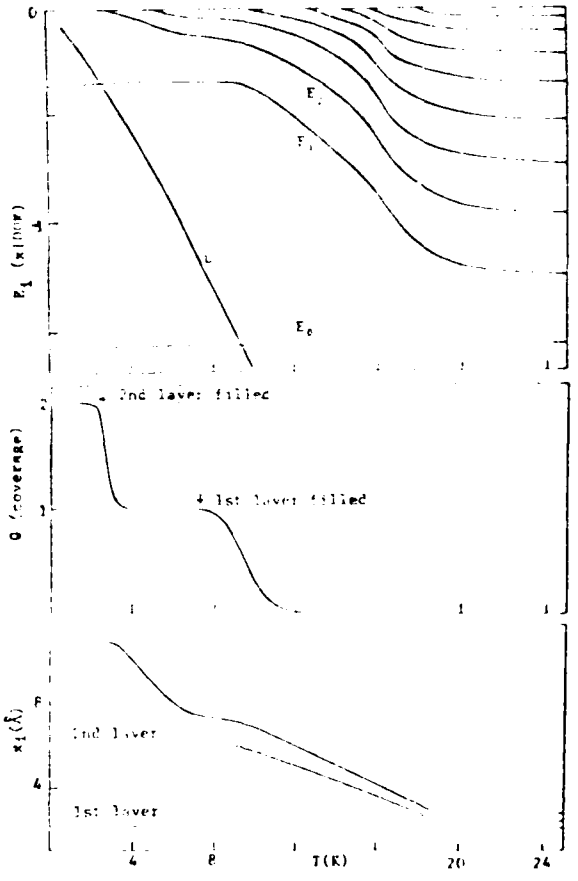

ION FORMATION FROM SOLID SURFACES DUE TO VERY RAPID ENERGY TRANSFER

Franz R. Krueger

Institut für Biophysik -Physik für Mediziner-, Universität Frankfurt, Haus 74, Th.-Stern-Kai 7, D-6000 Frankfurt/M. 70, West Germany

The transition probability P of a molecular species from a surface bound state to an ionized gaseous state by any quasi-adiabatic interaction can be separated into two independent probabilities: The probability P_1 to be launched into the activated surface state (energy hypersurface saddle point) times the probability P_2 to decay right away into the system of end-states considered. "Quasi-adiabatic" means, that there is an energy-hypersurface being well defined during transition, i.e. the hamiltonian of the whole system refers to good quantum states at any time. In this case the nuclear coordinates of the species may be well described within a potential formed by the electronic system at the surface. This quasi-adiabatic assumption is justified, if the electronic system is allowed to relax into the lowest eigenstate at any time during the nuclear movements, and, if the nuclear movements of the neighbour system forming the potential can be assumed to be completely decoupled. In this case the transitions will follow the paths of low activation energies with high probability. This does practically mean, that decomposition of thermally labile species is favored against evaporation without destruction.

The quasi-adiabatic assumption may become unvalid, however, if the forces acting on the molecular surface species alter more frequently than the nuclear system can response. This may be caused by very rapid energy transfer, either electronically by collective sound vibrations or by fast decomposition of the whole surrounding surface. Treated non-adiabatically the transition probability is now given by the overlap of the initial nuclear states with the energetically accessible free states, which is governed by the time-dependent correlation function being well known from quantum chemistry. The "diabaticity" is scaled to the ratio of decay time of the correlation function to the reciprocal mean frequency of the interaction. In the diabatic case even complex ions from fragile substances are formed with higher probability. This is seen by a semiquantitative treatment of nuclear correlation functions of typical ions and comparison with mass spectral data from fission-fragment induced and pulse-laser induced desorption, being "rapid" surface ion formation techniques in the above sense. Moreover, this diabatic evaporation treatment can explain the great similarity of surface ion formation by very different, but fast, interactions. Mass spectra are discussed under consideration of this non-adiabatic evaporation model.

A STUDY OF GAS CONDUCTION IN EVACUATED SOLAR ENERGY THERMAL COLLECTORS

B. Window and G. Harding

School of Physics
University of Sydney NSW 2006, AUSTRALIA

The major cause of degradation of performance in solar thermal collectors of the evacuated tubular all-glass design is the heat loss at elevated temperatures due to the buildup of gas within the vacuum space. These gases come from the bulk and the surfaces of the collector materials, and from permeation through the collection materials.

The pressures at which these heat losses become appreciable correspond to the free molecule regime, where the mean free path between gas atom collisions is much greater than the dimensions of the vessel, and the nature of the wall-molecule energy exchange is important in determining the heat flow for a given gas pressure. This interaction is usually described by an accommodation coefficient, which gives the fraction of available energy transferred to or from the wall by a gas molecule in a collision. Results for the rate of heat loss between two concentric cylinders, with the outer cylinder made of glass and held at 18 °C, and with the inner cylinder made of glass, sputtered copper or an iron-carbon selective surface and held at 60 °C to 300 °C have been obtained with small pressures (0.1-100 Pa) of hydrogen, helium, argon, nitrogen, carbon monoxide and water vapor in the vacuum. Accommodation coefficients are derived from this data for the different gases and surfaces over the temperature ranges. The results show correlations with molecular sizes, but are more dependent on the binding energies between gas molecules and the wall.

Results for the heat losses in closed collectors either with gas deliberately introduced or with gas produced by degrading the selective surface, were obtained. For gases such as hydrogen, helium, nitrogen and argon, it was possible to explain the observed behavior of a heat loss rate approximately linearly dependent on the temperature difference by using kinetic theory and the accommodation coefficients derived earlier. It was necessary in the case of water vapor and for some of the degraded collectors to include the absorption of gas molecules on the wall of the collector. The heat loss increased much faster than linearly with the temperature difference, corresponding to the release of molecules from the heated surface.

END

FILMED

8-83

DTIC